UNIVERSITÀ DEGLI STUDI DI MESSINA

Dipartimento di Scienze Chimiche, Biologiche, Farmaceutiche e Ambientali

---

DOTTORATO DI RICERCA IN SCIENZE CHIMICHE
XXX CICLO

Speciation of Al(III) with some classes of ligands in aqueous solution

Dott. Fausta Giacobello

Supervisor
Prof. Ottavia Giuffrè

Coordinator
Prof. Sebastiano Campagna

Academic Year 2016 - 2017

Index

Chapter 7

Amino acids: results and discussion 87

Chapter 8

Oligophosphate ligands: results and discussion 100

Chapter 9

Other inorganic ligands: results and discussion 116

Chapter 10

Nucleotides: results and discussion 121

Chapter 11

Sequestering ability and empirical relationships 132

Aim of the work

The importance of aluminium speciation

In recent years, the growth of the modern technology and the progress in many industrial fields caused an increase of the environmental pollution due to the discharge of heavy metal in natural systems, with relevant consequences on human life. Generally, metals can be classified as: (1) “essential”, if they are indispensable for the cell survivor, (2) “beneficial”, if their presence in an organism can give a health improvement, (3) “neutral”, if they do not cause beneficial or toxic effects and (4) “toxic”, if they are exclusively detrimental [1].

Despite heavy metals are natural components of earth’s crust, they are not degraded by biological or photochemical activity and, therefore, they can remain in the environment for many years. Man has managed to increase their emission in nature, by changing their natural transport and release rate with the rise of the industrial activity.

These “non-essential” metals, as already mentioned, have not beneficial effect to the organism and their exposure over certain limit can cause toxicity, because of their high persistence in human body and their tendency to bioaccumulate. This term indicates the process with which a persistent toxic substance accumulates in living tissues at concentrations higher than those found in the surrounding environment. It can directly occur with inhalation, swallowing, simple contact with the dangerous substance or through the food chain with the passage of this one from a food compartment to the other, until it reaches man, causing possible acute or chronic damages for health, such as poisoning, malformations, or central nervous system diseases. For these reasons, the exposure to the non-essential metals and their environmental distribution are topics of great interest in the field of analytical chemistry.

The only knowledge of the total metal concentration cannot provide all the required information about the impact of an element in biological or ecological systems. It is also insufficient to understand its speciation, that is the process for identifying and quantitatively determining the different chemical and physical forms of an element in a system [2]. Generally, this kind of investigation is of crucial importance to better understand the bioavailability, the toxicity and the environmental impact of the various chemical species of a certain element in a system. It was proved, indeed, that the biological and chemical activity of heavy metals is only ascribable to some chemical forms, such as cations or organic

derivatives, in which these elements are found in natural fluids. Some other factors as pH, temperature, ionic strength, redox potential and the presence of organic or inorganic complexing ligands in the considered system can influence the behaviour of the element, causing form changes in which it occurs. For example, in the case of aluminium, the subject of this thesis, a decrease of rainwater pH values, resulting from the burning of sulphur containing fossil fuels, can increase the leachability of this metal cation from minerals in soils, thus causing fishes death in receiving waters. Speciation, therefore, is of relevant importance not only in analytical chemistry, but also in many other scientific matters, such as geochemistry, biology, and medicine [3].

In the light of the above considerations, speciation study in aqueous solution achieved a key role, with the aim of examining and predicting a molecule behaviour in a natural fluid (seawaters, freshwaters, blood, plasma, etc.). This is possible by taking into account the formation equilibria of all the chemical species, thus considering acid - base properties of ligand molecules, metal hydrolysis, temperature, ionic strength, ligand-metal concentration ratio and pH. All these factors infuence the speciation of metal ions, modifying their potential toxicity and mobility in natural systems.

Metal speciation studies can mainly be performed through direct experimental measurements, by different analytical techniques, such as potentiometry, UV - Vis spectrophotometry, calorimetry, voltammetry, NMR spectroscopy and mass spectrometry. The experimental data sets can be processed by means of computer programs, with the purpose of achieving the better speciation model together with the values of formation constants and enthalpy changes. The validity of the results obtained from these calculations are directly correlated to the quality of the experimental data and the mathematical procedures used to determine an accurate equilibrium model, chosen by considering some important criteria such as, model simplicity, statistic parameters and literature data comparison [4].

Although aluminium is the most abundant metal of the earth's crust, it is not an essential element in biological systems, resulting, therefore, toxic for plants and animals. As detrimental element, it can be also considered a threat to the human health, causing many diseases, mostly related to the skeletal, nervous central and hematopoietic systems. There are two main different ways of Al(III) contamination: the first one due to the natural and industrial sources which can cause chronic intoxication, the second one due to high doses of Al(III)-containing therapeutic drugs which affect patients, leading to acute poisoning. The toxicity of this metal cation in aquatic and ground systems is related not only to its total concentration, but also to all its biological active forms, making the identification of its different chemical species indispensable in the environment. In particular, as it is a typical hard metal cation, Al^{3+} can interact with negative-charged oxygen donors in bio-systems,

especially molecules with carboxylate, phenolate, catecholate and phosphate groups [5-7]. This specific affinity is strictly related to its toxic effects, since biomolecules with these functions may be involved in the Al(III) transport and uptake processes into living organisms. Therefore, the extensive use of aluminium in many industrial fields, its natural distribution in the environment, the fact that it was recognized as the cause of several diseases and the relative lack of information on thermodynamic data of its species, made it of large interest for chemical speciation studies.

Aim of the thesis

In this thesis, as mentioned above, Al^{3+} speciation with several ligands of environmental and biological interest was studied.

A research of literature data concerning its speciation in natural fluids and the acid - base behaviour of the ligands under study was the first step.

The analysis of different Al(III)-ligand systems was, moreover, preceded by an experimental investigation on the metal cation hydrolysis, in different ionic media and ionic strength. Ligands chosen for this study can be distinguished by their organic or inorganic nature, the class of their compounds and the functional groups present in the molecules (-COOH, $-PO_4^{3-}$; -SH, $-NH_2$), classifying them as O-, S- and N-donors. Their properties will be discussed later.

On the light of the above considerations, the experimental analysis was developed in the following way:

1. Study of aluminium hydrolysis;
2. Determination of ligand acid - base properties;
3. Study of the Al(III) interactions with the different ligands under a wide range of experimental conditions. Stability constants of the species and speciation models were determined by means of potentiometric measurements. Enthalpy changes were obtained by calorimetric titrations. For some systems were also performed UV-spectrophotometric, ^{1}H or ^{31}P-$\{^{1}H\}$ NMR and MALDI-MS investigations.
4. Evaluation of the sequestering ability of the various ligands towards aluminium cation under different conditions.

Chapter 1

Aluminium

1.1 Historical notes

The aluminium term comes from the latin word "*alum*", which means "bitter salt" and identifies a mineral with chemical formula $KAl(SO_4)_2 \cdot 12H_2O$, already used in medicine as haemostatic to treat wounds in ancient Greek and Roman times. In that period, this stone was also fundamental in parchment prints, glass production, leather tanning and in statues, armours and weapons manufacture. The existence of this metal, not yet discovered at that time, was supposed by H. Davy in the 1807, who was not able to isolate it, but he was the first to give a name to the metal, proposing the "alumium" term and later agreed to change it into "aluminum". Two decades later, H. Oersted isolated this metal for the first time, by means of a potassium amalgam on the aluminium chloride. In 1827, H. Wöhler improved the operating method by using the metallic potassium and finally, in 1854, Henri Sainte-Claire Deville developed the first industrially exploitable process, by using sodium [8-10]. This method of production was complex, but had an advantage, since a french geologist had discovered a clay full of its content near the village of Les Baux, from which derives the name Bauxite. During that time, metallic aluminium was considered so valuable that, at the "Paris Exhibition" in 1855, it was shown next to the jewellery of the crown. Napoleon III himself, for that occasion, used cutlery made of this precious metal. In those years, Deville, after his discover, wrote a book, *Aluminium, Its properties, Its Production and Applications*, where he compared the extracted metal from clay to the silver [10]. At that time, the metal was considered so costly that some writers, as Jules Verne, spoke of it in his literary compositions. In his novel, *From the Earth to the Moon*, dated in 1865, he predicted its use as a material component of the spaceships. About a decade later, Charles Dickens wrote about aluminium in these terms: *"Within the course of the last two years ... a treasure has been divined, unearthed and brought to light ... what do you think of a metal as white as silver, as unalterable as gold, as easily melted as copper, as tough as iron, which is malleable, ductile, and with the singular*

quality of being lighter that glass? Such a metal does exist and that in considerable quantities on the surface of the globe" [10].

The Deville work was a starting point for Charles Hall and Paul Heroult, which, simultaneously and separately in USA and France, before the century end, worked out a not-expensive electrolysis process, through which aluminium could be extracted from its oxide, known as alumina, thus making the metal price lower. Later, Karl Josef Bayer, an Austrian engineer, improved the extraction methods, developing a process by which alumina could be educed from the mineral bauxite, a widespread and naturally aluminium source. This basic process, together with the Hall and Heroult one, is still used today. In the early twentieth century, aluminium has found its first industrial use in engines, such as that built in 1903 by Wright brothers to power their first biplane [11]. In 1910, the aluminium foils came into the market of the commerce and the following years, the alloy development, opened up new industrial fields. With the beginning of the Second World War, aluminium begun one of the most important and strategic metals, which uses included naval and airplane infrastructure constructions [10]. In the postwar period, American industry shifted its applications towards consumer goods and its production has continuously increased, as well as its uses, which completely affect our modern life [8]. Nowadays, thanks to is great peculiarities, such as lightweight, not-unbreakable, corrosion resistance, high thermal and electrical conductivity, high plasticity, excellent ductility and malleability, aluminium is employed to manufacture millions of products. Some aluminium components are essential for the aerospace industry and they are also very important in other industry areas, *i. e*. transports and constructions [9].

Regarding the etymology of the word, the International Union of Pure and Applied Chemistry (IUPAC) officially standardised the term *aluminium* in 1990. Despite this, many people in the scientific community use to call this metal *aluminum*, in particular in USA, where in 1925 the American Chemical Society decided to give back to this term, referring to the metal as "aluminum" still today [10, 12].

1.2 Chemical properties and solution chemistry

Aluminium is the most abundant metal of the earth's crust (8.8%); third element after oxygen and silicon. In nature it is mainly found in minerals, where it is always combined with other elements, forming oxides or silicates. It is not a heavy metal and, since it has not electrons unpaired into *d* and *f* orbitals, aluminium is not a transition metal, showing a fairly different redox behavior than Fe^{3+} [13]. It gains two diverse oxidation states, +3 and 0, but, as it is a metal very reactive, it does not exist in the environment as a single element. With a ionic radius of 54 pm, comparable in size to Fe^{3+} (65 pm) and Mg^{2+} (72 pm), it is a typical hard metal cation with a high charge density, which prefers to interact with small hard Lewis bases,

especially O-donors owning negative charge such as, carboxylates, phenolates, catecholates and phosphates. Fluoride also is a strong ligand for Al^{3+}[13, 14]. Due to its small size and its large charge, aluminium binding is mostly ionic rather than covalent type and, in minerals as well as in aqueous solutions, it prefers to interact through a six-fold coordination, giving complexes with octahedral structure. The aluminium solubility and bioavailability in natural and biological systems is strongly affected by its interaction with water components at different pH values in the absence of any ligands. It is well known that, in more acid solutions than pH = 4, at room temperature and intermediate ionic strength values, aluminium is present as exa-aquo ion, $Al(H_2O)_6^{3+}$ (usually indicated as Al^{3+}). At higher pH values, its solvating water molecules undergo deprotonation, leading to the formation of mononuclear species, such as $Al(OH)^{2+}$, $Al(OH)_2^{+}$ and $Al(OH)_3^{0}$ (water coordinate molecules are neglected). The latter species gives a precipitate at pH ≈ 4.5, which redissolves at pH ≈ 6.3 if the metal concentration is very low (≤ 0.5 μM) with the formation of the tetrahedral aluminate, $Al(OH)_4^{-}$. Polynuclear species, as $Al_2(OH)_2^{4+}$, $Al_3(OH)_4^{5+}$ and $Al_{13}(OH)_{32}^{7+}$, rise only in the case of high metal concentrations (not less than 10 μM) [15, 16]. The metal hydrolytic behaviour above mentioned can be strongly affected by the presence of competing ligands such as F^-, Cl^- or SO_4^{2-}; the formation of AlF_2^{+}, AlF_3^{0} and AlF_4^{-} can increase the aluminium solubility [17]. The exposure to oxygen and other oxidant agents, such as the water, causes the surface formation of a slightly aluminium oxide film, insoluble in the pH range 4.5 - 8.5, which confers resistance to the corrosion [13].

1.3 Sources and distribution in the environment

As mentioned in the previous paragraph, aluminium is the most abundant metal of the Earth's crust. Only the ^{27}Al isotope is present in nature and is obtained mainly from bauxite ores containing 40-60% alumina, from which the metal is extracted through Bayer process and succeeding Hall - Héroult electrolytic method [13]. In environment, it is also found as aluminium silicates in igneous minerals, such as clay and mica, as hydroxides in rocks and soils and as oxides in some gemstone, such as ruby and sapphire [12, 13].

In addition to natural sources, aluminium is introduced into ecosystems from anthropogenic ones, since its production is continuously growth, as well as its applications, that completely characterize our lifestyle [8]. This will be better discussed in one of the following paragraphs.

In natural waters, its content is mainly due to the action of atmospheric agents on rocks and minerals, such as acid precipitations that cause a massive descent of the metal from mountains to surface waters. Groundwater aluminium concentrations are generally less than those of the shallow waters. Unpolluted seawaters, instead, contain an amount of aluminium between 0.1 and 20 μg L^{-1}, which originates primarily from clay sediments on the seabed or in suspension.

This level is almost the same of that found in clear rivers and lakes with a concentration highly variable and dependent from pH [13]. The soluble species of aluminium include the $Al(H_2O)_6^{3+}$ free solvated cation, the Al^{3+}-OH^-,-F^- inorganic complexes and those bound to the dissolved organic matter (DOM), which concentrations seasonally change for the influence of soil acidification and microbial nitrification [18].

The increase in acid rain not only affects the distribution of aluminium in natural waters, but also in soils, where the Al^{3+} concentration is about 7.1% of the total composition. This depends almost exclusively by natural factors that increase the soil acidity and lead aluminium to complex with fluoride, phosphate and sulfate. The Al^{3+} hydrolytic species in soils are less than 1% of its total content, since it is present in significant quantities as fluoride, citrate, oxalate, humic and fulvic acids complexes. The last two mentioned are considered the main ligands in natural waters, without which the metal is present at acid pH values, lower than 4.5. Its distribution between soils and waters strictly depends on the reactions with ligands (included OH^-) and the different functional groups of clay and humic acids. The concentration of the exchangeable metal may achieve the order of mg kg^{-1}.

Besides the distribution of aluminium in natural waters and soils, it is necessary to make some notes about its presence in the atmosphere as well. It is due mainly to human sources, such as coal combustion, pumice, wastes burning, chalk and cement works. In urban and rural areas aluminium concentrations are in the ranges 0.1 - 5 and 0.05 - 0.5 μg m^{-3}, respectively, deriving principally from fossil fuel combustion by motor vehicles and industries. Aluminium is also found in coffee and tea plants cultivated on acid soils, where the metal is highly available. It is well known that about 25 plant families, mainly tropical and subtropical shrubs, bioaccumulate aluminium concentrations over 1g Kg^{-1} in their leaves. Also some algae, bryophytes, aquatic mosses and animals assimilate aluminium. Its accumulation in fishes increases with the pH decrease and its accumulation is principally in grills and in mucous. Moreover, older fishes show a lower metal concentration than larvae.

1.4 Sources of exposure and metabolism in humans

Aluminium is not an essential metal in biological processes, even if it is one of the main naturally occurring element on the terrestrial crest, as mentioned above. Probably, its exclusion from any metabolic pathway is due to its very low availability in nature as free metal, especially because of the formation of hydroxyl-alumino silicate complexes that reduce its environmental and biological distribution [19, 20]. Dietary is considered the main intake source of aluminium in humans, in absence of occupational subjection and chronic use of Al - containing medical preparations. Its oral absorption from drinking water and food is about 0.3% and 0.1%, respectively and, in particular, its daily exposure from aliments ranges from 3

to 10 mg [13, 17]. The metal concentration in nourishments is highly variable and dependent on different factors, such as methods of preparation, cooking and storage [8]. In fruit juice and carbonated beverage, the aluminium content is elevated; for example, in cola and several other drinks kept in lacquered aluminium cans, its estimated amount ranges between 0.10 and 0.61 mg L^{-1} [13]. The product provenance plays also a key role in the aluminium bioavailability from aliments. Food plants cultivate in acid soils present a highest aluminium concentration, such as tea and coffee (1 - 6 mg L^{-1} and 0.005 - 0.015 mg L^{-1}, respectively), whose infusions were recognized as the major sources of organism exposure [17]. Therefore, also environmental factors can cause an increase in the bioavailability of the metal, considering that its presence in soil from acid rains leads to its introduction into the food chain. Moreover, aluminium can be assimilated by inhalation through dusts in polluted environment from people living near industrial emission sources and from manufacturing and welding metal workers. The aluminium intake may be also increased by antiperspirants with transdermal absorption and by medicinal exposure, as vaccine injections, especially in children [8, 13, 17, 20]. Another possible source of accumulation is the use of tobacco, cannabis and drugs, such as heroin and cocaine, together vaporized on aluminum foils [8, 17]. The primary route of systemic aluminium intake is the assimilation into the gastrointestinal tract, in particular in the distal intestine, although the mechanism of absorption is not yet well known [17, 20]. Probably, most of the swallowed aluminium species are dissolved in the acidic stomach and, once reached the duodenum, soluble hydrated aluminium, $Al(H_2O)_6^{3+}$, precipitates as hydroxide or hydroxyphosphate, hindering the absorption [1]. Most of times, however, it does not happen, because the intake processes are influenced by the physiological acid environment of the digestive system, which can make the metal free from complexes formed in intestinal mucosa. Other different local factors can affect the absorption mode, such as food quality and the possibility of the metal to bind organic compounds present in aliments, making the metal available for assimilation. The dietary presence of both fatty acids and chelating agents, such as, gluconate, ascorbate, lactate, malate, oxalate and citrate, can increase, in fact, the aluminium absorption by solubilizing more of its salts [1]. Citric acid is also the main responsible of the aluminum transition from the intestinal barrier into the blood and it is recognized as the primary small aluminium binder into the plasma [16]. In particular, aluminium shows towards citrate a higher binding ability than Ca^{2+}; this competition in serum transport can lead to calcium metabolism diseases [17]. In blood and other tissue fluids, aluminium is also bound to other organic compounds, such as the transferrin protein, which is an important biomolecule involved in the iron transport. It can sequester about 90% of the free aluminium in serum, exploiting the iron - binding sites. It occurs only because transferrin has an iron deficiency of about 50 μM under physiological conditions. Aluminium, in fact,

cannot compete with iron replacing it, since the bond of Fe^{3+} with this protein is much stronger [17]. Lastly, aluminium can enter into the brain through the blood route or, directly, for inhalation from nasal cavities. The mechanisms by which the metal can cross membrane barriers are not yet well known. It was reported that most of aluminium in brain extracellular fluids is binding to citrate and only a small part to the transferrin [17]. However, the estimated aluminium amount in human whole-body is about 80 mg; normally for a healthy adult, taking into account the organ weights, about 60, 25, 10, 3 and < 1 % of the total Al amount in body is present in bone, lung, muscle and liver and blood, respectively [13]. Skeletal system, in fact, represents the major deposition site and a long-term reserve into the human body. The intake in bones starts with the metal transfer from citrate and transferrin, flowing in the blood, to the skeletal surfaces, where it is carried to the osteoclasts and later to the macrophages, which act as a temporary store releasing, then, the metal in the blood stream again. The main pathway of elimination is constituted by the kidneys, which, under physiological health conditions, excrete all the total aluminium absorbed with an urine concentration between 0.68 and 8 μg L^{-1} [8, 17]. Only ≈ 2 % is eliminated *via* bile [8]. In the following scheme (Fig 1.1) are outlined the different possible routes of aluminium entering in the human organism.

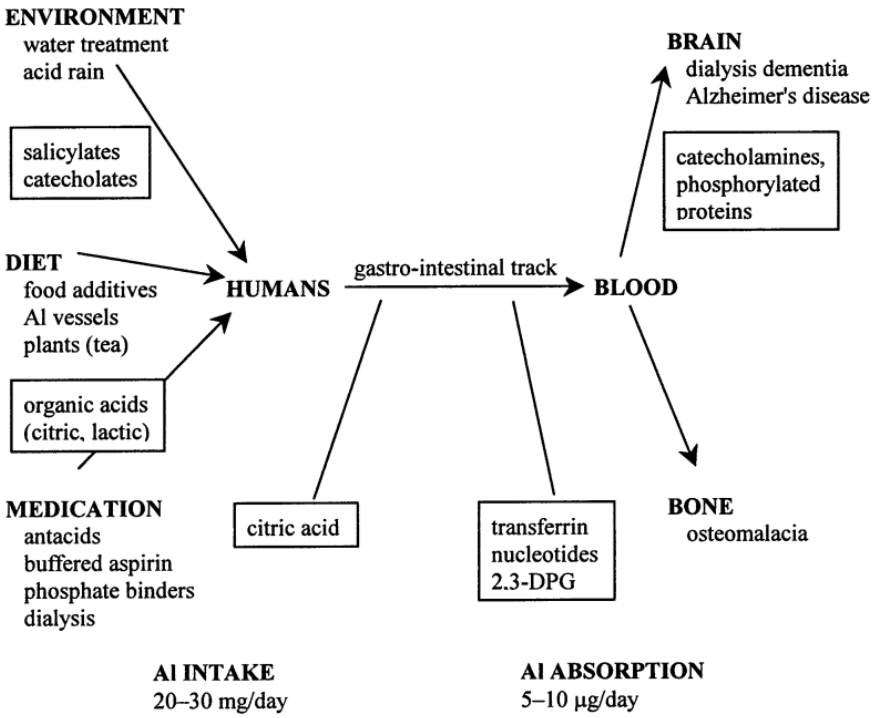

Fig. 1.1 Different patways of Al(III) entering in human body (from Ref. [15]).

1.5 Toxicological aspects and health effects

As underlined in the previous sections, there is no evidence of the aluminium essentiality in the biological processes, resulting, therefore, toxic for plants, animals and human beings. In all living organisms, aluminium is responsible of the enhanced production of reactive oxygen species, leading to an oxidative damage, which causes cell death, although the exact mechanism is not clear [8, 21].

This metal cation represents a potential threat for all people, which have to deal with its bioavailability increase from the environmental or occupational sources and all the patients who swallow its high doses derived from many drugs, in particular those affected by renal or peptic ulcer diseases [22]. Although in ordinary healthy conditions aluminium accumulated in human tissues is eliminated by kidneys, a high aluminium content in the skeletal system is observed in patients affected by renal pathologies, leading to osteomalacia and an adynamic bone disease. In people with chronic nephrologic disorders, who have undergone hemodialysis for a long time, microcytic anemia and dialysis encephalopathy syndrome are also observed [23]. In addition, aluminium is considered a neurotoxin and seems to have a tie with neurodegenerative disorders, such as Alzheimer and Parkinson's diseases, Gulf War syndrome, Amyotrophic Lateral Sclerosis (ALS) and dementia, though this correlation remains still controversial [8, 24]. The aluminium toxic effects are primary due to the homeostasis damaging of metals, such as iron, calcium and magnesium, of which aluminium imitates the actions, leading to biological alterations. The deposition of insoluble aluminium species in some tissues or the interaction with proteins, lipids or nucleotides are also causes of structural and functional disorders [8, 24]. Being a hard metal cation, aluminium tends to bind oxygen donor-ligands, promoting a strong interaction with phosphate groups, which are found in nucleosides, DNA and RNA, affecting the gene expression and metabolism processes.

With regard to the flora and fauna ground, the detrimental effects of this cation include the inhibition of the plant growth, the reduction and the alteration of the reproduction in aquatic animals, including invertebrates. Aquatic plants show a greater tolerance towards aluminium concentrations than fishes and other organisms, although it results dangerous for their growth.

Terrestrial shrubs and trees show highest absorbed aluminum amounts because of the soil contamination and its lower pH (detrimental effects are more common in grounds with pH < 5) [13]. As it is well known, the aluminium toxicity is attributed to the soluble monomeric and polymeric aluminium species. The target sites comprehend the plasma membrane and cell walls with an interaction that involves, probably, carboxyl and phosphate groups. $Al(OH)^{2+}$ and $Al(OH)_2^{+}$ are likely the most detrimental species for fish, which show a more sensitivity to the aluminium toxicity than invertebrate aquatic organisms. For amphibians aluminium

lethal levels occur from 0.15 mg L^{-1} [13]. The aluminium accumulation in aquatic and terrestrial environmental provides a route of entry into the whole food chain.

1.6 Applications

Aluminium is widely used in different industrial fields for its particular properties, such as brightness, resistance, high malleability and ductility, electrical and thermal capacity. Many of its alloys have good mechanical and stretching strength. Moreover, the ability of alloys to withstand corrosion in a wide range of pH (from 4.5 to 8.5), through the formation of an outward aluminium oxide film that blocks further oxidation, makes them of particular interest for numerous applications. Alloys with Mg, Cu, Mn, and Zn improve its mechanical properties, hardness especially. Its use is mainly exploited in building materials, automotive, aeronautic or naval transportation, space industry, containers and packaging. Aluminium compounds, such as $Al(OH)_3$, alumina and alum, are used in many technological processes and in the manufacturing of consumer goods. In particular, glass, ceramics, abrasive, furnace linings, wood preservation, waterproofing textiles, rubbers, adhesives, cosmetics and polishes are only a small part of the wide range of the products in which it is employed. Alum is used to control algal blooms in lake and to reduce elevated outflow winter phosphorus concentrations in a municipal wastewater treatment wetland, thus improving the water quality [13, 25]. Since Roman time, aluminium salts are added to drinking water to improve its appearance, in particular, to prevent its turbidity, acting as coagulant agent. This is due to the formation of $Al(OH)_3$ insoluble species, which lead to the absorption of turbidity [25]. Also in some foods, such as strawberries and cherries, aluminium is used as additive to make their aspect better [25]. Besides, it is present in bakery products as leavening agent (acidic sodium aluminium phosphate, E541) and nondairy creamers (sodium silicoaluminate, E554) [13].
Aluminium chlorohydrate, together with alum, is applied in antiperspirants which produce the $Al(OH)_3$ species on the skin, obstructing the sweat glands pores. Many deodorants stone are made principally of alum [13]. In addition to its applications in cosmetics, aluminium is widely employed also for pharmaceutical purposes. The topic medical usages of aluminium are many, such as antiseptic, astringent, antacid, styptic agents. It is also found in dental rinses and toothpastes to minimize dentinal hypersensitivity, in abrasive and in some acne cleaning preparations, in creams and ointments for dermatitis, insect stings or bites and sun protection. It is employed also as antibacterial to heal athlete's foot and as internal medicaments, which allow exploiting the adsorptive capacity of its compounds, as in antacids, vaccines and antibiotics [12, 13, 17]. Patients on dialysis are treat with oral aluminium hydroxide in order to reduce the serum phosphate amount [12].

Chapter 2

Ligands

2.1 General aspects

In the last decades, significant attention was focused to the Al^{3+} aqueous speciation, because of its tendency to form quite stable species with several inorganic and organic ligands [6, 26]. Due to its hard character, as previously underlined, Al^{3+} preferably binds hard Lewis bases, such as hydroxides, phosphates, sulphates, carboxylates, alcoholates [5-7, 27]. The most stable complexes formed by Al^{3+} are those involving multidentate ligands containing O-donor groups [5, 7] . Accordingly, the Al^{3+} speciation in the presence of several ligands, both having only O-donor groups and also having other functional groups, was studied.
The ligands under study can be classified in:

1. Carboxylic acids, or O-donor ligands;
2. Thiocarboxylic acids or S-, O-donor ligands;
3. Amino acids, or N-, O-donor ligands;
4. Oligophosphate (O-donor ligands) and other inorganic ligands;
5. Nucleotides.

The choice of studying these molecules was made on the basis of their importance in the biological and environmental systems and the lack of literature data regarding their interactions with the aluminium.

2.2 Carboxylic acids

As already mentioned above, aluminium, being a hard metal cation, shows a strong affinity towards O-donor ligands, forming quite stable complexes with inorganic and organic compounds, such as carboxylates [5, 7, 13, 15, 28]. Complex species, formed by the Al^{3+} interaction with these ligands, are of particular importance in aluminium biospeciation. Some of them, such as lactic, malic and malonic acids, are present in human body tissues and

biological fluids and may form stable complexes with Al^{3+}, able to cross biological membranes, thus promoting bioaccumulation [13, 15]. Moreover, also in environmental field, carboxylates are of great interest, because of their large distribution in natural waters [29]. The binding ability of organic O-donor compounds towards Al^{3+}, organic ligands, was studied. These molecules are shown below in Fig. 2.1.

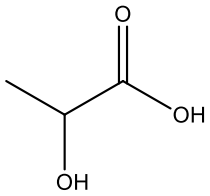

Lactic acid (*lac*)

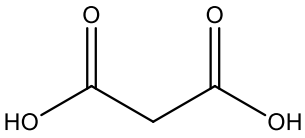

1,3-propanedicarboxylic acid or malonic acid (*mal*)

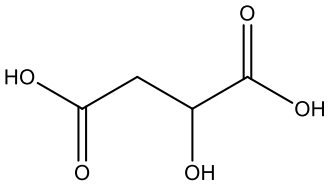

2-Hydroxybutanedioic acid or L-malic acid (*mala*)

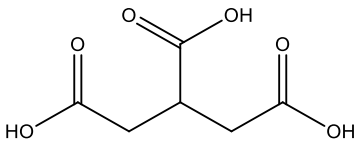

Propane-1,2,3-tricarboxylic acid or

tricarballylic acid (*tca*)

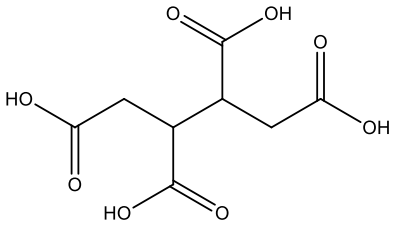

Butane-1,2,3,4-tetracarboxylic acid (*btc*)

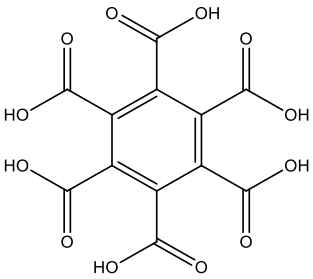

Benzene-1,2,3,4,5,6-hexacarboxylic acid or mellitic acid (*mlt*)

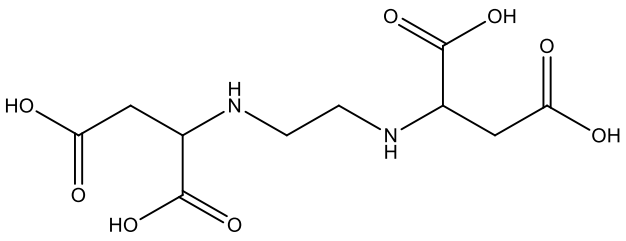

S,S-Ethylenediamine-N,N′-disuccinic acid (*EDDS*)

Fig. 2.1 Carboxylic acid under study.

Lactic acid (*lac*) plays a significant role in various biochemical processes. It is an anaerobic metabolism product, detrimental for the cells, whose accumulation in blood is correlated to the muscular effort. Its hematic concentration at rest is usually 1-2 mmol L^{-1}, but it can increase to over 20 mmol L^{-1} during an intense physical effort and reach up to 25 mmol L^{-1} later [30]. It is the simplest 2-hydroxycarboxylic acid with a chiral carbon and in nature it occurs in two enantiomeric forms: S, R or a mixture of them [31]. Because of its pK_a = 3.1 a T = 298.15 K, it is present almost entirely as lactate ion at physiological pH values. This hydroxocarboxylic compound is widely used in food industry, as a preservative, acidifying, aroma, pH buffer or antibacterial element. It is also used in many other applications, such as in chemical industry, including polymer technology, for the production of biodegradable plastics from renewable resources. It finds further employment in pharmaceutical field for cosmetics and topical preparations, in order to adjust acidity and prevent infections [31].

Malonic acid (*mal*), unlike the previous compound, is a dicarboxylic acid, whose esters and salts are named malonates. Its ionic form shows an inhibitory capacity towards the enzyme succinate dehydrogenase [32]. As well as being a precursor of many chemical compounds, it is widely used in the chemical industry to obtain resins, in alimentary field to control the acidity of foods, in pharmaceutical preparations to use it as excipient and as starting molecule to synthetize barbituric drugs, in cosmetic applications to obtain aromas and fragrances and in medicine to gain surgical adhesive.

Another dicarboxylic ligand, malic acid (*mala*), was taken into account, which differs from the precedent molecule for the presence of a hydroxyl group. It is a naturally occurring organic compound in fruit and vegetables. It is responsible of the sourness of green apples and other fruits. The food and beverage industries make an extensive use of this compound for its tartness. It is present in grapes and in most wines with concentrations that sometimes reach 5 g/L, giving to these a bitter taste [33]. From the chemical point of view, malic acid has two stereoisomers (L- and D-enantiomers), but only the L-isomer naturally occurs. Its anion form, well known as malate, acts as intermediate in the citric acid cycle. Together with succinate, malate is considered one of the most efficient antidote against acute aluminium toxicity in mice [34]. Tricarballylic acid (*tca*) is a powerful inhibitor of aconitase, a specific enzyme involved in the stereo-specific isomerization of citrate in iso-citrate in the Krebs cycle [35]. From the chemical point of view, it differs from citrate only for the hydroxyl group lack.

In this study, ligands with more O-donor groups, such as butane-*1,2,3,4*-tetracarboxylic acid (*btc*), mellitic acid (*mlt*) and ethylenediamine-N,N'-disuccinic acid (*EDDS*) were considered.

Butane-*1,2,3,4*-tetracarboxylic acid (*btc*), is a potential substitute of formaldehyde-relasing crosslinking agents in the permanent press fabrication of cotton and other fabrics. It was

considered a possible detrimental compound for the human development, although there are not literature data [36].

Mellitic acid (*mlt*) is a hexacarboxylic acid, also known as benzene-hexacarboxylic acid, discovered for the first time in the mineral mellite, which is its aluminium salt. This ligand is the most representative of the benzene - polycarboxylates class, which possesses interesting features such as, high charge density, high negative charge at pH > 6 and the presence in natural fluids as organic matter degradation products, with the possibility of forming several complexes species containing organic or inorganic cations [37, 38].

Lastly, ethylenediamine-N,N'-disuccinic acid, well known as *EDDS*, is an aminopolycarboxylic biodegradable compound used as strong chelating agent, with or without *EDTA* (Ethylenediaminetetraacetic acid), in the environmental remediation from heavy metal pollution [39]. However, this chelating action is only displayed by the (S,S) stereoisomer. *EDDS*, in fact, present two chiral centers, thus existing as the (S,S) and (R,R) enantiomeric form and as achiral meso (R,S) isomer [40]. Nowadays, S,S-*EDDS* is used in laundry detergent as tri-sodium salt, in hair products, in photographic development stage, in pulp bleaching, in many agricultural applications and for the metal removal in waste water and soil washing treatment [41].

2.3 Thiocarboxylic acids

Among all the different ligand classes under study, thiocarboxylic ligands were chosen for the presence of the carboxylic and sulphidrilic groups on their molecules. In particular, the investigated sulphur-containing ligands are shown in Fig 2.2.

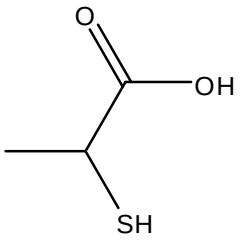

2-mercaptopropanoic acid or thiolactic acid (*tla*)

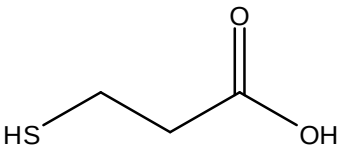

3-mercaptopropanoic acid (*mpa*)

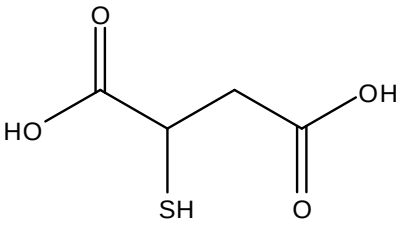

2-mercaptosuccinic acid or thiomalic acid (*tma*)

Fig. 2.2 Thiocarboxylic acids under study.

As it is well known, the most likely Al^{3+} binding sites are O-donors, such as carboxylates; amines and thiolates have not a good affinity towards Al^{3+}. However, if N- and S-donor

groups are in a chelating position with respect to an O-donor group, their binding ability may considerably increase [5]. Multidentate ligands with O-donor groups bind Al^{3+} with an affinity that increases with the number and the basicity of donor groups [28].
In general, these molecules are of large interest, because of thiols are ligands naturally present in the environment and they can be formed in many pathways. Indeed, sulphur-containing sites are present in fulvic and humic acids, as they derive mostly from sulphur containing amino acids, sulphate esters of polysaccharides, antibiotics and some vitamins [42]. Moreover, as in marine sediment interstitial waters and seawaters their concentration commonly change from nanomolar to millimolar [43].
Thiocarboxylic ligands are also important from a biological point of view. For example, thiomalic acid can be used as antidote against mercury, arsenic and cadmium poisoning [44].
Generally, the clinical chelation therapy for the mercury intoxication employes thiol compounds as dimercaptosuccinic acid and dimercaptopropionic sulphonate. Since they have two thio-groups available for chelate ring formation, these ligands are of great interest as sequestering agents for several metal ions [45].
Thiolactic acid is used as an antiarthritic and anti-rheumatic intramuscular, intravenous or oral drug [46] and lately it was employed in desfoliant-skin treatments known also as peeling [47].
3-mercaptopropanoic acid, structural isomer of thiolactic acid, is one of the main material used for the synthesis of PVC stabilizers. It is also employed in food packaging and personal care products. Recently, it have been found that this compound can act as β-oxidation inhibitor, while 2-mercaptopropanoic acid has no relevant effect on this pathway [48]. It can also lower the γ- butirric acid concentration in brain, causing convulsions in mice [49].

2.4 Amino acids

Amino acids are organic compounds constituted by an amino and a carboxylic group linked to a specific organic substituent *R*, known as *side chain*.
In particular, the term "*amino acid*" is often used to refer specifically to a natural molecule where the amino and carboxylic groups are attached to the same carbon atom of the chain, the first one, named also alpha-carbon (see Fig. 2.3). They can be classified according to the functional group position (α-, β-, γ-, δ-amino acids), the side chain type (aliphatic, aromatic containing sulphur or hydroxyl groups) and their polarity. Because of the carboxylic group acidity ($pK_a \approx 2.5$) and the basicity of the amino group ($pK_a \approx 9.4$), they are considered weak polyprotic acids. The presence of both groups in these compounds leads to the formation in aqueous solutions of the zwitterion form, that is a molecule with total neutral charge, in which the amino group is protonated, $-NH_3^+$, and the carboxylic group is deprotonated, $-COO^-$.

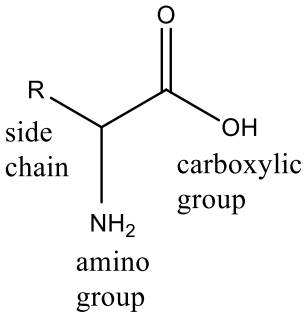

Fig. 2.3 General structure of an amino acid.

Amino acids have great importance in biochemistry, since they are constituent elements of proteins, precursors of hormones and molecules with a significant physiologic role, *i.e.* neurotransmitter.

In this thesis, the attention is focused on two α-amino acids, glycine and cysteine and the tranexamic acid, a synthetic molecule structurally ascribable to the lysine (see Fig. 2.4). The most common essential amino acids, namely ones that can be introduced into the body only by diet, are glycine-like compounds.

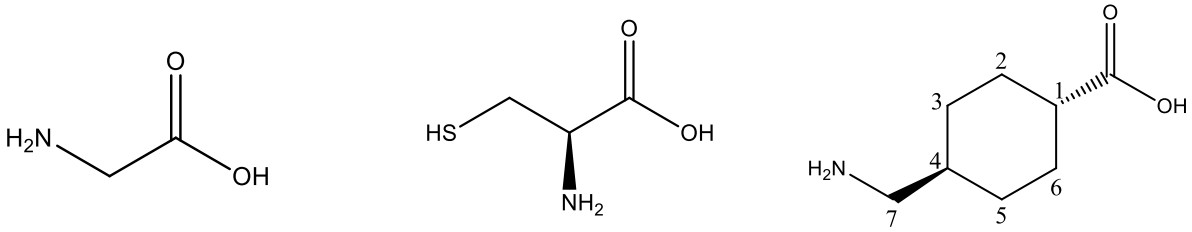

Glycine (*Gly*) L-Cysteine (*Cys*) Tranexamic acid (*tranex*)

Fig. 2.4 amino acids under study.

The study on these amino acids was carried out, because biomolecules with the same potential binding sites may be involved in the transport and uptake of aluminium. Furthermore, these ones can be considered model compounds for the binding ability study of aluminium with larger biomolecules, such as proteins.

Glycine (*Gly*) is the simplest amino acid and its side chain is represented by a single hydrogen atom. It is classified as non-essential amino acid, because it is synthesized in the body from serine. This amino acid is a basic element of the collagen, a fundamental protein for the formation of tendons and muscles. Indeed, it is present in the skin and connective tissue in large amount; it helps to repair the damages cutis, promoting its healing.

Moreover, glycine is an important regulator of nerve impulses, especially in the inhibition of the central nervous system and the spinal cord. It participates to the synthesis of creatine into liver, kidney and pancreas cellules and promotes the production of antibodies and immunoglobulins. It is also used for medical purposes, such as diuretics and in the treatment of schizophrenia and some musculoskeletal disorders [50].

Among the amino acids, cysteine (*Cys*) is the only one naturally occurring sulfur containing. For the adult human body it is not an essential amino acid, as it can be obtained from methionine under normal physiological condition.

It is widely diffused in many high-protein foods such as sausage meat, chicken, eggs, milk, and yogurt. Its presence in biological fluids demonstrates its involvement in many life processes. In blood plasma models it is present at the highest concentration, with a value ≥ 100 μmol L^{-1} [51]. Furthermore, in addition to glutamate and glycine, it is essential for glutathione biosynthesis and together with its derivatives it represents an active site in several peptides and proteins [52]. Two -SH groups, located in an oxidizing environment, may form bonds by means of a disulphide bridge (-S-S-), allowing to bind together two cysteine molecules in different point of a polypeptide chain or between two different peptides. In this way the ternary and quaternary structure of the proteins, from which the biological action depends, is shaped. It is recognized that cysteine can coordinate metal cations in several proteins and metal-enzymes through its -SH and -NH_2 sites, which may increase its binding ability [5].

Together these two amino acids, the binding ability of the tranexamic acid (*tranex*) towards aluminium was evaluated. This compound is a synthetic molecule used in medicine for the blood loss, especially in surgery and dentistry. It is included in the World Health Organization list of essential drugs. In addition to the anti-haemorrhagic capacity, it shows anti-inflammatory and antiallergic activity [53].

2.5 Oligophosphate ligands

Oligophosphate ligands are very important molecules in nature. They play a crucial role in many natural fluids, thus arousing a great interest in speciation studies. Since these compounds are present in human organisms and can be considered as models for largest biomolecules containing phosphate groups, the study of their interaction with aluminium is very significant. These compounds are, indeed, building blocks of biomolecules, such as RNA, DNA and nucleosides (ATP, ADP, AMP), which will be discussed in the next paragraph.

In this thesis, particular attention was addressed to four phosphate ligands, namely phosphate (PO_4^{3-}), pyrophosphate (*PP*), tripolyphosphate (*TPP*), shown in Fig 2.5, and

hexametaphosphate ions (*HMP*), of which the structure is not displayed, as it is a mixture of oligophosphates, both linear and cyclic.

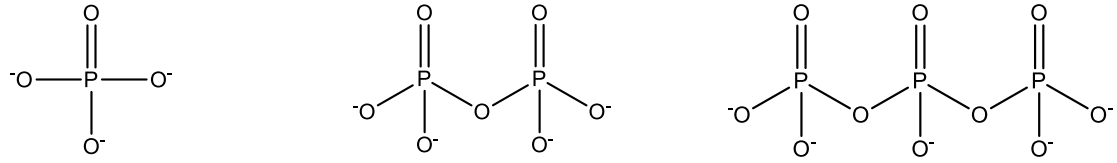

Phosphate (PO_4^{3-}) Pyrophosphate (*PP*) tri-polyphosphate (*TPP*)

Fig. 2.5 Oligophosphate under study.

In general, in seawater, PO_4^{3-} achieves a maximum amount of concentration at 1000 m depth in correspondence of the O_2 minimum one, whilst in the surface it is very low, because of the phytoplankton and other organism decomposition [54]. In biological systems, it plays a key role as buffering agent at physiological pH, together with HPO_4^{2-} and $H_2PO_4^-$ ions and in blood serum its concentration ranges from 0.07 to 0.3 mol L^{-1}[55].

In biochemistry, pyrophosphate, *PP*, is formed by the hydrolysis of ATP into AMP. It is the simplest condensed phosphate anion, formed by the binding of two orthophosphate ions. *PP* is present in synovial fluid, blood plasma, and urine at levels sufficient to block the accumulation of calcium salts in a body tissue [56].

Tripolyphosphate (*TPP*), instead, which differs from the previous ligand from a phosphate tetrahedral unit, is a food additive, known with the E number E451. It is especially used as preservative of meat, fish, poultry and animal fodders. In others industrial fields, it finds many applications, such as flame retardant, fermentation, anticorrosion pigments, antifreeze and textile manufactures [57]. *TPP* is also employed in toothpastes and detergents to improve its action [58, 59] and as a sequestrant of Mg^{2+} and Ca^{2+} cations to reduce water hardness [60].

Another ligand of significant interest for the environmental applications, chosen for the interaction studies with aluminium, is the Sodium Hexametaphosphate (*HMP)*. This compound is a hexamer, whose commercial product is typically a mixture of polymeric metaphosphate. It is usually employed in the hard water treatment, in food industry as additive, in detergents as sequestrant of calcium cation and in dentistry as anti-tartar ingredient in toothpastes [60].

2.6 Other inorganic ligands

Together with the previous class of compounds, the attention was also focused on other two inorganic ligands: carbonate and fluoride ions.

Carbonate is one of the main components of natural fluids and sedimentary rocks, made up principally of $CaCO_3$, such as calcite and dolomite. In natural waters (2.7 mmol L^{-1}, in seawater 35) it exists, together with bicarbonate, HCO_3^-, and carbon dioxide, CO_2, in a dynamic equilibrium, which is of great importance, since it regulates the seawater pH and control the CO_2 circulation in the atmosphere and oceans. This buffer system is closely related to the natural water alkalinity, which can be influenced strongly by the dissolution (or precipitation) of carbonate rocks, especially when these minerals are in contact with groundwater or seawater [61]. CO_3^{2-} is also a very important constituent of biological fluids (its concentration in human plasma ranges between 24 and 27 meq L^{-1}), operating as a pH buffer in living organisms blood. Its salts, such as sodium and calcium carbonate, are widely used in the paper and alimentary industry as additive, identified as E500 and E170, respectively. Furthermore, Na_2CO_3 is employed in the glass and detergent manufacture.

Fluoride is the smallest and simplest anion, deriving from fluorine that can exist in aqueous solutions. In terms of charge and size, the fluoride ion is similar to the hydroxide ion. This ligand does not give hydrolysis under normal conditions and tends to form quite strong hydrogen bonds. As well as carbonate, it is one of the major components of natural waters with a concentrations of 0.7 mmol L^{-1} in seawater 35 [62]. Fluoride ion is naturally present in the environment as primary constituent of several minerals, such as fluorite, and in natural water in trace quantities. As a result of human activities, through industrial waste release, fertilizers and pesticides, an increase of this anion in both ground and surface waters, can occurs. It is also used for medical purpose, to promote healthy bone growth and to prevent dental caries [63].

2.7 Nucleotides

Nucleotides are organic molecules that form nucleic acids, DNA and RNA, polymeric biological macromolecules, essential for living organisms. These repeating units are featured by:

1) An azotate base (purine or pyrimidine);
2) A pentose sugar that forms a nucleoside together with nitrogen base;
3) A terminal phosphate group.

The general structure of nucleotides is depicted as follow in Fig 2.6.

The study of the aluminium interactions with these biological building blocks is essential for the knowledge of this metal cation effect in biological systems. In general, nucleotides contain three different aluminium - binding sites: a carbonyl or amino group, respectively O- and N-donors in the nucleic base, alcoholic or hydroxyl functions in the sugar moiety and phosphate groups in the mono-, di- or tri-phosphate sides. In this type of compounds, the first binding site for Al^{3+} is the terminal phosphate with pK ≈ 6 [15, 64].

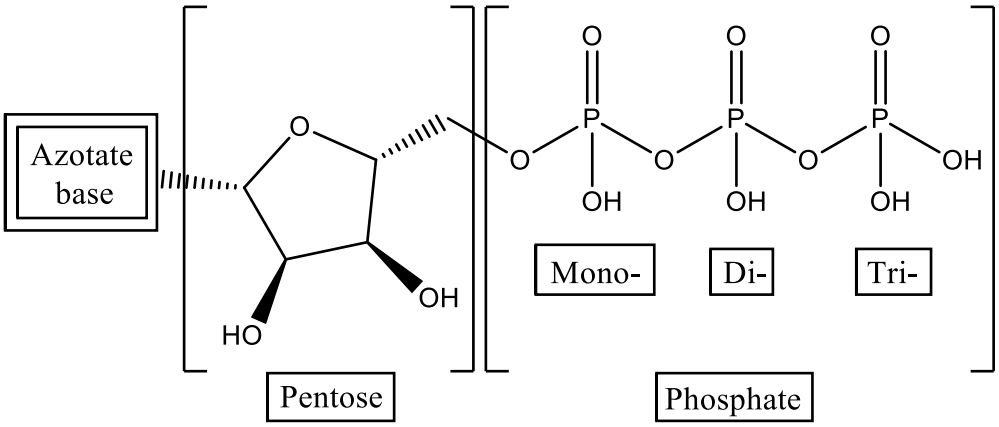

Fig 2.6 General structure of nucleotides.

Particular attention was given to three important nucleotides: adenosine-5'-tri-, di- and monophosphate, whose structures are shown in Fig 2.7.

The adenosine-5'-triphosphate, *ATP*, is a nucleotide formed by an adenine molecule as azotate base and a chain of three phosphate groups bound to the ribose sugar. It acts as coenzyme in cells with the main function of energy carrier in biological process [9]. The addition and the removal of the PO_4^{3-} functions inter-converts *ATP* into adenosine-5-di-, or monophosphate. This can be occur in metabolic processes that exploit *ATP* as energy source. It is continually recovered in the human body and, besides its role in energy metabolism, it is also found into nucleic acids by polymerases in the processes of DNA replication and transcription.

Almost all cellular reactions and biological processes in the organism that require energy, such as transmission of nerve impulses, muscle contraction, active transports through plasma membranes, protein synthesis and cell division, are fed by the conversion of *ATP* to *ADP*.

As mentioned previously, the adenosine-5-diphosphate (*ADP*), as well as the adenosine-5-monophosphate (*AMP*), are product deriving from the loss of a phosphate group from the *ATP*

and *ADP* respectively, with resulting energy release (*ATP* → *ADP* + PO_4^{3-} and *ADP* → *AMP* + PO_4^{3-}).

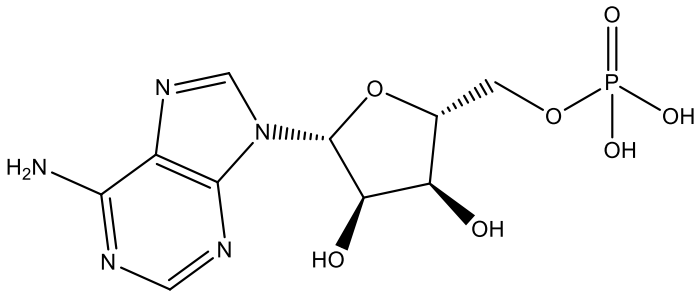

Adenosine-5'-monophosphate, *AMP*

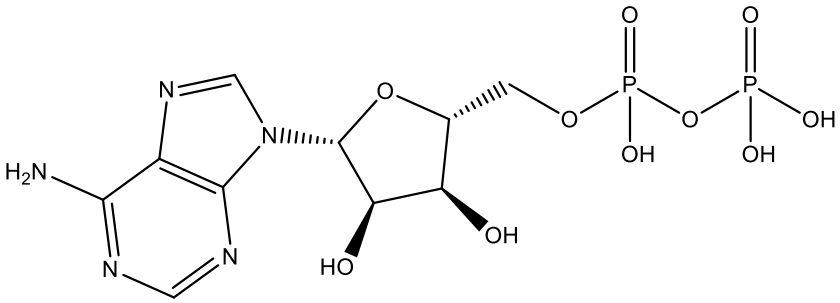

Adenosine-5'-diphosphate, *ADP*

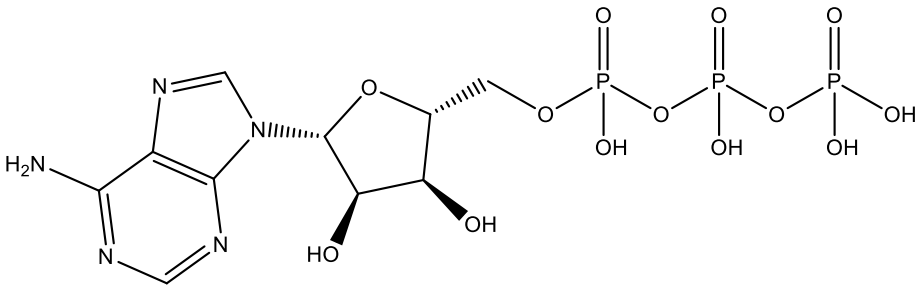

Adenosine-5'-triphosphate, *ATP*

Fig 2.7 Nucleotides under study.

It occurs with the help of an enzyme, known as ATPase, which can easily break the bonds between the different *ATP* phosphate groups into the cell. In general, the breaking of a bond among phosphate groups generates about 34 kJ mol^{-1} in energy. *ADP* is produced by an exergonic reaction and it is then used to produce *ATP* again with an endergonic reaction; this

occurs continually via mitochondrial aerobic respiration in humans, whilst in plants this happens through the photosynthesis [65].

AMP is a constituent of the RNA and can be assimilated to an ester of the phosphoric acid and the nucleoside adenosine. Besides the hydrolysis of an *ADP* phosphate group, it can be formed, starting from *ATP*, with the loss of an orthophosphate molecule or during the process of *ATP* synthesis by means of the combination of two *ADP* molecules in the presence of the enzyme adenylate kinase. This nucleotide exists in two isomers: a linear (*5'AMP*), inactive, and a cyclic (*3'-5'AMP* or *AMP* cyclic or *cAMP*), biologically active. Its main functions are the activation of the kinase proteins to regulate the calcium transmembrane passage through ionic channels and the regulation of the glucose metabolic process. Cyclic adenosine monophosphate (*cAMP)* plays also an important role in intracellular signaling, acting as mediator in the action of different hormones, such as serotonin, acetylcholine and prostaglandins, thus influencing several metabolic processes.

Chapter 3

Experimental section

Several analytical techniques were used in order to investigate the different systems under study.

In this chapter are described:

1) all the procedures for the preparation of each reagent;

2) each analytical technique used to perform the experimental measurements;

3) the calculation programs to elaborate the experimental data.

3.1 Chemicals

Aluminium solutions were prepared by weighing the Sigma-Aldrich product $AlCl_3 \cdot 6H_2O$ salt, having a purity ≥ 99 %. Its concentration was verified by a back-titration with a standard EDTA solution, using a standard $CuSO_4$ solution as titrant and NET (Eriochrome Black T) as indicator. All ligands, described in this thesis and purchased from different sellers, are summarized in table 3.1. They are of analytical grade and were used without any further purification. Their purity was checked potentiometrically by alkalimetric titrations (always > 99.5%, except *AMP*, 94%; *ADP*, 95%; *EDDS*, 80.5%; *HMP*, 96%). The effective purity was taken into account in the calculations of the concentration ligands.

For *HMP*, HPLC analysis showed that the ligand salt used was a mixture of various polyphosphates. For the calculation purposes this ligand was assumed to be tribasic [66]. Hydrochloric acid and sodium hydroxide solutions were prepared from concentrated Fluka ampoules and standardised using sodium carbonate and potassium biphtalate respectively, previously dried at 383.15 K. NaOH was stored in dark bottles and preserved by CO_2 through soda lime traps. Sodium chloride and sodium nitrate solutions were prepared by weighing the pure salt (Fluka, puriss.), pre-dried in an oven at 383.15 K. All solutions were prepared using ultrapure water (conductivity < 0.1 μS cm^{-1}) and grade A glassware.

Table 3.1 Ligands under study and their information

Ligands	Counter ion	Abbreviation or acronym used	Sellers
Lactic acid	-	*lac*	Fluka
1,3-propanedicarboxylic acid or malonic acid	-	*mal*	Fluka
2-Hydroxybutanedioic acid or L-malic acid	-	*mala*	Fluka
Propane-1,2,3-tricarboxylic acid or tricarballylic acid	-	*tca*	Fluka
Butane-1,2,3,4-tetracarboxylic acid	-	*btc*	Fluka
Benzene-1,2,3,4,5,6-hexacarboxylic acid or mellitic acid	-	*mlt*	Fluka
Ethylenediamine-N,N′-disuccinic acid	-	*EDDS*	[a]
2-mercaptopropanoic acid or thiolactic acid	-	*tla*	Sigma - Aldrich
3-mercaptopropanoic acid	-	*mpa*	Sigma - Aldrich
2-mercaptosuccinic acid or thiomalic acid	-	*tma*	Fluka
Glycine	-	*Gly*	Fluka
L-Cysteine	-	*Cys*	Fluka
Tranexamic acid	-	*tranex*	[a]
Carbonate	Na^+	CO_3^{2-}	Sigma - Aldrich
Fluoride	Na^+	F^-	Sigma - Aldrich
Phosphate	Na^+	PO_4^{3-}	Sigma - Aldrich
Pyrophosphate	Na^+	*PP*	Sigma - Aldrich
Tripolyphosphate	Na^+	*TPP*	Sigma - Aldrich
Hexametaphosphate	Na^+	*HMP*	[a]
Adenosine-5'-monophosphate	Na^+	*AMP*	Sigma - Aldrich
Adenosine-5'-diphosphate	Na^+	*ADP*	Sigma - Aldrich
Adenosine-5'-triphosphate	Na^+	*ATP*	Sigma - Aldrich

[a] Kindly provided by the Procter & Gamble Ltd.

3.2 Potentiometry

3.2.1 General aspects

Potentiometry is one of the most reliable analytical technique, whose application fields include acid - base, complexation, precipitation and redox titrations [2]. This analytical method allows to indirectly derive the concentration of a test substance, measuring the variation of the e.m.f., due to the addiction of a titrant, in an electrochemical cell under zero current conditions. The potential variation can be observed by placing two electrodes in the sample solution:

- the *external reference electrode*, characterized by a constant potential once ionic strength and temperature are fixed;
- the *indicator electrode*, also known as working electrode, whose potential depends on the concentration of a single ion. It is separated from the sample solution by a membrane, selectively permeable to the analyte under study [67, 68].

The above-mentioned potentiometric apparatus is shown in Fig 3.1.

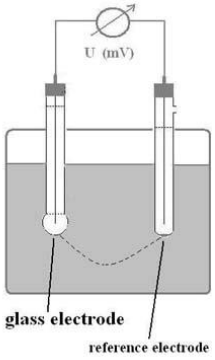

Fig. 3.1 Potentiometric cell.

In this thesis an ion-selective electrode ISE-H^+, also called *glass electrode* and specific to H^+ ions, was used for the determination of proton exchange in acid - base equilibria.
It consists of a thin membrane sensitive to the pH, welded at the bottom of a glass or polymer tube, in which is contained a known concentration of H^+ ions in a small volume of a buffer or a diluted hydrochloric acid solution, saturated with AgCl. A reference electrode Ag /AgCl can be present into the same cylindric probe [67]. In this case, it is a combined glass electrode, as shown in Fig. 3.2.

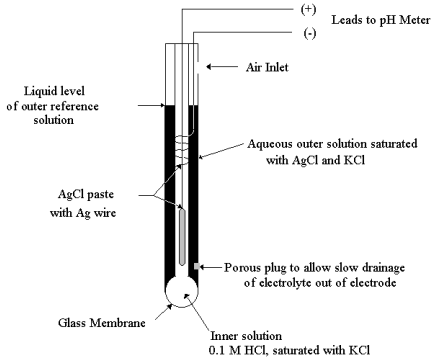

Fig. 3.2 Glass electrode

The potential difference observed during the potentiometric measurement is due to the difference of the H^+ ion activity between the internal and external solutions in contact with the membrane. Being constant the proton activity into the electrode, this variation is only function of the proton activity of the external solution under study. This dependence can be described by the following Nernst equation:

$$E = E' - s\log\frac{a_{H^+}(int)}{a_{H^+}(ext)} \tag{3.1}$$

where E is the measured potential, E' is the formal potential, and s (the nernstian slope up to pH ≈ 11) is 2.303RT/nF (59.16 and 29.58 mV for monovalent and divalent ions, respectively, at T = 298.15 K).

The formal potential, in addition to the standard electrode potential, is a sum of different contributions, such as the asymmetry potential and the junction potential. The first one is given by small differences between the two glass membrane surfaces, due to some abrasions caused by the use or determined at the time of fabrication [67]. This non-ideal behavior can be corrected by calibrating the same electrode with a titration of strong base or acid standard solutions. The junction potential is developed at the interface between the salt bridge and each half-cell, due to the different mobility of ions in solution and, in particular, to their different diffusion from a side of the junction surface, generating a charge separation and a potential as a consequence [67, 69].

This problem can be solved by utilizing a double junction electrode as reference, in which the salt bridge owns the same ionic medium of the analyte solution.

3.2.2 Instrumental equipment and procedure

The potentiometric measurements were carried out by using an automatic system consisting of a Metrohm model 809 titrando coupled with Metrohm 800 Dosino dispenser and equipped with a Metrohm 750 combined glass electrode, as shown in Fig. 3.3. This device was connected to a PC and the titrations were performed using the Metrohm TIAMO 2.2 software to control titrant delivery, data acquisition and e.m.f. stability. This software allows to manage some parameters necessary for a correct acquisition of experimental data, such as the interval time between two readings, max number of readings, max number of cycles needed to reach the stability of the e.m.f. readings, maximum and minimum addiction of titrant.
The estimated accuracy of the potentiometric system was ±0.15mV for e.m.f. and ±0.002 mL for titrant volume readings.

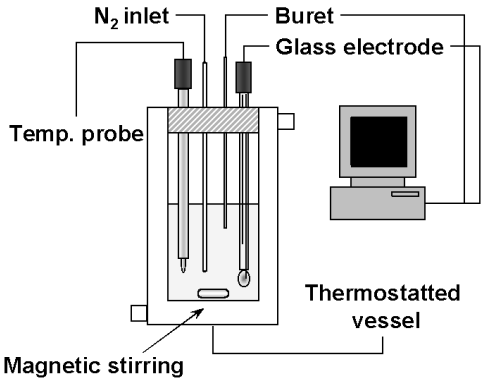

Fig. 3.3 Schematization of the instrumental apparatus used for the potentiometric titrations.

All measurements were performed into glass jacket cells thermostated at T = 298.15 ± 0.1 K (also T = 283.15 ± 0.1 K and T = 318.15 ± 0.1 K also, for lactic acid and Al^{3+}-lactate system) under magnetic stirring and bubbling pure N_2 through the solutions to avoid O_2 and CO_2 inside.
In this thesis only some ligand protonation constants were determined, since most of them were already studied in the past by the research group.
For these investigations, a volume of 25 mL containing the ligand under study and the ionic medium, in order to reach the prefixed ionic strength values, was titrated with standard NaOH. For the aluminium hydrolysis study, some solutions of 25 mL, containing the metal cation together with the ionic medium, NaCl, $NaNO_3$ or mixtures of $NaNO_3$ / NaCl, were titrated with standard NaOH. The study of aluminium-ligand interactions was performed by titrating with NaOH a solution of 25 mL in which different amounts of ligand and metal cation were dissolved, together with the ionic medium (NaCl or $NaNO_3$) and hydrochloric or

nitric acid when it was required. For each experiment, independent titrations of hydrochloric acid with sodium hydroxide standard solutions were performed in the same experimental conditions of temperature and ionic strength as the systems under study, in order to determine the formal electrode potential. The details of the experimental conditions used are shown in Tables 3.2 - 3.3.

Table 3.2 Experimental conditions of aluminium hydrolysis by potentiometric investigations, at T = 298.15 K

C_{Al} [a)]	Ionic medium	C_{Cl} [a)]	C_{NO3} [a)]	I [a)]	n[b)]
10-20	NaCl	0.11	—	0.1	3
10-20		1.02	—	1	4
10-20	$NaNO_3$	—	0.16	0.1	4
10-20		—	1.03	1	3
5-20	NaCl / $NaNO_3$	0.26	0.28	0.5	6
5-20		0.26	0.76	1	6
5-20		0.75	0.27	1	6
20		0.50	0.55	1	2

[a)] mol L^{-1}; [b)] number of titrations.

Table 3.3 Experimental conditions of all the investigated systems by potentiometry, at $0.15 < I$ / mol $L^{-1} < 1$ and $T = 298.15$ K

System	c_M [a]	c_L [a]	M/L ratio	Ionic Medium	pH range	n [b]
H^+-*lac*	—	10.0	—	NaCl	2.0 - 11.0	14
H^+-CO_3^{2-}	—	5.0	—	NaCl	2.0 - 11.0	6
H^+-*AMP*	—	2.0	—	NaCl	2.0 - 11.0	2
H^+-*ADP*	—	2.0	—	NaCl	2.0 - 11.0	2
Al^{3+}-*lac*	4.0 - 7.0	6.0 - 15.0	0.33 - 1.0	NaCl	2.0 - 4.0	48
Al^{3+}-*lac*/F^-	1.0 - 2.0	6.0 - 12.0 / 1.5 - 3.0	0.05 - 0.11	NaCl	2.0 - 5.5	9
Al^{3+}-*mal*	1.0 - 2.0	4.5 - 8	0.2 - 0.44	NaCl	2.0 - 6.5	12
Al^{3+}-*mala*	1.0 - 2.0	4.5 - 8	0.2 - 0.44	NaCl	2.0 - 6.9	12
Al^{3+}-*tca*	1.0 - 2.0	4.5 - 8	0.2 - 0.44	NaCl	2.0 - 4.9	12
Al^{3+}-*btc*	1.0 - 2.0	4.5 - 8	0.2 - 0.44	NaCl	2.0 - 4.9	12
Al^{3+}-*mlt*	0.75 - 1.0	2.25 - 8	0.1 - 0.33	NaCl	2.0 - 4.9	12
Al^{3+}-*EDDS*	0.5 - 0.8	0.8 - 1.0	0.5 - 2.0	NaCl	2.0 - 10.0	12
Al^{3+}-*tla*	2.0 - 6.0	6.0 - 12.0	0.25 - 1.0	NaCl	2.0 - 5.0	24
Al^{3+}-*mpa*	2.0 - 6.0	6.0 - 12.0	0.25 - 1.0	NaCl	2.0 - 5.0	24
Al^{3+}-*tma*	2.0 - 6.0	6.0 - 12.0	0.25 - 1.0	NaCl	2.0 - 5.0	24
Al^{3+}-*Gly*	2.0 - 6.0	6.0 - 12.0	0.25 - 1.0	NaCl	2.0 - 4.5	24
Al^{3+}-*Cys*	2.0 - 6.0	6.0 - 12.0	0.25 - 1.0	NaCl	2.0 - 5.0	24
Al^{3+}-*tranex*	2.0 - 6.0	6.0 - 12.0	0.25 - 1.0	NaCl	2.0 - 5.0	24
Al^{3+}-CO_3^{2-}	0.6 - 1.0	1.7 - 4.0	0.25 - 0.55	NaCl	2.0 - 5.0	24
Al^{3+}-F^-/*lac*	1.0 - 2.0	1.5 -12.0	0.05 - 0.11	NaCl	2.0 - 5.5	9
Al^{3+}-PO_4^{3-}	1.0 - 4.0	5.0 - 12.0	0.17 - 0.33	NaCl	2.0 - 5.0	12
Al^{3+}-*PP*	0.5 - 3.0	1.0 - 6.0	0.2 - 1.0	NaCl	2.0 - 6.0	12
Al^{3+}-*TPP*	0.5 - 3.0	1.0 - 6.0	0.2 - 1.0	NaCl	2.0 - 8.0	12
Al^{3+}-*HMP*	1.0 - 2.0	1.0 - 6.0	0.2 - 1.0	$NaNO_3$	2.0 - 8.0	12
Al^{3+}-*AMP*	0.5 - 0.8	3.0 - 4.0	0.14 - 0.2	NaCl	2.0 - 5.0	4
Al^{3+}-*ADP*	0.5 - 2.0	2.0 - 4.0	0.2 - 0.5	NaCl	2.0 - 7.5	4
Al^{3+}-*ATP*	1.0 - 2.5	1.0 - 6.0	0.25 - 1.0	NaCl	2.0 -7.5	12

[a] mmol L^{-1}; [b] number of titrations.

3.3 UV - Vis Spectroscopy

3.3.1 General aspects

Spectroscopic techniques are based on the energy exchange that occurs between an incident electromagnetic radiation and the matter. In particular, UV - Vis spectroscopy deals the absorption phenomena of luminous radiations belonging to the visible (380 -780 nm) and near ultraviolet (200 -380 nm) spectral range. An electromagnetic radiation can be described as a particle, better known as photon, and like a wave consisting of an oscillating electric and magnetic field perpendicular to each other and to the direction of the radiation propagation. When an ultraviolet or visible photon is absorbed by a molecule, an increase of the absorbing species internal energy occurs, involving vibrational, rotational and electronic transitions from the ground state to those at higher energy, causing changes in the distribution of the molecule electron cloud. It can only happen if the incident photon energy and the ΔE between the fundamental state and the exited one are the same. The allowed transitions for this kind of spectroscopic technique are:

- $\sigma \rightarrow \sigma^*$
- $\pi \rightarrow \pi^*$
- $\pi \rightarrow \sigma^*$
- $n \rightarrow \pi^*$
- $n \rightarrow \sigma^*$

These ones are given by transition metals or molecules with double or triple bonds that are called chromophores.

Measuring the absorbed radiation intensity, it is possible to draw the analyte information and carry out qualitative or quantitative analysis. The results of this measurement can be expressed graphically by means of a spectrum, which is a diagram of the intensity of the radiation absorbed as a function of wavelength.

For qualitative analysis purposes, this one is compared with other spectra proposed by literature or collected in special databases. The quantitative determination is carried out, instead, on the basis of the *Lambert - Beer's law*, which correlates the intensity of the absorbed radiation to the analyte concentration and the thickness of the traversed medium.

When a molecule is struck by an incident radiation, the attenuation of the incident ray, due to the absorption by an analyte solution, can be explained as *Transmittance* (*T*):

$$T = I_1/I_0 \tag{3.2}$$

where I_0 is the intensity of the incident radiation and I_1 is the intensity of the transmitted radiation by the solution.
The absorbed radiation is more commonly measured as *Absorbance* (*A*) and it is related to the *Transmittance* (*T*) through the following relation:

$$A = \log 1/T = \log I_1/I_0 \tag{3.3}$$

By knowing *A*, it is possible to obtain the concentration of the absorbent species, thanks to *Lambert - Beer's law* which correlates these two ones.

$$A = \varepsilon\, b\, c \tag{3.4}$$

where:
ε = molar extinction coefficient (L mol^{-1} cm^{-1}), dependent on the wavelength of the absorbed radiation, on the solvent and chemical species that lead to the absorption;
b = thickness of the cell or optical path of the solution (cm), generally equal to 1 cm;
c = concentration of the absorbent species (mol L^{-1}) [67].

The *Lambert - Beer's law* is, however, a limit law, as it applies to dilute solutions, *i.e.* for concentrations ≤ 0.01 mol L^{-1}.
The spectrophotometric measurements can be also used to follow the course of a titration using a titrant or analyte chromophore, as in the research work reported in this thesis.

3.3.2 Instrumental equipment and procedure

Spectrophotometric measurements on Al^{3+}-ligands containing solutions have been carried out using a Varian Cary 50 UV - Vis spectrophotometer, equipped with an optical fiber probe, having a path length equal to 1 cm, able to investigate the ultraviolet and visible electromagnetic spectrum area and a Metrohm 750 combined glass electrode in order to register the pH values.
The optical fiber is a filament made of siliceous material or glass, suitable for the transmission of light pulses contained into a cable that allows the use over long distances. the medium used for the transmission of the signal is the light, which takes place thanks to the total internal reflection. So that it occurs, it is necessary that the transmitting fiber is coated with a material whose refractive index is lower than the one of the material with which the fiber was built.
The system is connected to a PC for the acquisition of the spectra and for the modification or setting of important parameters for the measurement (range of wavelengths, scanning speed, correction of the baseline).

Each experiment was carried out into the same glass jacket cells and apparatus described in the previous potentiometric equipment and procedure paragraph.

The experimental determinations of the complex species formation constants were performed on 25 mL of Al^{3+}-ligands containing solutions, by recording the absorption spectra by varying the potential, after the addition of known volumes of base titrant in a range of wavelengths between 220 and 280 nm. The metal and ligand concentrations used in the measurements at T = 298.15 K and I = 0.15 mol L^{-1}, using NaCl as supporting electrolyte, are shown in Table 3.4.

Table 3.4 Experimental conditions of all the investigated systems by UV - Vis spectrophotometry, at I = 0.15 mol L^{-1} and T = 298.15 K

System	c_M [a)]	c_L [a)]	C_M/C_L **ratio**	**Ionic Medium**	**pH range**	**Wavelength range**	**n** [b)]
Al^{3+}-*mpa*	1.0 - 2.0	2.0 - 4.0	1.0 - 0.25	NaCl	2.3 - 8.4	220 - 280	4
Al^{3+}-*Cys*	1.0 - 2.0	2.0 - 4.0	1.0 - 0.25	NaCl	2.4 - 7.0	220 - 280	4

[a)] mmol L^{-1}; [b)] number of titrations.

3.4 Calorimetry

3.4.1 General aspects

The direct calorimetry is a kind of analytical technique which allows to measure the variation of heat, absorbed or developed in a chemical reaction, as a function of the titrant addition. The system used for the investigation reported in this thesis is an isoperibolic calorimeter, made up of an adiabatic reaction cell, named dewar, immersed in a thermostated bath.
The temperature variation in the reaction vessel is proportional to the temperature difference between this one and the bath and it is, usually, due to a physical interaction or chemical reactions between the simple solution and the titrant, which involves the formation of new species in solution. The data obtained by this analysis, expressed as heat *vs.* added titrant volume, are useful to determine the ΔH thermodynamic parameter.

3.4.2 Instrumental equipment and procedure

Calorimetric measurements were performed at 298.150 ± 0.001 K using a CSC (Calorimetry Science Corporation) 4300 Isoperibol Titration calorimeter coupled with a computer for the acquisition of calorimetric data.
It is made up of:

- a water bath of 25 liters capacity, thermally insulated, equipped with a system of temperature control (accuracy ± 0.0002 °C);
- a glass reaction vessel (dewar), covered with a layer of silver, of the capacity of 25 or 50 mL;
- a glass stirrer connected to a motor;
- a Wheatstone bridge that includes a temperature sensor (thermistor) and a heater absorbed in the reaction vessel;
- an electrical junction box.

The titrant was delivered by a 2.5 mL capacity Hamilton syringe, model 1002TLL and the recorded data were collected by means of CALOR8 computer program, that is also used to set the parameters for the measurement.

They are:

- the rate of buret delivery in mL/min and the delay of the burette in seconds (both measured previously),
- the initial volume,
- total times and intervals time, expressed in seconds, for the readings of the baselines, the calibrations and the titration;
- the values of HTRI and HTRV (the voltage across the standard resistor and the heating resistance calibration, respectively) and the starting potential of the measurement.

Before the first measurement of the day, the voltage across the Wheatstone bridge was always checked out and set to zero.

Moreover, for each investigation, the heats of the pure solvent solution were also determined, using the same titrant of the measurements.

The accuracy of the apparatus for the measured heat was $Q \pm 0.008$ J and for the volume $v \pm 0.001$ mL. It was checked, periodically, by titrating a THAM [tris-(hydroxymethyl)amino-methane] buffer with HCl.

For the protonation enthalpies, a solution of 25 mL, containing the ligand salt and ionic medium, was titrated with standard HCl.

The investigations of metal - ligand species were carried out by adding the ligand under study as sodium salt to a solution of 25 mL containing aluminium, ionic medium and sometimes HCl.

The details of the experimental conditions used are shown in Tables 3.5 - 3.6.

Table 3.5 Experimental conditions of ligand protonation enthalpies by calorimetry, at I = 0.15 mol L^{-1} and T = 298.15 K

System	c^T_H [a)]	C_L [b)]	**Ionic medium**	**pH range**
H^+-*mala*	0.1	4.7	NaCl	3.2 - 5.3
H^+-*tma*	0.1	2.5	NaCl	3.0 - 10.0
H^+-*tranex*	0.5 - 0.1	10	NaCl	2.6 - 11.0
H^+-*HMP*	0.1	10	NaCl	2.0 - 7.6
H^+-*ATP*	1	10	NaCl	2.0 - 7.7

[a)] mol L^{-1}; [b)] mmol L^{-1}.

Table 3.6 Experimental conditions of all the investigated metal - ligand systems by calorimetry, at I = 0.15 mol L^{-1} and T = 298.15 K

System	c^{T}_{L} [a)]	c_M [b)]	C_H [b)]	**Ionic medium**	**pH range**
Al^{3+}-*mal*	0.15	3.8	-	NaCl	2.0 - 6.5
Al^{3+}-*mala*	0.3	3.8	-	NaCl	2.0 - 6.9
Al^{3+}-*tca*	0.15	3.8	-	NaCl	2.0 - 4.9
Al^{3+}-*btc*	0.15	4	1.5	NaCl	2.0 - 4.9
Al^{3+}-*mlt*	0.075	3.8	4	NaCl	2.0 - 4.9
Al^{3+}-*EDDS*	0.1	4	2	NaCl	2.0 - 10.0
Al^{3+}-*tla*	0.1	2	4	NaCl	2.0 - 5.0
Al^{3+}-*mpa*	0.1	4	4	NaCl	2.0 - 5.0
Al^{3+}-*tma*	0.1	4	4	NaCl	2.0 - 5.0
Al^{3+}-*Gly*	0.1	4	3	NaCl	2.0 - 4.5
Al^{3+}-*Cys*	0.1	4	1	NaCl	2.0 - 5.0
Al^{3+}-*tranex*	0.1	4	4	NaCl	2.0 - 5.0
Al^{3+}-PO_4^{3-}	0.15	4	2.5	NaCl	2.0 - 5.0
Al^{3+}-*PP*	0.15	4	5	NaCl	2.0 - 6.0
Al^{3+}-*TPP*	0.22	4	4	NaCl	2.0 - 8.0
Al^{3+}-*HMP*	0.11	2	-	$NaNO_3$	2.0 - 8.0
Al^{3+}-*ATP*	0.75	2	-	NaCl	4.0 - 6.6

[a)] mol L^{-1}; [b)] mmol L^{-1}.

3.5 ^{1}H - ^{31}P - {^{1}H} NMR

3.5.1 General aspects

Nuclear Magnetic Resonance spectroscopy (NMR) is an important analytic technique that takes advantage of the magnetic properties of some nuclei to provide information about molecular structures and their conformations. It also can be employed to study some particular phenomena in solution, as equilibria between isomeric forms, exchange of hydrogens acids, reaction kinetics and often the identification of protonable sites in a molecule.

The operating principle is based on the nuclei ability of the sample molecule to absorb the radio - frequency radiations when it is immersed in an external magnetic field, thanks to their magnetic properties. This absorption occurs when the molecules of the sample compound have some particular atom groups as, ^{1}H, ^{13}C, ^{15}N, ^{19}F and ^{31}P, that are characterized by spin ½. When these nuclei are immersed in an external strong magnetic field, there are two energetic levels, classified as ½ and -½. The lowest energy level is a little bit more populated than the higher one and the ΔE between them is given by the following equation:

$$\Delta E = (h\gamma/2\pi)\, B_0 \tag{3.5}$$

Where h is the Planck constant, γ is the *gyromagnetic ratio* (typical of each nucleus and proportional to the magnetic moment nuclear spin, μ and the spin I) and B_0 is the external strong magnetic field.

Considering that ΔE is correlated to the radiation frequency by the relation:

$$\Delta E = h\nu \tag{3.6}$$

it follows that:

$$\nu = (\gamma/2\pi)\, B_0 \tag{3.7}$$

This one is the fundamental NMR equation, that relates the radio-frequency applied to the magnetic field.

When the enforced radiation energy is equivalent to ΔE and the eq. (3.7) is satisfied, the system is in resonance, the active NMR nuclei absorb the radio-frequency applied and it is possible to record the spectrum, *i.e.* a graph of the absorption picks intensity *vs*. frequency.

As a proton in a molecule is shielded from its electronic cloud, whose density varies with the chemical around, the fundamental equation becomes:

$$\nu = (\gamma/2\pi)\, B_0\, (1-\sigma) \qquad (3.8)$$

where σ is the shielding constant deriving from the electronic cloud. The electrons move under the influence of a magnetic field, generating in this way a little own magnetic field that is opposed to the applied one.
For this reason, the recorded frequency is lower than the enforced one. This variation causes a difference in the absorption position of a given active NMR nucleus (^{1}H - ^{31}P -{^{1}H} in this thesis) with respect to that of a reference compound.
Shielding depends on the density of circulating electrons and the inductive effect of the groups adjacent to the active NMR nuclei [70].

3.5.2 Instrumental equipment and procedure

A Bruker AMX R-300 spectrometer, operating at 300 MHz, was used to record ^{1}H and ^{31}P -{^{1}H}NMR solution spectra of some ligands and Al^{3+}-ligand system containing under study. Investigations were performed in a 9:1 H_2O:D_2O mixture, suppressing the water signal by presaturation pulse sequence, at T = 298.15 K. In the case of ^{1}H NMR spectra recorded, the chemical shifts were measured with respect to 1,4-dioxane as internal reference and converted relative to TMS (δ_{dioxane} = 3.70 ppm). The measurements on ligands were carried out on 8 or 10 mmol L^{-1} solutions in a large range of pH (between *ca.* 2 and 10) in order to obtain log β^{H} and chemical shifts of the protonated species. Conversely, ^{1}H and ^{31}P -{^{1}H}NMR titrations on metal-containing solutions were performed in different pH range, due to the formation of poorly soluble species at higher pH values. Depending on the system under study, NMR investigations have been carried out by varying metal - ligand ratios as well as metal and ligand concentrations. The individual chemical shifts belonging to the metal - ligand complexes were calculated assuming fast mutual exchange.
More in detail, the experimental conditions are reported in Tables 3.7 - 3.8.

Table 3.7 Experimental conditions for the determination of ligand protonation constants by ^{1}H NMR and ^{31}P - {^{1}H} NMR, at I = 0.15 mol L^{-1} and T = 298.15 K

	System	C_L [a)]	Ionic medium	pH range
^{1}H NMR	H^+-*tla*	10.0	NaCl	2.6 - 10.5
	H^+-*tma*	10.0	NaCl	2.0 - 10.9
	H^+-*Cys*	10.0	NaCl	2.1 - 10.9
	H^+-*mal*	8.0	NaCl	2.4 - 6.0
	H^+-*mala*	8.0	NaCl	2.7 - 6.9
	H^+-*tranex*	10.0	NaCl	3.1 - 11.5
	H^+-*ATP* [b)]	8.0	NaCl	1.85 - 8.05
^{31}P - {^{1}H} NMR	H^+-*TPP*	10.0	NaCl	1.6 - 10.2

[a)] mmol L^{-1}; [b)] I = 0.1 mol L^{-1}.

Table 3.8 Experimental conditions for the determination of all the Al^{3+}-ligand systems by ^{1}H NMR and ^{31}P - {^{1}H} NMR, at I = 0.15 mol L^{-1} and T = 298.15 K

	System	C_L [a)]	C_M [a)]	C_M/C_L ratio	Ionic medium	pH range
^{1}H NMR	Al^{3+}-*tla*	10.0	5 - 10	0.5 - 1.0	NaCl	2.2 - 4.7
	Al^{3+}-*tma*	10.0	5 - 8	0.5 - 0.8	NaCl	2.2 - 4.7
	Al^{3+}-*Cys*	10.0	6 - 8	0.6 - 0.8	NaCl	3.7 - 6.3
	Al^{3+}-*mal*	8.0	3 - 4	0.37 - 0.5	NaCl	2.0 - 5.5
	Al^{3+}-*mala*	8.0	3 - 5	0.37 - 0.62	NaCl	2.5 - 6.9
	Al^{3+}-*tranex*	10.0	5 - 6	0.5 - 0.8	NaCl	3.0 - 4.6
	Al^{3+}-*ATP* [b)]	8.0	4 - 6	0.5 - 0.8	NaCl	2.0 - 7.6
^{31}P - {^{1}H} NMR	Al^{3+}-*TPP*	10.0	5 - 7	0.7 - 0.8	NaCl	1.5 - 8.2

[a)] mmol L^{-1}; [b)] I = 0.1 mol L^{-1}.

3.6 Mass Spectrometry (MALDI LD/MS)

3.6.1 General aspects

Mass spectrometry is an analytical technique used to identify unknown products, for quantitative determinations of known compounds and to clarify the structural and chemical properties of molecules. It is commonly used in combination with separating techniques, such as gas chromatography and liquid phase chromatography (HPLC), or with the induction plasma. Unlike spectroscopic techniques, this is a destructive analytical method (the molecule does not remain intact after analysis) and it is not based on the interaction between radiation and matter. The operating principle is based on the possibility of separating a mixture of ions depending on their mass / charge ratio, generally through static or oscillating magnetic fields. This blend of ions is obtained by ionizing the sample molecules, by passing them through an electron beam of known energy. More in detail, after the ionization, a molecule loses an electron becoming a radical, named *molecular ion;* the latter is partially fragmented by giving molecules and / or neutral radicals (which the instrument does not detect), or cations and / or radical cations, called *fragment ions*. These ones are, lastly, discriminated on the basis of their mass / charge ratio and revealed by a detector. The adopted revelation technique depends on the ion separation method. Nowadays, mass spectrometers are interfaced with a computer, which controls the instrumental operations and records the spectrum in both graphic and tabular form. This technique allows to measure both nominal and exact molecular masses, by determining the specific fragmentation profile of each compound. The result of the experiment is a mass spectrum representing the relative abundance of the ions depending on their mass / charge ratio. In general, there are two methods of ionization, namely hard and soft ones. Hard ionization operates at high energies, leading to a large degree of fragmentation; soft techniques, instead, work at lower energy, providing little fragmentation.

Laser desorption (LD) ionization, employed for our investigations, is a soft method that uses a laser beam to ionize the sample. This radiation can be constituted by CO_2, which emits in the far infrared, or Nd/YAG (neodymium / yttrium-aluminum-garnet), which releases energy in the UV region. The potentiality of this soft method is enhanced if the laser desorption technique is coupled with a support matrix (MALDI) [70].

MALDI technique is based on the absorption of the sample on a matrix, which can be made of various materials, especially organic, such as glycerol, picolinic, succinic, caffeic, synaptic (SA) and α-Cyano-4-hydroxycinnamic (α-CHA) acids. It must have particular chemical-physical properties:

1) it must be easily evaporated, but it should not be significant during the preparation of the sample or prior to performing the measurements;
2) it must have a given acidity, in order to act as a source of protons by promoting the ionization of the analyte;
3) it must have a strong optical absorption in the UV region, in order to absorb the laser radiation efficiently;
4) it must, eventually, have polar groups and be water soluble.

Once brought the analyte into solution, it is bombed with the laser beam. The matrix attenuates the effects of the laser beam, by providing adequate protection to the analyte, which is ionized and vaporized. Often the MALDI technique is combined with spectrometers equipped with a flight time analyzer.

3.6.2 Instrumental equipment and procedure

A MALDI TOF-TOF Analyzer (AB SCIEX) was employed to perform LD MS and MS/MS investigations. This system, equipped with a Nd/YAG laser, operates in reflection positive-ion mode with a mass accuracy of 5 ppm. In the MS mode, 4000 laser shots were accumulated with laser pulse rate of 400 Hz, whilst in the MS/MS mode, spectra are recorded by means of 5000 laser shots with a pulse rate of 1000 Hz. MS/MS investigations were carried out at 1 kV collision energy, by using ambient air as gas at a medium pressure of 10^{-6} Torr. After acquisition, Data Explorer 4.0 was used to manage spectra. For *PP*, *TPP* and *HMP*, at pH = 3.5 and 6.5, a ligand amount of 2 equivalent was added to 1 mL of $AlCl_3$, dissolved in water under magnetic stirring for 20 minutes. LD MS and MS/MS were performed by direct spotting of the reaction mixture. MALDI MS and MS/MS were carried out with the sandwich method layer by spotting of a simple/matrix (α-CHA and SA) premixed solution (1:5 - 1:25 v/v ratio).

3.7 Calculations

3.7.1 Computer programs

The experimental data collected from the different instrumental techniques were elaborated by means of different computer programs that allow to obtain the stability constants of the complex species and their thermodynamic parameters for the dependence on the ionic strength and temperature.
These computer programs are described as it follows:

- STACO and BSTAC [71]: both use the nonlinear least square minimization method and allow the calculation of all the analytical parameters from potentiometric titration at constant or different ionic strength, considering also the variation of the ionic strength during a titration. These programs especially can calculate the stoichiometry of the species and thermodynamic protonation and complex formation parameters. The programs can refine also the dependence of the stability constants on ionic strength. Concerning the refinement procedure, STACO minimizes the sum of squares of the residuals relatives to the volume delivering, while BSTAC makes the same operation on the e.m.f. readings:

$$U_V = \sum_n w_n \left(v_n^{exp} - v_n^{calc}\right)^2 \qquad \text{STACO} \qquad (3.9)$$

$$U_E = \sum_n w_n \left(E_n^{exp} - E_n^{calc}\right)^2 \qquad \text{BSTAC} \qquad (3.10)$$

where:

$$w_n = 1/\sigma_n^2 \qquad (3.11)$$

$$\sigma_n^2 = \sigma_V^2 + \left(\delta v_i / \delta E_i\right)^2 \sigma_E^2 \qquad \text{STACO} \qquad (3.12)$$

$$\sigma_n^2 = \sigma_E^2 + \left(\delta E_i / \delta v_i\right)^2 \sigma_v^2 \qquad \text{BSTAC} \qquad (3.13)$$

Alternatively, $w_n = 1$, usually this last assumption is made when using STACO, because the partial derivative in eq. (3.12) is null. For both programs, it is possible to execute two refinements processes, the first one with unit weight, and the second one with weight described in eq. (3.11), where σ is taken form the first cycle.
The possibility to perform two cycles allows the operator to give minor weight, in the second cycle, to the data points affected by higher errors (σ).

- LIANA (Linear and Nonlinear Analysis) [72]: this is a software written in Pascal code and used for general fitting and optimization of experimental data, with some features:
  a. it can be used for the parameter calculation of linear and not linear equations;
  b. the equations can be written by operator;
  c. the equation can be splitted into several partial equations;
  d. several equations can be written in the same input and the parameters can be present in several equations;
  e. it is possible to give different weights to different variables and multi-variables fitting can be solved;
  f. some graphics can be displayed for a more rapid evaluation of the results;
  g. it is possible to solve linear systems, two or more problematic in the same time;
  h. it has a great number of library equations.

- ES5CM99 [73]: it is a computer program for calculating enthalpy changes of complex formation in solution from direct calorimetric measurements.

- ES4ECI and ES4SEQ2 [72, 74]: this software is useful for the calculation of the formation percentage of the species present in a multicomponent solution at the equilibrium. It allows to draw the speciation and the sequestration diagrams, from stability constants data and analytical concentrations of the components.

- HYPSPEC [75]: it is a Windows application that allows the determination of equilibrium constants from spectrophotometric data. This program can process UV/visible, infrared, Raman, luminescence and fluorescence data, (the spectral intensity of each chemical species should be proportional to their concentration in solution). The spectral data may be obtained by titration or from a set of individual solutions (batch data). It is possible to perform a manual simulation (manual fitting), with the aim of optimize the values of stability constants from a good fit or display the results of a cycle of refinement.

- HYPNMR [76]: this program can be used to determine equilibrium constants from chemical shifts in NMR spectra. It is assumed that the equilibrium is attained rapidly on the NMR time-scale and the observed chemical shift, δ, for a particular nucleus is the average of the chemical shifts of that nucleus in the various species present, weighted according to their fractional populations.

  Data input include the frequencies (i.e. chemical shifts) of the NMR peaks in relation to the analytical concentrations of reagents in the solution and (optionally) its pH. The software can manage the data in which the chemical shift(s) of one or more nuclei may be

assigned in some spectra and not in others. The refinement process yields the values of both the equilibrium constants and the individual chemical shifts of each nucleus in each chemical compound. At each refining cycle, the chemical shifts of the individual species, δ, are calculated by linear least-squares using the current set of stability constants. The output file contains information, not only on the refined stability constants, but also on all the species, concentrations, calculated chemical shifts, etc.

3.7.2 Equilibrium constants

Ligand protonation constants, reported in the text, are given by their decimal logarithm and they are expressed according to the following equilibria:

$$iH^{+} + L^{z-} = H_iL^{(z-i)-} \qquad \beta_i^H \qquad (3.14)$$

or

$$iH^{+} + H_{i-1}L^{(z-i+1)-} = H_iL^{(z-i)-} \qquad K_i^H \qquad (3.15)$$

where i represent the protonation step.
The formation constants refer to the following equilibria:

$$pM^{3+} + qL^{z-} + rH^{+} = M_pL_qH_r^{(3-qz+r)} \qquad \beta_{pqr} \qquad (3.16)$$

or

$$pM^{3+} + L_qH_r^{-(qz+r)} = M_pL_qH_r^{(3-qz+r)} \qquad K_{pqr} \qquad (3.17)$$

The metal hydrolysis is given as follows:

$$jM^{n+} + iH_2O = M_j(OH)_i^{(j\cdot n-i)} + iH^{+} \qquad \beta_i^{OH} \qquad (3.18)$$

3.7.3 Models for the ionic strength dependence

The evaluation of the formation constants at different temperature and ionic strength values is of great importance for the application to real systems, such as natural waters or biological fluids, having very variable composition. For this reason, the dependence on the ionic strength of the ligand protonation constants, metal hyrolysis and complex species formation constants were taken into account in quite wide ionic strength interval, by using mathematical models.
In an ideal aqueous solution system, the activity *a* of a component is equal to its concentration *m*. In the real case, where electrolytes are present, $a \neq m$, because long - range electrostatic

interactions occur, even in very diluted solutions. More in detail, $a = \gamma \cdot m$, where γ is the activity coefficient, which describes the linearity deviation of the real system from the ideal one.

This deflection from the linearity can be explained through the Debye - Hückel Theory, which assumes that ions in solutions are point masses whose interactions are only of electrostatic nature. This is a limit law valid up to $I \leq 0.001$ mol L^{-1} and it can be expressed as it follows:

$$\log \gamma_{\pm} = -A \left| z_{+} \cdot z_{-} \right| \sqrt{I_m} \tag{3.19}$$

where, A is a constant depending on the temperature and solvent (it is equal to 0.5100 $mol^{-1/2}\, kg^{1/2}$ at $T = 298.15$ K), z_+ and z_- are the charges of anions and cations and I_m is the ionic strength expressed in the molal concentration scale.

In a subsequent study, Debye and Hückel gave to the ions a dimensional property, admitting that they cannot approach distances lower than the sum of their radii. They stated, thus, an extension of this law that can be written:

$$\log \gamma_{\pm} = -A \frac{\left| z_{+} \cdot z_{-} \right| \sqrt{I_m}}{1 + 1.5 \sqrt{I_m}} \tag{3.20}$$

Starting from this law, valid up to $I \leq 0.01$ mol L^{-1}, Davis obtained another expression which consider another factor $L(I)$ [77]. It can be written as follows:

$$\log \gamma_{\pm} = -A \frac{\left| z_{+} \cdot z_{-} \right| \sqrt{I_m}}{1 + 1.5 \sqrt{I_m}} + L(I) \tag{3.21}$$

where $L(I) = CI$.

C is an empirical parameter characteristic of the electrolyte and it depends on the ionic strength. It can be explained as:

$$C = c_0 p^{*} + c_1 z^{*} \tag{3.22}$$

where p is a stoichiometric coefficient and $p^* = \sum p_{reagents} - \sum p_{products}$, z indicates the ion charges and $z^* = \sum z^2_{reagents} - \sum z^2_{products}$. This term is often sufficient to explain experimental data in a wide ionic strength range, where the supporting electrolyte is an alkali metal salt in a ratio 1:1.

In the past, many different approaches were used to model the dependence of equilibrium constants on ionic strength. As it is strictly depending on the activity coefficients and their modifications, a modified Debye - Hückel type equation, like that reported below, was used.

$$\log\beta = \log^{T}\beta - A\frac{z^{*}\sqrt{I}}{1+1.5\sqrt{I}} + CI \qquad (3.23)$$

where β is the stability constant at a specific ionic strength value and $^{T}\beta$ is the stability constant at infinite dilution.

3.7.4 Dependence of the equilibrium constants on the temperature

The dependence of equilibrium constants on temperature can be evaluated by means of the Van't Hoff equation, reported below [78]:

$$\log^{T}\beta = \log\beta_{\theta} + \frac{1}{2.303R}\Delta H_{\theta}^{0}\left(\frac{1}{\theta}-\frac{1}{T}\right) \qquad (3.24)$$

where:
$\log {}^{T}\beta$ = equilibrium constant at a given temperature (expressed in Kelvin);
θ = reference temperature (expressed in Kelvin);
$\log \beta_{\theta}$ = equilibrium constant at T = 298.15 K;
R = 8.314472 J K^{-1} mol^{-1}, when ΔH_{θ} is expressed in J mol^{-1}.

By means of eq. 3.24 it is possible to calculate the enthalpy changes related to a given formation reaction species, knowing its logβ values at different temperatures, or to estimate logβ values at a given temperature, if the ΔH_{θ}^{0} is obtained by calorimetric measurements. This equation can be applied both to molar and molal concentration scales.
The dependence of enthalpy changes on ionic strength can be modelled by using a modified Debye - Hückel type equation, reported below, which allow to calculate the corresponding values at infinite dilution [78].

$$\Delta H_{i} = \Delta H_{i}^{T} - z^{*}\cdot 1.5\frac{\sqrt{I}}{1+1.5\sqrt{I}} + p_{i}I \qquad (3.25)$$

The *i* index indicates a given species present in the speciation model, p_i term is an empirical parameter which can be expressed as a function of the ionic strength.

From the knowledge of the enthalpy changes, ΔH_i, and the formation constant species, $\log\beta_i$, it is possible to calculate the Gibbs free energy, ΔG_i, and $T\Delta S_i$ values, by means of the following relations:

$$\Delta G_i = -RT \ln \beta_i \tag{3.26}$$

$$\Delta G_i = \Delta H_i - T\Delta S_i \tag{3.27}$$

The Van't Hoff equation is valid if the enthalpy changes are approximately constant in a given temperature range. These ΔH values can be also calculated considering a Taylor's series expansion, cut off after the second term if a small temperature range is taken into account.
On the basis of these considerations, it is possible to express another single equation which allows to assess both the dependence on ionic strength and temperature of the stability constants [79]:

$$\log\beta = \log^{T}\beta - z^{*}\cdot 1.5\frac{\sqrt{I}}{1+1.5\sqrt{I}} + CI + EI^{2} + P(T) \tag{3.28}$$

The dependence on the temperature of the formation constants was evaluated by the *P(T)* term:

$$P(T) = \left(\Delta H^{0} - z^{*}\cdot\left(1.5\frac{\sqrt{I}}{1+1.5\sqrt{I}}\right) - C_{T}I - \Delta C_{p}(T-\theta)\right)\cdot\left(\frac{1}{\theta}-\frac{1}{T}\right)\cdot 52.23 \tag{3.29}$$

where θ is the reference temperature (298.15 K), T is the temperature expressed in Kelvin, ΔH^{0} is the enthalpy change expressed in J mol^{-1} at infinite dilution and C_T and ΔCp are parameters for the dependence on the ionic strength and temperature of the ΔH values.

Chapter 4

Aluminium hydrolysis: results and discussion

Aluminium, as already pointed out in the Chapter 1, is a typical hard metal cation with high charge density, which prefers to interact with small hard Lewis bases, especially O-donors owning negative charge such as, carboxylate, phenolate, catecholate and phosphate [13]. The knowledge of the Al^{3+} acid - base properties is still today a crucial topic for evaluating its role in natural and biological systems, featured by a very variable composition.

In aqueous solution, it gives rise to complexes with octahedral structure and quickly hydrolyses in the absence of competing ligands, leading to the formation of several mono- and poly-nuclear complexes, which are strongly dependent on concentration [15, 80]. A large number of species were reported in the literature: the monomeric species, AlOH, $Al(OH)_2$, $Al(OH)_3$, (also known as gibbsite, which precipitates at pH ≈ 4 and slowly redissolves at higher pH values), $Al(OH)_4$, and the polymeric ones, $Al_2(OH)_2$, $Al_3(OH)_4$, $Al_{13}(OH)_{32}$, formed only in the case of high metal concentrations, as already discussed in the Section 1.2. The study of Al^{3+} hydrolysis is often difficult because of the slow kinetic rate of the species formation reactions, in particular the poly-nuclear ones, and the possible interferences due to the presence of the precipitate. The knowledge of thermodynamic parameters, especially of the latter species, is not complete and many discrepancies are present in literature data [81]. Despite this, polymeric ones are involved in many different processes, such as in geochemistry, to evaluate the mineral formation, in water treatment, to understand the functional mechanism and to act as coagulants agent, and in biology, to increase the rigidity of cell membranes.

Aluminium hydrolysis in different ionic media, such as NaCl, KCl, $NaNO_3$ and $NaClO_4$, was quite studied in the past [80, 82], even not in a wide range of ionic strength.

In this Chapter, Al^{3+} acid - base properties in NaCl, $NaNO_3$, and NaCl/$NaNO_3$ mixed ionic medium aqueous solutions was discussed on the basis of potentiometric data, at T = 298.15 K and ionic strength between 0.1 and 1 mol L^{-1}.

4.1 Al^{3+} hydrolysis

Al^{3+} hydrolysis study was conducted at different metal concentrations, different ionic strength values ($0.1 \leq I$ / mol $L^{-1} \leq 1$ in NaCl) and T = 298.15 K, in order to define the stoichiometry, the stability constants of the hydrolytic species and the speciation profile. The experimental details are reported in the Section 3.2.2. Several speciation models were checked in order to obtain the best one, which is featured by two species, $Al_3(OH)_4$ and $Al_{13}(OH)_{32}$ ones. Under the experimental conditions characterized by high metal concentrations (5 - 20 mmol L^{-1}), poly-nuclear species are preferred, whilst mono-nuclear species, such as AlOH and $Al(OH)_2$ ones, are formed in very low amount and only in specific conditions of metal concentration (5 mmol L^{-1}). This speciation model was found for all the investigated ionic media, at different ionic strength values. The experimental formation constants of $Al_3(OH)_4$ and $Al_{13}(OH)_{32}$ species are expressed as $\log\beta_i^{OH}$, according to the reaction (3.18) and are reported in Table 4.1, at T = 298.15 K and I = 0.1 - 1 mol L^{-1} in NaCl, $NaNO_3$ and NaCl/$NaNO_3$ mixed ionic medium. The speciation profile, showed in Fig 4.1, indicates the presence of the $M_{13}(OH)_{32}$ species with very high metal fraction already at pH = 4, at I = 0.01 mol L^{-1}, typical of the fresh waters. With the increase of the ionic strength, from I = 0.01 to 0.7 mol L^{-1}, which represents the average ionic strength value of seawater, its formation is slightly shifted towards higher pH values, *approx.* 4.2. The other poly-nuclear species, $M_3(OH)_4$, is formed with lower fractions of over 0.2, at pH = 4 at I = 0.7 mol L^{-1} and its amount decreases significantly in the case of the ionic strength of fresh waters.

Table 4.1 Experimental hydrolytic constants of Al^{3+}, in NaCl, $NaNO_3$, NaCl/$NaNO_3$, at different ionic strengths and at T = 298.15 K

Ionic medium	I [a]	C_{Cl} [a]	C_{NO3} [a]	$\log\beta_i^{OH}$ [b]	
				$M_3(OH)_4$	**$M_{13}(OH)_{32}$**
NaCl	0.142	0.11	—	-13.324(3) [c]	-108.48(2) [c]
	0.946	1.02	—	-13.618(3)	-112.72(1)
$NaNO_3$	0.167	—	0.16	-13.272(3)	-108.376(5)
	0.963	—	1.03	-13.320(3)	-110.43(1)
NaCl/$NaNO_3$	0.505	0.26	0.28	-13.248(4)	-109.88(2)
	0.939	0.26	0.76	-13.241(5)	-110.62(1)
	0.949	0.75	0.27	-13.314(3)	-111.30(1)
	0.919	0.50	0.55	-13.304(7)	-110.970(2)

[a] In mol L^{-1}; [b] according to the reaction (3.18), charges omitted for simplicity; [c] least-squares errors on the last significant figure are given in parentheses.

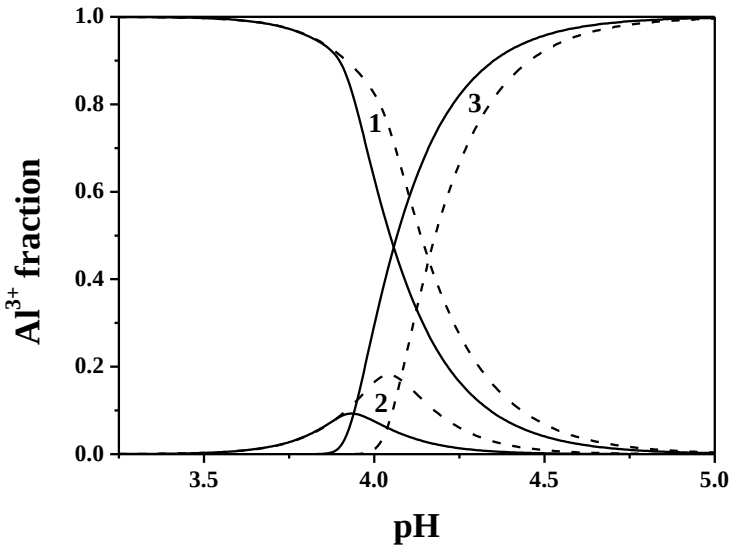

Fig 4.1 Speciation diagram of Al^{3+} hydrolytic species in NaCl at I = 0.01 (solid line) and I = 0.7 mol L^{-1} (dotted line), T = 298.15 K. Experimental conditions: C_M = 20 mmol L^{-1}. Species: **1. M; 2.$M_3(OH)_4$; 3. $M_{13}(OH)_{32}$.**

4.2 Ionic strength dependence

The dependence of the formation constants of the Al^{3+} hydrolytic species on the ionic strength was evaluated, by taking into account the experimental values reported in Table 4.1, analysed by means of an extended Debye - Hückel type equation (eq. 3.23). The obtained values of $\log^T\beta$ together with the empirical parameter *C* for the dependence on ionic strength are reported in Table 4.2 for aqueous NaCl, $NaNO_3$ and NaCl/$NaNO_3$ solutions.
For $M_3(OH)_4$ species, *C* parameter is always negative. More in detail, *C* = -0.562, -0.244, -0.219 in NaCl, $NaNO_3$ and NaCl/$NaNO_3$ mixed ionic medium solutions, respectively. As $M_{13}(OH)_{32}$ species concerns, *C* parameter shows different values in the various ionic media. The determination of the stability constants at I = 0 mol L^{-1} and *C* parameters are of great importance, in order to calculate their values at any ionic strength in the investigated range.

Table 4.2 Formation constants for Al^{3+} hydrolytic species at infinite dilution, together with *C* parameter of eq. (3.23), in NaCl, $NaNO_3$, NaCl/$NaNO_3$, at T = 298.15 K

Species [a]	Ionic medium	$\log^T\beta$	*C*
$M_3(OH)_4$	NaCl	-13.490(1) [b]	-0.562(6) [b]
$M_{13}(OH)_{32}$		-103.81(6)	-1.75(7)
$M_3(OH)_4$	$NaNO_3$	-13.490(1)	-0.244(6)
$M_{13}(OH)_{32}$		-103.81(6)	0.69(8)
$M_3(OH)_4$	NaCl/$NaNO_3$	-13.490(1)	-0.219(2)
$M_{13}(OH)_{32}$		-103.81(6)	0.1(1)

[a] According to the reaction (3.18), charges omitted for simplicity; [b] least-squares errors on the last significant figure are given in parentheses.

4.3 Thermodynamic parameters of Al^{3+} hydrolysis

By considering all together the results regarding the formation constants of hydrolytic species here reported ($M_3(OH)_4$ and $M_{13}(OH)_{32}$), with the ones of the paper of Cigala *et al*. [83], and literature thermodynamic data ones [80, 82, 84, 85] of MOH, $M(OH)_2$, $M(OH)_3$, $M(OH)_4$, $M_2(OH)_2$, $M_3(OH)_4$ and $M_{13}(OH)_{32}$ species, the thermodynamic parameters for the hydrolysis of Al^{3+}, reported in Table 4.3, were obtained.
These ones were taken into account for the calculations performed on all the Al^{3+}-ligand systems.

Table 4.3 Thermodynamic parameters for the hydrolysis of Al^{3+} at T = 298.15 K and at different ionic strength (NaCl)

		logβ [a)]		***ΔH*** [a); b)]
Species [a)]	***I* = 0.15** [c)]	***I* = 0.5** [c)]	***I* = 1** [c)]	***I* = 0.15** [c)]
MOH	-5.30	-5.43	-5.45	46
$M(OH)_2$	-11.20	-11.41	-11.49	94
$M(OH)_3$	-17.84	-18.04	-18.09	167
$M(OH)_4$	-23.31	-23.48	-23.57	180
$M_2(OH)_2$	-7.75	-7.72	-7.68	78
$M_3(OH)_4$	-13.66	-13.58	-13.54	150
$M_{13}(OH)_{32}$	-104.2	-106.5	-108.3	1260

[a)] According to the reaction (3.18); [b)] in kJ mol^{-1}; [c)] mol L^{-1}.

4.4 Literature comparisons

A fair amount of data regarding the aluminium hydrolysis, obtained under different experimental conditions of ionic strength and temperature, are present in the literature. These values are reported in Table 4.4. More in detail, Marklund and Ohman found a logβ = -105.5 for the $M_{13}(OH)_{32}$ species, at T = 298.15 K and I = 0.6 mol L^{-1} in NaCl, whilst Hedlund and co-workers, reported the MOH species, in addition to $M_3(OH)_4$ and $M_{13}(OH)_{32}$ ones, with logβ = -5.52, -13.57, -109.2, respectively. These values are in good agreement with the ones here recalculated and reported in Table 4.3 at I = 0.5 mol L^{-1}. Moreover, Brown *et al.*, found logβ = -13.13, -107.47 for $M_3(OH)_4$ and $M_{13}(OH)_{32}$, respectively, at T = 298.15 K and I = 0.1 mol L^{-1} in $NaNO_3$, against logβ = -13.272, -108.376 here reported at I = 0.167 mol L^{-1} in $NaNO_3$.

In the past, the study on Al^{3+} hydrolysis in $NaNO_3$ was also carried out by this research group, at I = 1 mol L^{-1} and different temperatures, using very high aluminum concentrations ($20 \leq C_M$ / mmol $L^{-1} \leq 200$) [83]. This last paper reported for $M_3(OH)_4$ and $M_{13}(OH)_{32}$, logβ = -13.71, -109.13, respectively, at I = 1 mol L^{-1} in $NaNO_3$ and T = 298.15 K, fairly close to the ones obtained by using the parameters shown in Table 4.2 for $NaNO_3$ ionic medium (logβ = -13.49, -109.73), for $M_3(OH)_4$ and $M_{13}(OH)_{32}$, respectively.

Table 4.4 Al^{3+} hydrolysys literature data

***T*/K**	***I*** [a)]	**Ionic medium**	**log β** [b)]													**Ref.**
Species [c)]			1 1	1 2	1 3	1 4	2 2	2 4	3 4	3 6	4 3	4 2	13 32	13 35	14 34	
298.15	0	—	-5.00	-10.3	-16.7	-22.7	-7.7	—	-13.9	—	—	—	-98.7	—	—	[84]
298.15	0	—	-4.97	-9.3	-15.0	-23.0	-7.7	—	-13.94	—	—	—	-98.73	—	—	[80]
298.15	0	—	-5.0	-10.3	-16.2	-22.2	—	—	—	—	—	—	—	—	—	[82]
298.15	0	—	-5.17	—	—	—	-6.95	—	—	—	—	—	-100.7	—	—	[82]
298.15	0	—	-4.99	—	—	—	—	—	—	—	—	—	—	—	—	[82]
298.15	0	—	-5.02	—	—	—	—	—	—	—	—	—	—	—	—	[82]
298.15	0	—	-4.98	—	—	—	—	—	—	—	—	—	—	—	—	[82]
298.15	0	—	-5.1	—	—	—	—	—	—	—	—	—	—	—	—	[82]
298.15	0	—	-4.5	—	—	—	—	—	—	—	—	—	—	—	—	[82]
298.15	0	—	-4.60	—	—	—	—	—	—	—	—	—	—	—	—	[82]
288.15	0	—	-5.11	—	—	—	-8.03	—	—	—	—	—	—	—	—	[82]
293.15	0	—	-4.93	—	—	—	—	—	—	—	—	—	—	—	—	[82]
303.15	0	—	-4.61	—	—	—	-7.44	—	—	—	—	—	—	—	—	[82]
323.15	0	—	-4.6	—	—	-23.7	—	—	—	—	—	—	—	—	—	[82]
298.15	0.1	NaCl	-5.31	—	—	—	—	—	—	—	—	—	—	—	—	[82]
310.15	0.15	NaCl	—	—	—	-21.031	—	—	—	—	—	—	—	—	—	[82, 86]
298.15	0.60	NaCl	—	—	—	—	—	—	—	—	—	—	-105.5	—	—	[82, 87]
298.15	0.60	NaCl	—	—	—	-23.46	—	—	—	—	—	—	—	—	—	[82]
298.15	0.60	NaCl	-5.52	—	—	—	—	—	-13.57	—	—	—	-109.2	—	—	[82, 88]
298.15	3.0	NaCl	—	—	—	—	-7.53	-16.50	-13.44	—	—	—	—	—	—	[82]
298.15	3.0	NaCl	-5.52	—	—	—	—	—	-13.96	—	—	—	-113.35	—	—	[82]
298.15	0.1	KCl	-4.81	—	-14.17	—	—	—	-13.82	—	—	—	—	—	—	[82]
335.15	1.0	KCl	—	—	—	—	-5.90	—	-10.74	—	—	—	—	—	—	[82]
372.15	1.0	KCl	—	—	—	—	-4.81	—	-8.20	—	—	—	—	—	-67.9	[82]

303.15	3.0	KCl	—	—	—	—	-6.68	—	—	-20.90	—	—	-104.45	-117.78	—	[82]
298.15	0.1	LiCl	-5.62	-9.74	—	—	—	—	-13.7	—	—	—	—	—	—	[82]
298.15	1.0	$NaClO_4$	-5.48	-10.3	—	—	-8.0	—	-13.47	—	—	—	-104.8	—	—	[82]
298.15	1.0	$NaClO_4$	-4.31	—	—	—	—	—	—	—	—	—	—	—	—	[82]
298.15	2.0	$NaClO_4$	—	—	—	—	-7.07	—	—	—	—	—	-104.5	—	—	[82]
298.15	8.0	$NaClO_4$[b)]	—	—	—	—	—	—	—	—	-11.7	-25.8	—	—	—	[82, 89]
298.15	0.1	$NaNO_3$	-5.33	-10.91	—	—	—	—	-13.13	—	—	—	-107.47	—	—	[82, 90]
283.15	1.0	$NaNO_3$	-5.46	—	—	—	—	—	-14.98	—	—	—	-120.94	—	—	[83]
298.15	1.0	$NaNO_3$	-5.01	—	—	—	—	—	-13.71	—	—	—	-109.13	—	—	[83]
298.15	3.0	$NaNO_3$	—	—	—	—	-7.55	-16.41	-13.24	—	—	—	—	—	—	[82]
293.15	0.12	$BaNO_3$	-5.74	—	—	—	-8.06	—	—	—	—	—	—	—	—	[82]
293.15	0.6	$BaNO_3$	-5.97	—	—	—	-8.24	—	—	—	—	—	—	—	—	[82]

[a)] In mol L^{-1}; [b)] According to the reaction (3.18), charges omitted for simplicity; [c)] Other species: $M_5(OH)_4$, $M_5(OH)_3$, $M_6(OH)_5$, $M_6(OH)_4$, $M_6(OH)_3$, $M_7(OH)_5$, with log β = -35.4, -17.0, -45.1, -31.2, -17.0, respectively.

Chapter 5

Carboxylic ligands: results and discussion

The Al^{3+} interaction with some carboxylic ligands (*lac, mal, mala, tca, btc*, *mlt, EDDS*) is here reported. As already explained in the chapter dedicated to the different ligand classes, many of them, contaning O-donor groups, are of great importance in Al^{3+} speciation, because of their presence in natural waters, biological fluids and tissues of the human body. In particular, complex species formed by aluminium with these organic ligands can cross biological membranes and lead to bioaccumulation, since this hard metal cation shows a strong affinity towards molecules having hard character.
For each system, the speciation models were critically analysed. For all the systems, thermodynamic formation parameters were determined by potentiometric and calorimetric titrations. In addition, spectroscopic investigations (^{1}H NMR) were performed for Al^{3+}-*mal* and -*mala* systems, in order to confirm the reliability of the formation constants values obtained by potentiometry. For the determination of the complex stability constants, aluminium hydrolysis constants, described in the previous chapter, and ligands protonation constants were taken into account.

5.1 Ligand protonation constants

Before evaluating the Al^{3+} interaction with the different carboxylates under study, an accurate knowledge of the acid - base properties of the metal and of all the ligands is necessary. As concerns the protonation constants at different ionic strength ($0.15 \leq I$ / mol $L^{-1} \leq 1$) in NaCl and T = 298.15 K, for *mal, mala, tca, btc, mlt, EDDS*, literature data were used and reported in Table 5.1. *Lac* protonation constants were experimentally determined by potentiometry at different ionic strength ($0.1 \leq I$ / mol $L^{-1} \leq 1$) in NaCl, at different temperatures ($288.15 \leq T$ / K ≤ 318.15). These data are also listed in Table 5.1.

Table 5.1 Protonation constants of *lac*, *mal*, *mala*, *tca*, *btc*, *mlt*, *EDDS* at different ionic strength in NaCl

					$\log\beta^H$		Ref.
***T*/K**	**Ligand**	**Species** [a]	***I* = 0.1** [b]	***I* = 0.15** [b]	***I* = 0.5** [b]	***I* = 1** [b]	
288.15		**LH**	3.757 (3) [c]			3.670 (4) [c]	This thesis
298.15	*lac*	**LH**	3.615 (1)		3.71 (3) [c]	3.523 (2)	
318.15		**LH**	3.801 (3)		3.71 (3)	3.832 (3)	
298.15	*mal* [d]	**LH**		5.22	5.071	5.009	[91]
		LH_2		7.99	7.615	7.547	
298.15	*mala* [d]	**LH**		4.61	4.483	4.445	[91]
		LH_2		7.98	7.641	7.592	
298.15	*tca*	**LH**		5.819	5.528	5.429	[91]
		LH_2		10.311	9.847	9.730	
		LH_3		13.729	13.218	13.081	
298.15	*btc*	**LH**		6.21	5.912	5.793	[91]
		LH_2		11.31	10.801	10.602	
		LH_3		15.39	14.733	14.512	
		LH_4		18.55	17.798	17.551	
298.15	*mlt*	**LH**		6.390			[92]
		LH_2		11.623			
		LH_3		15.743			
		LH_4		18.500			
		LH_5		20.176			
		LH_6		20.898			
298.15	*EDDS*	**LH**		9.98	9.79	9.78	[93]
		LH_2		16.86	16.55	16.55	
		LH_3		20.75	20.32	20.31	
		LH_4		23.83	23.38	23.42	
		LH_5		25.2	24.79	24.88	

[a] According to the reaction (3.14), charges omitted for simplicity; [b] in mol L^{-1}; [c] least-squares errors on the last significant figure are given in parentheses; [d] for *mal* and *mala*, protonation constants were also confirmed by ^1H NMR measurements and discussed in the dedicated following section.

5.2 Al^{3+}-carboxylate complexes

The study on the Al^{3+}-carboxylate systems was conducted at different metal - ligand ratios, reported in the experimental section 3.2.2, different ionic strength values ($0.1 \leq I$ / mol $L^{-1} \leq 1$

in NaCl) and T = 298.15 K, in order to define the stoichiometry, the stability constants of the complexes and the speciation profiles. For the Al^{3+}-lactate system, the measurements were carried out also at different temperature values (288.15 ≤ T / K ≤ 318.15), with the aim of studying the dependence of the stability constants on the temperature and calculating the enthalpy changes of the complex species at I = 0 mol L^{-1} by means of the equation (3.28). Formation constants of Al^{3+} with the ligands under study are expressed as $\log\beta_{pqr}$, according to the reaction (3.16). Moreover, the complex species formation of some ligands with aliphatic hydroxyl groups, such as lactate and malate (whose protonation constants are too high to be determined by means of the potentiometry), are governed by the following equilibrium reaction:

$$M^{3+} + L^{z-} = MLH_{-1}^{(3-z-1)} + H^{+} \qquad (5.1)$$

where -1 subscript indicates the proton displaced on the ligand.

The formation constants described by the above reported equilibrium are named displacement constants and are taken into account when these ones cannot be expressed by considering the fully deprotonated ligand, although the proton is displaced by the metal ion. The speciation models and formation constants of all the systems, except for Al^{3+}-*lac*, are reported in Table 5.2, at different ionic strengths (0.15 ≤ I / mol L^{-1} ≤ 1 in NaCl) and T = 298.15 K. The equilibrium constants of Al^{3+}-*lac* system, instead, are shown in Table 5.3 at different ionic strength in NaCl (0.1 ≤ I mol L^{-1} ≤ 1) and different temperatures (288.15 ≤ T / K ≤ 318.15). For all the systems under study, the formation of the ML species was found. The stability of this species changes on the basis of the specific carboxylate ligand. At T = 298.15 K and I = 0.15 mol L^{-1}, for example, $\log\beta_{110}$ = 6.40, 4.25, 4.765, 5.87, 5.89, 17.60 for *mal*, *mala*, *tca*, *btc*, *mlt* and *EDDS*, respectively. The higher $\log\beta_{110}$ value of *mal*, compared to the one of the other ligands, except *EDDS*, is probably related to its ability to act as bidentate ligand, forming cyclic structures. In addition to ML species, other complexes are found for the different systems, *i.e.* ML_2, MLH_{-1}, ML_2H_{-1}, ML_2H_{-2} for Al^{3+}-*lac* system, ML_2 for Al^{3+}-*mal* system, MLH_{-1}, ML_2H_{-1}, $ML(OH)H_{-1}$ for *mala* containing system, MLH_2 and MLH for Al^{3+}-*mlt* system, MLOH for Al^{3+}-*tca* and -*EDDS* systems and, lastly, MLH in *btc* containing system. All the systems were investigated at different pH ranges, as the formation of sparingly soluble species was experimentally observed. The speciation profiles drawn in Fig. 5.1 - 5.7, show the experimental window useful to study the interaction of Al^{3+} with these O-donor ligands. In the Al^{3+}-*lac* system, depicted in Fig. 5.1, although significant fractions of the free metal are present for all the investigated pH range, the complexation becomes significant starting from pH ≈ 3 with the ML, ML_2 and MLH_{-1} species, which achieve a maximum Al^{3+} fraction of about 0.2, 0.3 and 0.4 at pH ≈ 3, 3.6 and 4, respectively.

Table 5.2 Experimental formation constants for Al^{3+} *-mal, -mala, -tca, -btc, -mlt, -EDDS* species obtained by potentiometry at T = 298.15 K and different ionic strengths in NaCl

		logβ		
Ligand	**Species** [a]	I **= 0.15** [b]	I **= 0.5** [b]	I **= 1** [b]
mal	**ML**	6.40 (3) [c]	5.933 (9) [c]	5.835 (9) [c]
	ML_2	11.40 (3)	10.278 (7)	10.152 (4)
mala	**ML**	4.25 (3)	3.85 (2)	3.11 (2)
	MLH_{-1}	1.14 (1)	0.46 (2)	-0.17 (2)
	ML_2H_{-1}	4.03 (4)	3.63 (2)	3.22 (1)
	$ML(OH)H_{-1}$	-4.83 (5)	-4.84 (2)	-4.48 (1)
tca	**ML**	4.765 (5)	4.124 (4)	3.785 (6)
	MLOH	0.02 (1)	-0.418 (7)	-0.680 (7)
btc	**MLH**	10.17 (1)	8.71 (5)	8.03 (5)
	ML	5.87 (2)	5.26 (1)	4.959 (4)
mlt	**MLH_2**	14.69 (1)		
	MLH	10.788 (9)		
	ML	5.89 (2)		
EDDS	**ML**	17.60 (4)	15.75 (3)	15.01 (3)
	MLOH	12.24 (4)	11.15 (2)	10.87 (2)

[a] According to the reactions (3.16), (5.1), charges omitted for simplicity; [b] mol L^{-1}; [c] least-squares errors on the last significant figure are given in parentheses.

Table 5.3 Experimental formation constants for Al^{3+}*-lac* species obtained by potentiometry at different ionic strengths (in NaCl) and temperatures

		logβ[a]				
T**/K**	I**/mol** L^{-1}	**ML**	**ML_2**	**MLH_{-1}**	**ML_2H_{-1}**	**ML_2H_{-2}**
288.15	0.1	1.93 (4)[b]	4.85 (1) [b]	-1.365 (7) [b]	-0.19 (5) [b]	-4.14 (3) [b]
	1.0	1.66 (6)	4.42 (1)	-1.87 (1)	-0.61 (1)	-4.65 (2)
298.15	0.1	2.26 (1)	4.88 (2)	-1.095 (4)	0.55 (4)	-3.75 (3)
	0.5	2.12 (2)	4.66 (3)	-1.40 (1)	0.31 (5)	-3.92 (4)
	1.0	2.07 (2)	4.60 (3)	-1.52 (1)	0.05 (9)	-4.11 (4)
318.15	0.1	2.51 (2)	5.19 (3)	-0.77 (1)	1.59 (4)	-2.75 (3)
	1.0	2.34 (4)	5.07 (3)	-1.12 (2)	1.26 (3)	-3.03 (3)

[a] According to the reaction (3.16), charges omitted for simplicity; [b] least-squares errors on the last significant figure are given in parentheses.

ML_2H_{-1} and ML_2H_{-2} mixed hydrolytic species reach lower fractions. With the increase of the ionic strength from I = 0.1 to 1 mol L^{-1}, a slight increase of the ML_2 formation is observed, whilst ML and MLH_{-1} fractions decrease. For Al^{3+}-*mal* system, shown in Fig. 5.2, the complexation is significant already starting from pH = 2 with the formation of ML species, present in the pH range between 2 and 4.5, with a fraction of over 0.7 at pH = 2.5. Despite this, ML_2 is the main species, since its formation is observed from pH = 2.5 to 6.5, reaching a maximum fraction of over 0.9 in the range of pH = 4.5 - 6 at I = 0.15 mol L^{-1}. Its decrement is observed with the increase of the ionic strength from 0.15 to 1 mol L^{-1}, together with a little raise of the ML species. In the case of Al^{3+}-*mala* system, displayed in Fig. 5.3, MLH_{-1} is the main species in a wide pH range between 3 and 6, at I = 0.15 mol L^{-1}, with a maximum Al^{3+} fraction of over 0.7 at pH = 4. At the same ionic strength value, the other species ML, ML_2H_{-1}, $ML(OH)H_{-1}$ reach maximum fractions of about 0.3, 0.4 and 0.6 at pH ≈ 3.3, 5.3 and 6.5, respectively. By increasing the ionic strength from 0.15 to 1 mol L^{-1}, the speciation profile of MLH_{-1} and $ML(OH)H_{-1}$ significantly change: MLH_{-1} fraction decreases from 0.7 to 0.3 at pH = 4, whilst $ML(OH)H_{-1}$ fraction increases from 0.6 to over 0.9 at pH = 6.5. The distribution diagram related to Al^{3+}-*tca* system, shown in Fig. 5.4, is different with respect to the previous ones, as the complexation becomes significant starting from pH ≈ 3.75 to approximately 5. The main species is ML, which reaches a maximum Al^{3+} fraction of over 0.5 at pH = 4.5 and I = 0.15 mol L^{-1}, whilst the formation of MLOH species is observed in the pH range between 3.75 and 4.75, with a maximum fraction of about 0.3. With the increasing of the ionic strength, the distribution curves significantly change, with a decrement of ML fractions from 0.5 to 0.3 at pH = 4.5. Al^{3+}-*btc* system, reported in Fig. 5.5, shows a speciation profile quite similar to the previous one, in which the formation of the complex species becomes important starting from pH = 3.6 up to pH ≈ 5. At I = 0.15 mol L^{-1}, MLH and ML species achieve maximum fractions of 0.4 and 0.7 at pH = 4.2 and 4.75, respectively. With the increasing of the ionic strength, a significant decrease of the MLH species (from 0.4 to 0.08 at pH = 4.2) and an increase of the ML species (from 0.7 to 0.8 at pH = 4.75) are observed. For Al^{3+}-*mlt* system, the distribution diagram is displayed in Fig 5.6 only at I = 0.15 mol L^{-1}. Similarly to previous speciation profiles, the complexation is significant starting from pH = 3.25 with the formation of MLH_2. The main species is MLH, which reaches a maximum Al^{3+} fraction of 0.5 at pH = 4.5. ML species, instead, is formed with a lower fraction at pH = 4.75. Al^{3+}-*EDDS* distribution profile, reported in Fig 5.7, shows a wide pH range, from 2 to 8, where, ML and MLOH are present at I = 0.15 mol L^{-1} with a maximum fraction of almost 1.0 at pH = 4 and 8, respectively. With the increasing of the ionic strength, ML fraction decreases to 0.8 at pH = 3.5, whilst the formation of MLOH is shifted to lower pH values, reaching a maximum fraction of almost 1.0 at pH = 6.5.

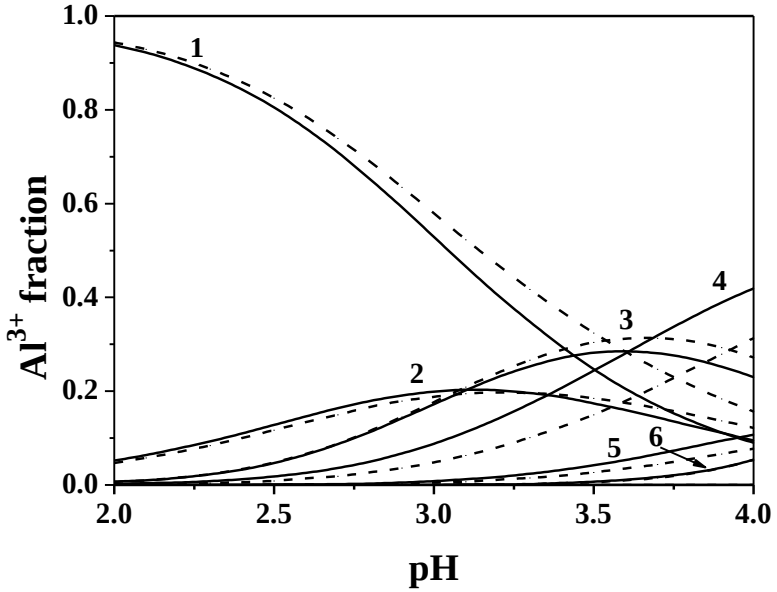

Fig. 5.1 Speciation diagram of Al^{3+}-*lac* system in NaCl at I = 0.1 mol L^{-1} (solid line) and I = 1 mol L^{-1} (dotted line), T = 298.15 K. Experimental conditions: C_M = 5 mmol L^{-1}, C_L = 15 mmol L^{-1}. Species: **1. M; 2. ML; 3. ML_2; 4. MLH_{-1}; 5. ML_2H_{-1}; 6. ML_2H_{-2}.**

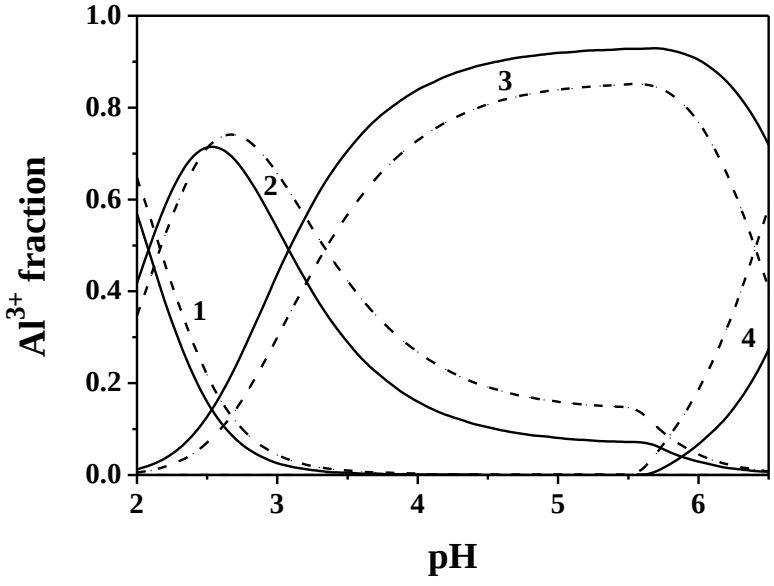

Fig. 5.2 Speciation diagram of Al^{3+}-*mal* system in NaCl at I = 0.15 (solid line) and I = 1 mol L^{-1} (dotted line), T = 298.15 K. Experimental conditions: C_M = 2 mmol L^{-1}; C_L = 4 mmol L^{-1}. Species: **1. M; 2. ML; 3. ML_2; 4. $M_{13}(OH)_{32}$.**

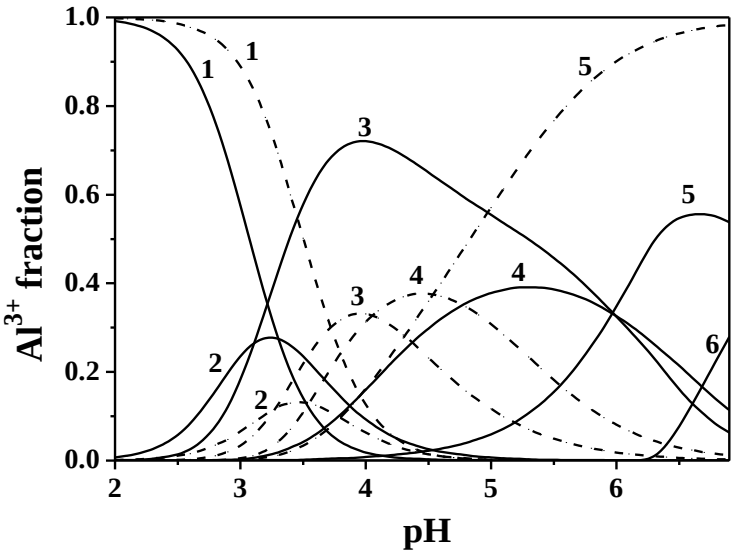

Fig. 5.3 Speciation diagram of Al^{3+}-*mala* system in NaCl at I = 0.15 (solid line) and I = 1 mol L^{-1} (dotted line), T = 298.15 K. Experimental conditions: C_M = 2 mmol L^{-1}; C_L = 4 mmol L^{-1}. Species: **1. M; 2. ML; 3. MLH_{-1}; 4. ML_2H_{-1}; 5. $ML(OH)H_{-1}$; 6. $M_{13}(OH)_{32}$.**

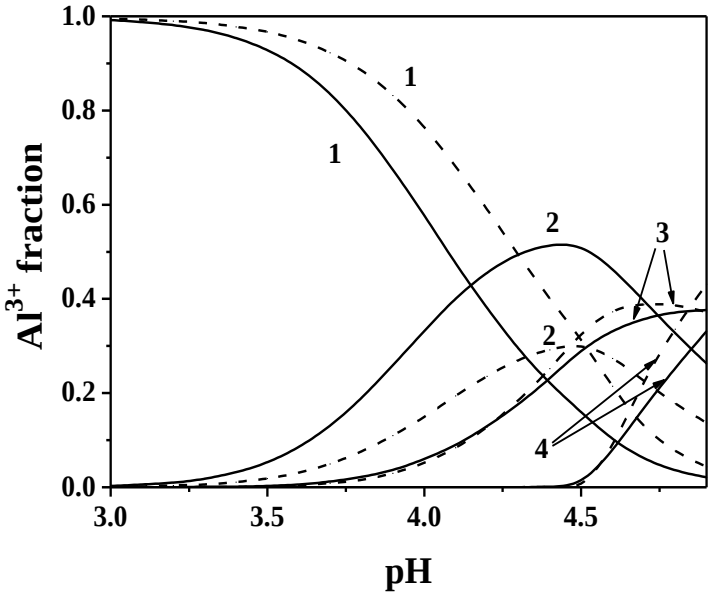

Fig. 5.4 Speciation diagram of Al^{3+}-*tca* system in NaCl at I = 0.15 (solid line) and I = 1 mol L^{-1} (dotted line), T = 298.15 K. Experimental conditions: C_M = 2 mmol L^{-1}; C_L = 4 mmol L^{-1}. Species: **1. M; 2. ML; 3. MLOH; 4. $M_{13}(OH)_{32}$.**

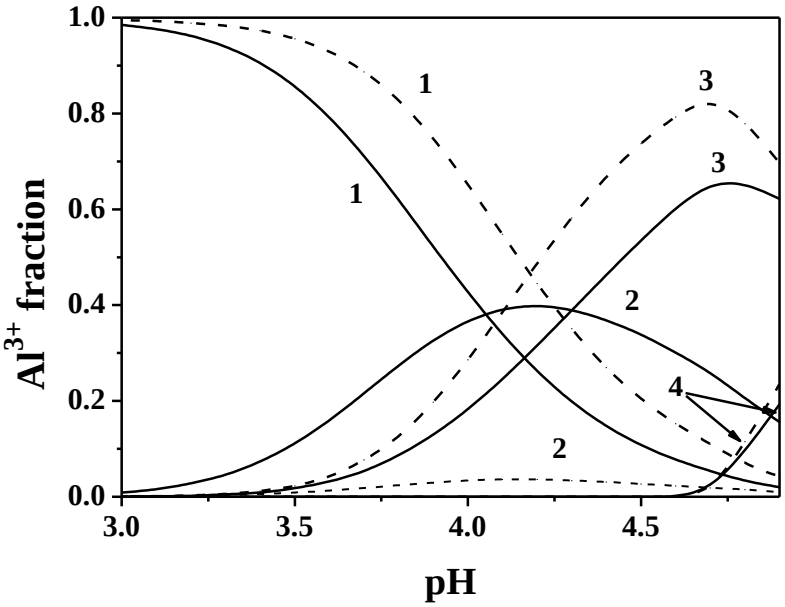

Fig. 5.5 Speciation diagram of Al^{3+}-*btc* system in NaCl at I = 0.15 (solid line) and I = 1 mol L^{-1} (dotted line), T = 298.15 K. Experimental conditions: C_M = 2 mmol L^{-1}; C_L = 4 mmol L^{-1}. Species: **1. M; 2. MLH; 3. ML; 4. $M_{13}(OH)_{32}$.**

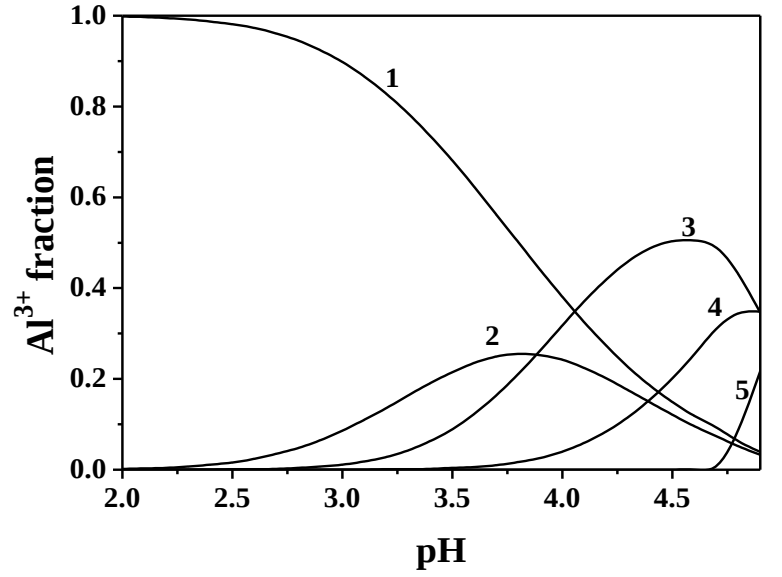

Fig. 5.6 Speciation diagram of Al^{3+}-*mlt* system in NaCl at I = 0.15 (solid line) and I = 1 mol L^{-1} (dotted line), T = 298.15 K. Experimental conditions: C_M = 1 mmol L^{-1}; C_L = 2 mmol L^{-1}. Species: **1. M; 2. MLH_2; 3. MLH; 4. ML; 5. $M_{13}(OH)_{32}$.**

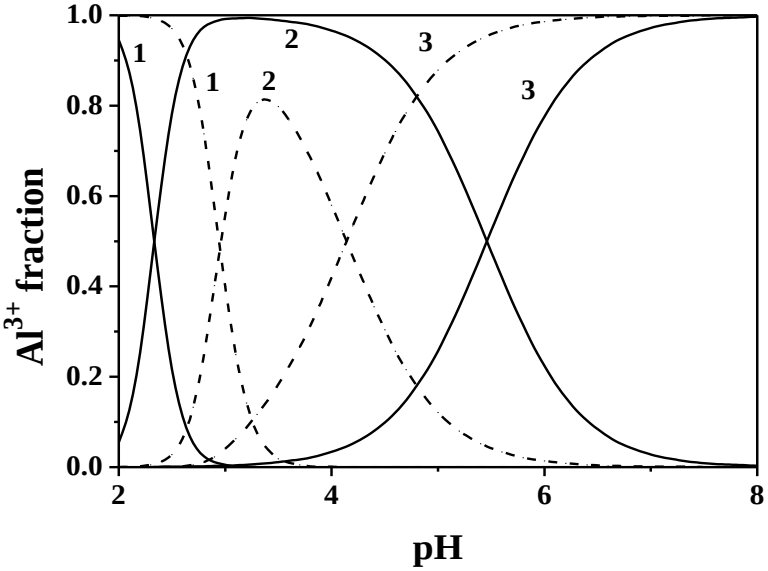

Fig. 5.7 Speciation diagram of Al^{3+}-*EDDS* system in NaCl at I = 0.15 (solid line) and I = 1 mol L^{-1} (dotted line), T = 298.15 K. Experimental conditions: C_M = 0.5 mmol L^{-1}; C_L = 1 mmol L^{-1}. Species: **1. M; 2. ML; 3. MLOH.**

5.3 Ionic strength dependence

For all the Al^{3+}-carboxylate systems here reported, except for Al^{3+}-*mlt* one, the dependence of the formation constants on the ionic strength was studied, analysing the stability constant values in a range of ionic strength between 0.1 and 1 mol L^{-1}, by using an extended Debye - Hückel type equation (3.23) (for Al^{3+}-*lac* system eq. (3.28) was employed), as previously done for many other systems [94-97].

Values of formation constants extrapolated at infinite dilution (I = 0 mol L^{-1}), are reported in Table 5.4, together with the empirical parameter C. The determination of the stability constants at I = 0 mol L^{-1} and C parameters are of great importance, in order to calculate their values at any ionic strength in the investigated range.

Table 5.4 Formation constants for Al^{3+}-*lac, -mal, -mala, -tca, -btc, -EDDS* species at infinite dilution, together with C parameter for the ionic strength dependence (eq. (3.23) (3.28)) in NaCl, at T = 298.15 K

Ligand	Species [a]	$\log^T\beta$	C
lac	**ML**	2.84 (1) [b]	-0.4(1) [b]
	$\mathbf{ML_2}$	5.99 (8)	-0.7(1)
	MLOH	-0.25 (6)	0.3(1)
	$\mathbf{ML_2OH}$	1.59 (8)	0.5(1)
	$\mathbf{ML_2(OH)_2}$	-2.81 (6)	0.37 (8)
mal	**ML**	7.81 (5)	0.47 (7)
	$\mathbf{ML_2}$	13.3 (2)	0.1 (3)
mala [c]	**ML**	5.9(1)	-0.3(2)
	$\mathbf{MLH_{-1}}$	2.71(6)	-0.5(1)
	$\mathbf{ML_2H_{-1}}$	5.53(9)	0.1(1)
	$\mathbf{ML(OH)H_{-1}}$	-3.79(2)	1.42(4)
tca	**ML**	6.28 (5)	-0.07 (7)
	MLOH	1.97(7)	0.6 (1)
btc	**MLH**	13.4(1)	-0.1(2)
	ML	8.7(1)	1.1(2)
EDDS	**ML**	20.6 (2)	-0.8 (3)
	MLOH	14.6 (2)	0.3 (2)

[a] According to the reaction (3.16), charges omitted for simplicity; [b] least-squares errors on the last significant figure are given in parentheses; [c] according to the reaction (5.1).

5.4 Temperature dependence

In order to complete the thermodynamic parameter framework, it is very important to determine enthalpy changes referring to complex species, as performed for several other systems [96, 98-103].

The study of the temperature effect on the formation constants is of crucial importance, in order to calculate their values at other different temperatures, under the conditions of different natural or biological fluids, by means of Van't Hoff equation (3.24). Enthalpy changes, here reported, were determined at T = 298.15 K by calorimetric titrations for all the systems, except for Al^{3+}-*lac* one, since for this system they were calculated from potentiometric data previously obtained at different temperatures, by using an extended Debye - Hückel type equation, combined with the Van't Hoff one (eq. 3.28).

Enthalpy change values of the protonation ligands (except for *lac*) at T = 298.15 K and at I = 0.15 mol L^{-1} in NaCl are reported in Table 5.5. Enthalpy change values of Al^{3+}-*mal, -mala, -tca, -btc, -mlt, -EDDS* systems, are listed in Table 5.6, together with ΔG and $T\Delta S$ values. Thermodynamic parameters for the temperature dependence of Al^{3+}-*lac* complex species, obtained by using the eq. 3.28 at infinite dilution and T = 298.15 K, are shown in Table 5.7. The dependence on temperature of Al^{3+}-*lac* stability constants can be evaluated by observing the trend in Fig 5.8, where formation constants for ML_2, MLOH, ML_2OH and $ML_2(OH)_2$ species are plotted vs. the inverse of T.

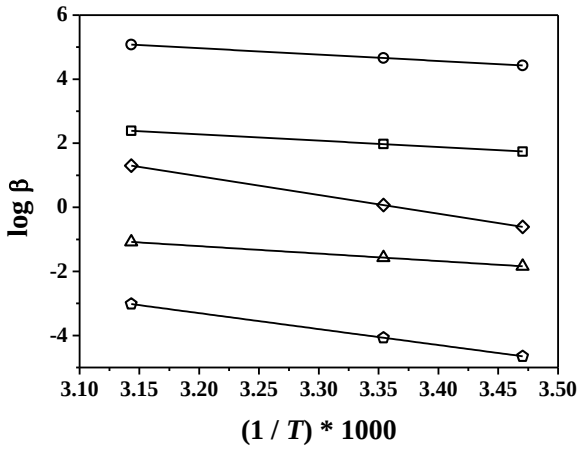

Fig. 5.8 Dependence of $\log\beta_{110}$ (squares), $\log\beta_{120}$ (circle), $\log\beta_{11-1}$ (triangles), $\log\beta_{12-1}$ (pentagons) and $\log\beta_{12-2}$ (triangles) of Al^{3+}-*lac* species on ionic strength, at I = 1.0 mol L^{-1} in NaCl and $288.15 \leq T / K \leq 318.15$.

Since the interaction between Al^{3+} and O-donor ligands is typical hard - hard, as expected, the enthalpy changes obtained, for all the systems under study are endothermic, except for Al^{3+}-*EDDS* interactions, where ΔH = -20.5, -4 kJ mol^{-1} for ML and MLOH, respectively. For this

type of electrostatic interaction, the contribution to the free energy is mainly entropic in nature, due to the change of orientation of the hydration water molecules into the coordination sphere.

Table 5.5 Protonation thermodynamic parameters of *mal, mala, tca, btc, mlt, EDDS* at T = 298.15 K and at I = 0.15 mol L^{-1}in NaCl

	ΔH [a) b)]						Ref.
Ligands	**LH**	**LH_2**	**LH_3**	**LH_4**	**LH_5**	**LH_6**	
mal	4.8	4.6					[104]
mala [c)]	0	-2					[105]
tca	3.3	3.9	-0.4				[104]
btc	6.1	5.4	3.9	1.4			[104]
mlt	12.7	10.1	7.6	5.0	2.8	0.4	[105]
EDDS	-24.0	-44.0	-53.5	-56.5	-43.5		[106]

[a)] According to the reaction (3.14), charges omitted for simplicity; [b)] in kJ mol^{-1}; [c)] according to the reaction (5.1).

Table 5.6 Thermodynamic parameters of Al^{3+}-*mal, -mala, -tca, -btc, -mlt, -EDDS* complex species obtained by titration calorimetry at I = 0.15 mol L^{-1} in NaCl and T = 298.15 K

Ligand	**Species** [a)]	$-\Delta G$ [b)]	ΔH [b)]	$T\Delta S$ [b)]
mal	**ML**	36.5	21 (1) [c)]	57
	ML_2	65.0	28 (2)	93
mala [d)]	**ML**	24.3	7 (3)	31
	MLH_{-1}	6.5	53.0 (6)	59.5
	ML_2H_{-1}	23.0	68.9 (7)	91.9
tca	**ML**	27.2	15.0 (7)	42.2
	MLOH	0.1	58.2 (8)	58.3
btc	**MLH**	58.1	35 (4)	93
	ML	33.5	19 (3)	52
mlt	**MLH_2**	83.8	25 (3)	109
	MLH	61.5	50 (1)	111
EDDS	**ML**	100.5	-20.5 (4)	80.0
	MLOH	69.9	-4 (2)	66

[a)] According to the reactions (3.14), charges omitted for simplicity; [b)] In kJ mol^{-1}; [c)] least-squares errors on the last significant figure are given in parentheses; [d)] according to the reaction (5.1).

Table 5.7 Calculated thermodynamic parameters for the temperature dependence (eq. 3.28) of Al^{3+}-*lac* complex species at infinite dilution and T = 298.15 K

Ligands	Species [a]	$-\Delta G^0$ [b]	ΔH^0 [b]	$T\Delta S^0$ [b]	C_T
	ML	16.2 (5) [c]	28 (4) [c]	44 (4) [c]	10 (2) [c]
	ML_2	34.2 (4)	31 (3)	32 (3)	14 (2)
lac	**MLOH**	-1.4 (3)	21 (3)	55 (3)	17 (3)
	ML_2OH	9.1 (4)	95 (4)	104 (4)	17 (3)
	$ML_2(OH)_2$	-16.0 (3)	82 (2)	98 (3)	14 (2)

[a] According to the reactions (3.14), charges omitted for simplicity; [b] In kJ mol^{-1}; [c] least-squares errors on the last significant figure are given in parentheses.

5.5 ^{1}H NMR spectroscopy

In the study of these systems, ^{1}H NMR titrations were also employed, as performed for several other systems, in order to confirm the speciation models obtained by the potentiometric technique [107-110]. For Al^{3+}-*mal* and -*mala* systems, ^{1}H NMR investigations in H_2O/D_2O solutions were performed. Before to study the ^{1}H NMR spectra of the complexes, the individual NMR parameters, related to each protonated ligand form, were calculated. A wide number of spectra were collected in the pH range dependent on the specific system, by varying the metal - ligand ratio and the concentrations of metal and ligand as well. The chemical shifts obtained from each ^{1}H NMR spectra, allowed to calculate, by HypNMR software program [76], the formation constants of the species and the chemical shift values for each complex. Moreover, the program can recalculate the average chemical shift at each experimental pH.

For *mala* containing system, a single set of resonances related to each proton is observed in all the spectra. This is indicative of a fast mutual exchange on the NMR time scale of all the species present at equilibrium. Regarding *mala* ligand solutions, a resonance shift from 4.4 to 4.26 ppm of the CH signal is noted in the pH range between 2.75 and 5.3, due to the proton loss of the close carboxylic group. At higher pH values, no change of this signal was recorded. A similar trend, was observed also for the CH_2 signal, whose resonance is shifted from 2.8 to 2.45 ppm, in the pH range between 2.75 and 6.3, thus indicating the deprotonation of the other carboxylic group. In Fig. 5.9 the spectrum of the metal free *mala* solution at pH 6.30 is shown.

For Al^{+3}-*mala* complexes, the metal presence does not cause any change in the chemical shifts of the ligand resonances, for any solution with different metal - ligand ratios. The high

stabilization to the coordination with the metal, attributed to the presence of a hydroxyl group on the molecule, as it was found for the diethyltin(IV), here was not observed [111].

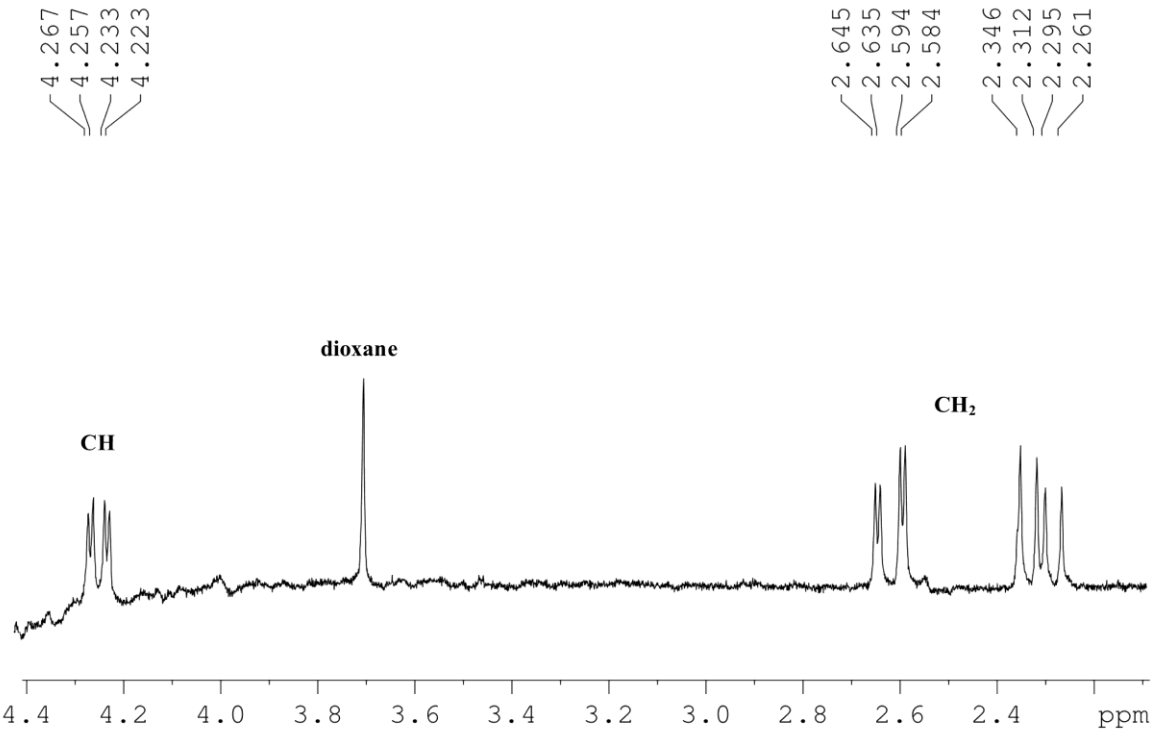

Fig. 5.9 ^{1}H NMR spectrum of *mala* at C_L = 8 mmol L^{-1}, pH = 6.30, I = 0.15 mol L^{-1} in NaCl and T = 298.15 K.

The only difference, due to the presence of the metal in *mala* containing solutions, is given by an alteration of the signal form for methylene carbon, occurring from pH = 5.5, with a considerable broadening of the peaks. From the observed shape related to the resonance signals, the *mala* coordination site towards Al^{3+} can not be established with certainty. Furthermore, it was not possible to investigate this system at pH above 6.5, because of the formation of sparingly soluble hydrolytic species.

As the experimental spectra collected for *mala* and Al^{+3}-*mala* solutions have shown both a single resonance for each kind of proton, the direct measurements of the chemical shifts related to each single complex was not allowed. From the direct observation of the spectra, in fact, it was not possible to detect the signals due to bound and free ligand.

The stability constants of the species and the corresponding chemical shifts obtained by the fit of the observed average resonances are reported in Table 5.8. These results, with the excellent agreement between the calculated and observed chemical shifts (Fig. 5.10), confirm the speciation model and the formation constant values found by potentiometric study (logβ = 4.25, 1.14, 4.03, -4.83, for ML, MLH_{-1}, ML_2H_{-1}, $ML(OH)H_{-1}$, respectively) as shown in Table 5.9.

Table 5.8. Protonation constants of *mala*, formation constants and calculated chemical shifts of Al^{3+}-*mala* species obtained by ^1H NMR at I = 0.15 mol L^{-1} in NaCl and T = 298.15 K

Species [a]	logβ	δ_{CH}	δ_{CH2}
L		4.243(1) [b]	2.453(1) [b]
LH	4.753(6) [b]	4.317(1)	2.687(1)
LH_2	8.06(1)	4.556(1)	2.842(1)
ML	4.4(3)	4.481(7)	2.66(4)
MLH_{-1}	1.2(1)	4.339(7)	2.68(4)
ML_2H_{-1}	3.9(2)	4.207(7)	2.41(4)
$ML(OH)H_{-1}$	-4.3(2)	4.243(7)	2.45(4)

[a] According to the reactions (3.14), (5.1), charges omitted for simplicity; [b] least-squares errors on the last significant figure are given in parentheses.

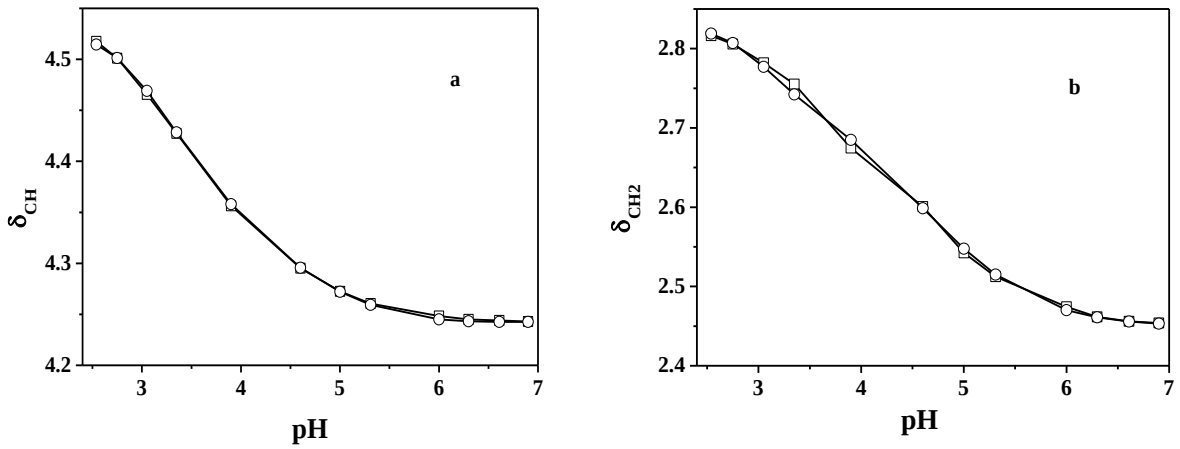

Fig. 5.10 Observed (□) and calculated (○) values of selected chemical shifts of the ligand *vs.* pH in Al^{3+}-*mala* (**a**, **b**) at C_M = 3 mmol L^{-1}, C_L = 8 mmol L^{-1}, I = 0.15 mol L^{-1} in NaCl and T = 298.15 K.

Table 5.9. Comparison between experimental stability constants of Al^{3+}-*mala* species obtained by ^1H NMR and potentiometry at I = 0.15 mol L^{-1} (NaCl) and T = 298.15 K

Species [a]	$\log\beta_{\ H\ NMR}$	$\log\beta_{\ ISE\ H+}$
ML	4.4(3) [b]	4.25(3) [b]
MLH_{-1}	1.2(1)	1.14(1)
ML_2H_{-1}	3.9(2)	4.03(4)
$ML(OH)H_{-1}$	-4.3(2)	-4.83(5)

[a] According to the reaction (5.1), charges omitted for simplicity; [b] least-squares errors on the last significant figure are given in parentheses.

As far as it is concerned the investigation of *mal* containing solutions, the collected spectra showed a single signal due to the only methylenic group, whose resonance shifted to higher fields with the pH increase. Unlike the previous system, in Al^{3+}-*mal* solutions spectra, a new resonance at *ca*. 3.30 ppm was present, beside the peak due to the species involved in a rapid exchange. The latter showed a similar free *mal* behavior, whilst the new signal, referred as bound, did not shift largely, regardless of the metal - ligand ratio and solution pH. The intensity of the bound peak underwent a significant change with the pH increasing: the signal appeared slightly smaller than the other one at lower pH values, then, starting from pH = 3, it achieved higher intensity than the signal of the free ligand and, at the same time, its shape was broader. In addition, in the solutions with a metal - ligand ratio of 0.5, starting from pH = 4.3, the peak referred to the free ligand disappeared. This experimental evidence suggested that the bound methylene signal could be assigned to the ML_2 complex, as supported by the speciation model coming from potentiometry, whereas all the other *mal* containing species rapidly exchanged in the NMR time scale. The calculated chemical shifts together with the stability constants of the complex species were collected in Table 5.10. The results found by NMR titrations were comparable to those already determined by potentiometric investigations ($\log\beta$ = 6.40, 11.40, for ML and ML_2 respectively), as reported in Table 5.11. Furthermore, the good agreement between the observed and calculated chemical shifts, shown in Fig. 5.11, allowed to validate the speciation model.

Table 5.10. Protonation constants of *mal* and formation constants of Al^{3+}-*mal* species obtained by ^{1}H NMR at I = 0.15 mol L^{-1} in NaCl and T = 298.15 K

Species [a)]	**logβ**	**δ_{CH2}**
L		3.059(1) [b)]
LH	5.25(2) [b)]	3.207(1)
LH_2	7.88(3)	3.466(1)
ML	6.63(7)	3.427(9)
ML_2	11.4(7)	3.185(9)

[a)] According to the reactions (3.14) and (3.16), charges omitted for simplicity; [b)] least-squares errors on the last significant figure are given in parentheses.

Table 5.11. Comparison between experimental stability constants of Al^{3+}-*mal* species obtained by ^{1}H NMR and potentiometry at I = 0.15 mol L^{-1} (NaCl) and T = 298.15 K

Species [a]	$\log\beta_{\text{H NMR}}$	$\log\beta_{\text{ISE H+}}$
ML	6.63(7) [b]	6.40(3) [b]
ML_2	11.4(7)	11.40(3)

[a] According to the reaction (3.16), charges omitted for simplicity; [b] least-squares errors on the last significant figure are given in parentheses.

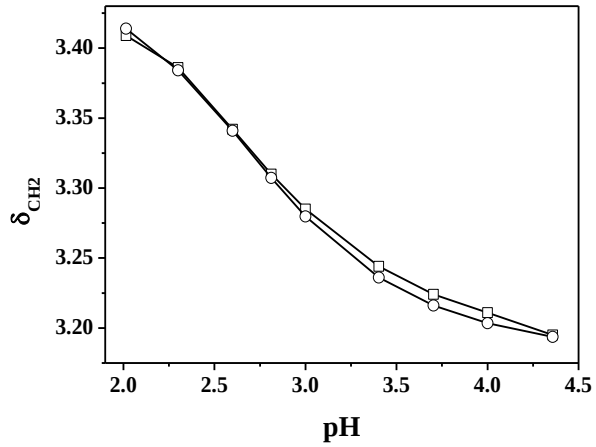

Fig. 5.11 Observed (□) and calculated (○) values of selected chemical shifts of the ligand *vs.* pH in Al^{3+}-*mal* mixtures, at C_M = 3 mmol L^{-1}, C_L = 8 mmol L^{-1}, I = 0.15 mol L^{-1} in NaCl and T = 298.15 K.

5.6 Literature comparisons

Literature reports few data dealing with the interaction between Al^{3+} and polycarboxylic ligands under study, except for Al^{3+}-*lac*, -*mal*, -*mala* and -*tca* species [15, 28, 87, 112-115], as shown in Table 5.12.

For Al^{3+}-*lac* system, Marklund *et al.* found a logβ = 2.36 for ML species at I = 0.6 mol L^{-1} in NaCl and T = 298.15 K by NMR and potentiometric measurements [87]. This value is comparable to the one here reported ($\log\beta_{110}$ = 2.12 at I = 0.5 mol L^{-1} in NaCl and T = 298.15 K) (this thesis and [116]). Rubini and co-workers provided a speciation model with five species, namely ML, ML_2, ML_3, MLH_{-1}, ML_2H_{-1} [15], quite similar to the one reported in this thesis, with the only difference that ML_2H_{-2} species here is found instead of ML_3 one. These results are in agreement also with those reported in a paper of Kiss and other co-authors [117], which provided a logβ = 2.48 for ML species, at I = 0.2 mol L^{-1} in KCl and T = 298.15 K.

For Al^{3+}-*mal* system, Powell and Town reported logβ = 6.711, 11.53 for ML and ML_2, respectively, at I = 0.1 mol L^{-1} in KCl and T = 298.15 K [114], which are close to those here presented, namely logβ = 6.40, 11.40 for ML and ML_2, respectively, at I = 0.15 mol L^{-1} in NaCl and T = 298.15 K. As concerns Al^{3+}-*mala* interactions, the ML and MLH_{-1} formation constant values reported in different papers are in good agreement to those of this study. More in detail, Venturini-Soriano and Berthon proposed a speciation model with a high number of species, such as MLH, ML_2H, M_2LH_{-2}, M_2LH_{-3}, $M_2L_2H_{-3}$, $M_2L_2H_{-4}$, $M_2L_3H_{-1}$, $M_3L_4H_{-4}$, $M_4L_4H_{-5}$, in addition to ML and MLH_{-1} here reported. For these two common species, the stability constants result logβ = 4.519, 1.268, respectively, at I = 0.15 mol L^{-1} in NaCl and T = 310.15 K [115], against logβ = 4.25, 1.14, respectively, at I = 0.15 mol L^{-1} in NaCl and T = 298.15 K of this study. The presence of dimeric and trimeric species in the model presented by Venturini and Berthon is probabily due to the different experimental conditions of metal - ligand concentration ratios employed, in particular to the high metal concentrations (C_{Al} = 1 - 10 mM) with respect to the ligand (C_{mala} = 5 - 10 mM). On the contrary, in this study, the investigations were carried out with lower aluminium amounts, in order to hinder the formation of sparingly soluble species. Moreover, Kiss and other co-workers found a logβ = 3.84, 1.32, 4.74, for ML, MLH_{-1}, ML_2H_{-1}, respectively, at I = 0.2 mol L^{-1} in KCl and T = 298.15 K [117]. These values are comparable to those here obtained (logβ = 4.25, 1.14, 4.03 for ML, MLH_{-1}, ML_2H_{-1}, respectively, at I = 0.15 mol L^{-1} in NaCl and T = 298.15 K), considering the different ionic strength and ionic medium employed. In addition, Martell *et al.* reported a speciation model with ML_2H, MLH, ML, and ML_2 [28], whilst Findlow *et al.* provided only two species, namely ML and ML_2 [112].

As far as Al^{3+}-*tca* concerns, Jackson presented some thermodynamic data related to this system, with a ML formation constant value of 5.44 at I = 0.15 mol L^{-1} in NaCl and T = 310.15 K [113], quite similar to the one here reported (logβ = 4.765 at I = 0.15 mol L^{-1} in NaCl and T = 298.15 K).

To the best of our knowledge, there are no papers, which provide information regarding the interaction between Al^{3+} and *EDDS* ligand. Despite this, since *EDDS* is a structural isomer of *EDTA* (etylenediaminetetraacetic acid) and exhibits metal complexes with comparable stability (except for the alkaline heart ones), it is possible to confront *EDDS* thermodynamic data here obtained to those related to the Al^{3+}-*EDTA* system. Martell *et al.* give a log$K$ = 16.5 for ML species of *EDTA* at I = 0.1 mol L^{-1} and T = 298.15 K [28], whilst log$K$ for Al^{3+}-*EDDS* complex here provided is 17.60 at I = 0.15 mol L^{-1} in NaCl and T = 298.15 K.

Furthermore, it is also possible to make a comparison between Al^{3+}-carboxylate stability and the humic substance one. Elkins and Nelson reported log$K$ = 5 - 6 [118], comparable to log$K$ = 4.25, 4.765 for ML species of Al^{3+}-*mala* and -*tca* complexes, respectively.

Table 5.12 Literature data on Al^{3+}-polycarboxylate systems

			logβ [a]				Ref.
***T*/K**	***I*/mol L^{-1}**	**Ligand**	**ML**	**ML_2**	**MLH_{-1}**	**ML_2H_{-1}**	
298.15	0.6 [b]	*lac*	2.36	—	—	—	[87]
	0.2 [c]		2.48	—	—	—	[117]
298.15	0.1 [c]	*mal*	6.711	11.53	—	—	[114]
310.15	0.15 [b]	*mala*	4.519	—	1.268	—	[115]
	0.2 [c]		3.84	—	1.32	4.74	[117]
310.15	0.15 [b]	*tca*	5.44	—	—	—	[113]

[a] According to the reactions (3.16), (5.1), charges omitted for simplicity; [b] in NaCl; [c] in KCl.

Chapter 6

Thiocarboxylic ligands: results and discussion

The interaction between Al^{3+} and thiocarboxylic ligands was not yet studied. To the best of our knowledge, thermodynamic data on these systems were not reported in the literature yet.
As already discussed in the Chapter 2, this class of ligands was chosen for the presence of the sulphidrilate group in their molecules, in addition to the carboxylate ones.
Generally, thiolates do not show a good affinity towards Al^{3+}, because of their soft character, which does not allow to a good interaction with hard metals. However, if S-donor groups are in a chelating position with respect to an O-donor group, their binding ability may considerably increase [28].
Speciation models and thermodynamic formation parameters of the complexes formed by Al^{3+} with some thiocarboxylic ligands, namely *tla*, *mpa* and *tma*, at T = 298.15 K and $0.15 \leq I$ / mol $L^{-1} \leq 1$ in NaCl, are here reported. These systems were mainly discussed on the basis of potentiometric and calorimetric data. In addition to these techniques, spectrophotometric UV - Vis titrations for Al^{3+}-*mpa* system and ^1H NMR spectroscopic investigations for Al^{3+}-*tla* and -*tma* systems, were performed, in order to confirm the reliability of the formation constants values obtained by potentiometry. For the determination of the stability constants, aluminium hydrolysis reactions, described in the Chapter 4, and the protonations of the ligands were taken into account.

6.1 Ligand protonation constants

In order to study the interaction between Al^{3+} and thiocarboxylic ligands, protonation constants of *tla*, *mpa* and *tma*, were previously studied by the research group [119]. These data, reported in Table 6.1, were recalculated at the same ionic strength and temperature conditions of the metal - ligand complexes ($0.15 \leq I$ / mol $L^{-1} \leq 1$ in NaCl and T = 298.15 K). Moreover, for *tla* and *tma*, these values were confirmed by ^1H NMR investigations.

Table 6.1 Protonation constants of *tla, mpa, tma* at different ionic strength in NaCl

			$\log\beta^H$		Ref.
Ligand	**Species** [a]	I **= 0.15** [b]	I **= 0.5** [b]	I **= 1** [b]	
tla	**LH**	10.02	9.95	9.92	[119]
	LH_2	13.52	13.409	13.421	
mpa	**LH**	10.03	9.98	10.00	[119]
	LH_2	14.37	14.07	14.13	
tma	**LH**	10.227	9.962	9.839	[119]
	LH_2	14.997	14.352	14.109	
	LH_3	18.507	17.402	16.999	

[a] According to the reaction (3.14), charges omitted for simplicity; [b] in mol L^{-1}.

6.2 Al^{3+}-thiocarboxylate complexes

With the aim to define the speciation models and the stability constants of the different species, the study on the Al^{3+}-thiocarboxylate systems was performed by potentiometry at different metal to ligand ratios, reported in the experimental section 3.2.2, different ionic strength values ($0.1 \leq I$ / mol $L^{-1} \leq 1$ in NaCl) and T = 298.15. The experimental formation constants of the complexes, reported in Table 6.2, are expressed as $\log\beta_{pqr}$, according to the equilibrium reaction (3.16). The gained results show quite similar speciation models for each system, with the presence of two common species, ML and MLH. Furthemore, the formation of MLOH and ML_2OH species was observed for Al^{3+}-*tla* system, ML_2 and ML_2OH for Al^{3+}-*mpa* and, lastly, MLH_2 and MLOH for Al^{3+}-*tma.*

The stability of the ML species of Al^{3+} with the investigated thiocarboxylate compounds changes depending on the specific S-donor ligand. At T = 298.15 K and I = 0.15 mol L^{-1}, for example, $\log\beta_{110}$ = 8.33, 8.756, 9.87 for *tla*, *mpa* and *tma*, respectively. As expected, it follows the trend:

$$tla < mpa < tma$$

The higher logβ value of *tma* compared to the other two ligands is probably related to the presence on its molecule of another carboxylic group with respect to *tla* and *mpa*, which gain only two potential binding site (a carboxylate and a thiolate). More in detail, for ML species, $\Delta\log K_{TMA\text{-}TLA}$ = 1.54 and $\Delta\log K_{TMA\text{-}MPA}$ = 1.114, at T = 298.15 K and I = 0.15 mol L^{-1} in NaCl, were found. These results are in agreement with Martell *et al*. assertions, according to which

the affinity of Al^{3+} towards multidentate ligands containing O-donor groups increases with the number and the basicity of the donor groups [28].

Table 6.2 Experimental equilibrium constants for Al^{3+}-*tla*, -*mpa*, -*tma* species (in NaCl) obtained by potentiometry at different ionic strengths and at T = 298.15 K

		logβ		
Ligand	**Species** [a]	I **= 0.15** [b]	I **= 0.5** [b]	I **= 0.94** [b]
tla	**MLH**	12.462(6) [c]	12.675(7) [c]	12.665(6) [c]
	ML	8.33(1)	8.41(1)	8.25(1)
	MLOH	3.62(2)	3.30(3)	2.98(5)
	ML_2OH	11.42(2)	11.53(1)	11.28(1)
mpa	**MLH**	12.71(1)	12.95(1)	12.45(1)
	ML	8.756(6)	8.41(2)	8.11(1)
	ML_2	16.14(3)	16.14(3)	15.41(6)
	ML_2OH	11.47(2)	11.38(3)	10.44(4)
tma	**MLH_2**	17.57(2)	17.30(2)	16.09(3)
	MLH	14.30(1)	13.56(3)	12.16(5)
	ML	9.87(5)	9.58(2)	8.47(1)
	MLOH	6.06(2)	5.34(3)	4.05(3)

[a] According to the reaction (3.16), charges omitted for simplicity; [b] mol L^{-1}; [c] least-squares errors on the last significant figure are given in parentheses.

All the three systems were investigated in a limited pH range ($2 \leq pH \leq 5$), as the formation of sparingly soluble species was experimentally observed. The speciation diagrams, drawn in Figs. 6.1 - 6.3, show significant metal fractions of the complex species over the pH experimental window.

As Al^{3+}-*tla* system concerns, MLH is the predominant species, since it is formed over all the pH range investigated and reaches a maximum fraction of 0.45 at pH = 3.5 and I = 0.15 mol L^{-1}. The formation of ML species is observed in a small pH range, between 3.75 - 4.75, with a maximum Al^{3+} fraction of about 0.35. At pH = 5, where the $M_{13}(OH)_{32}$ hydrolytic species is significant, MLOH and ML_2OH show lower metal fractions, namely 0.15 and 0.4 respectively, at I = 0.15 mol L^{-1}. With the increase of ionic strength, from 0.15 to 1 mol L^{-1} these two minor species decrease, with a metal fraction of 0.1 and 0.3, respectively. On the contrary, MLH species achieves a maximum metal fraction of about 0.6 at I = 1 mol L^{-1}.

The speciation profile of Al^{3+}- *mpa* system is quite similar to the *tla* one, with the significant formation of the MLH species in the pH range from 2 to 4.5, reaching a maximum metal fraction of about 0.3 and 0.6 at I = 0.15 and 1 mol L^{-1}, respectively. In the pH range between 4

and 4.5 ML species is the predominant, reaching a maximum fraction at pH = 4.3 of over 0.5 at I = 0.15 mol L^{-1} and 0.35 at 1 mol L^{-1}. Moreover, for this system, at pH = 5, the $M_{13}(OH)_{32}$ hydrolytic species is significant, where the minor species ML_2 and ML_2OH display lower metal fractions of about 0.15 and 0.3 at I = 0.15 mol L^{-1}, respectively.

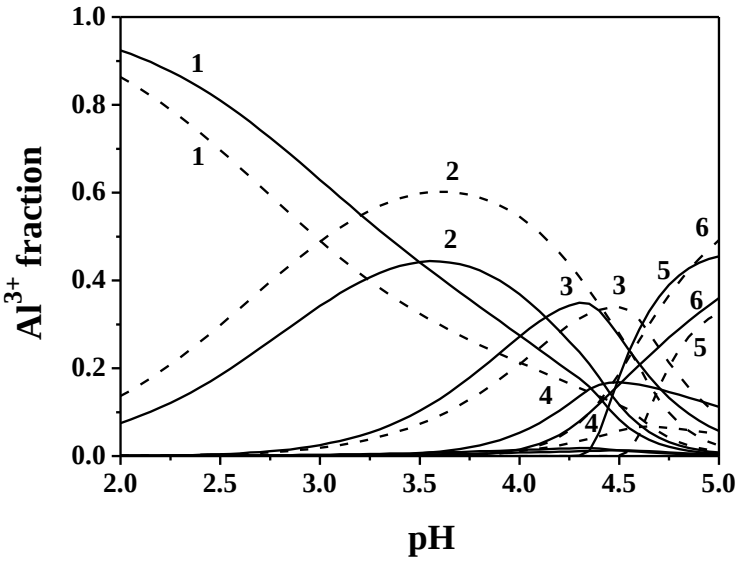

Fig. 6.1 Speciation diagram for Al^{3+}-*tla*, system in NaCl at I = 0.15 (solid line) and I = 1 mol L^{-1} (dotted line), T = 298.15 K. Experimental conditions: C_M = 5 mmol L^{-1}; C_L = 10 mmol L^{-1}. Species: **1. M; 2. MLH; 3. ML; 4. MLOH; 5. ML_2OH; 6. $M_{13}(OH)_{32}$.**

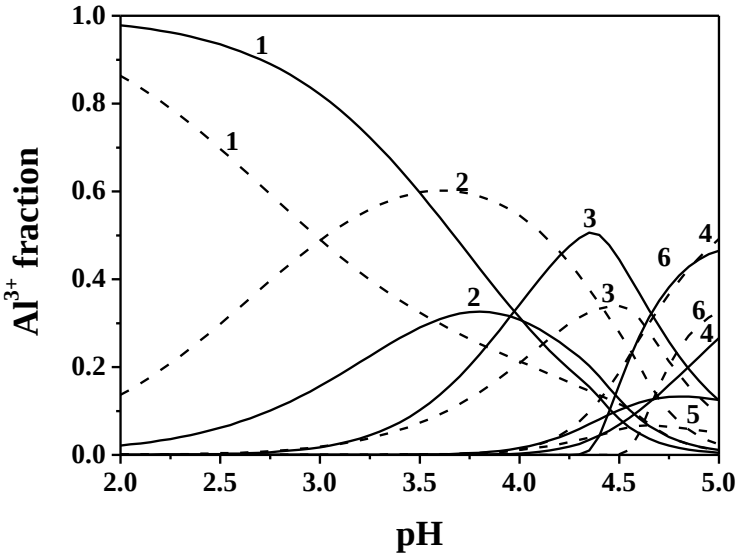

Fig. 6.2 Speciation diagram for Al^{3+}-*mpa* system in NaCl at I = 0.15 (solid line) and I = 1 mol L^{-1} (dotted line), T = 298.15 K. Experimental conditions: C_M = 5 mmol L^{-1}; C_L = 10 mmol L^{-1}. Species: **1. M; 2. MLH; 3. ML; 4. ML_2OH; 5. ML_2; 6. $M_{13}(OH)_{32}$.**

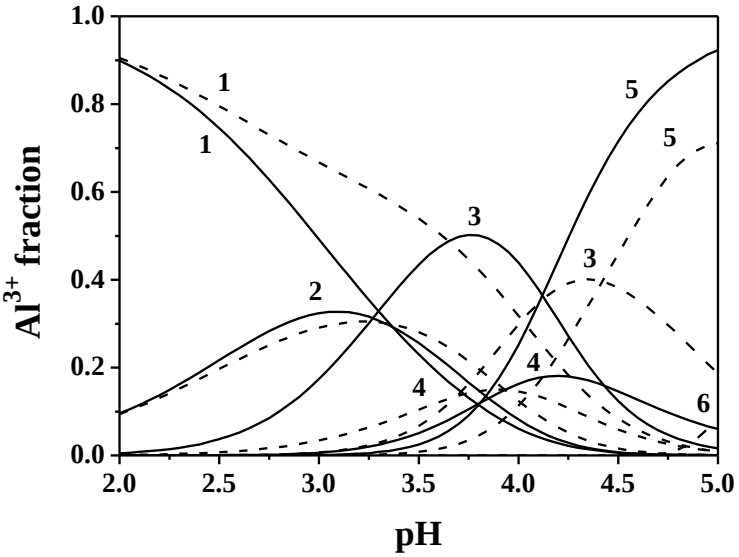

Fig. 6.3 Speciation diagram for Al^{3+}-*tma* system in NaCl at I = 0.15 (solid line) and I = 1 mol L^{-1} (dotted line), T = 298.15 K. Experimental conditions: C_M = 5 mmol L^{-1}; C_L = 10 mmol L^{-1}. Species: **1. M; 2. MLH_2 3. MLH; 4. ML; 5. MLOH; 6. $M_{13}(OH)_{32}$.**

In the case of Al^{3+}-*tma*, the speciation profile is quite different with respect to the previously ones and the metal hydrolysis is suppressed by the formation of the complex species. The formation of MLH_2 achieves a maximum fraction of over 0.3 at pH = 3, whilst MLH is the predominant species at pH = 3.8 with a fraction of about 0.5 at I = 0.15 mol L^{-1}. From pH 4.2 to 5, MLOH species prevails, with a metal fraction of 0.9 at I = 0.15 mol L^{-1}. By increasing the ionic strength from 0.15 to 1 mol L^{-1}, the MLH formation is shifted at higher pH with a maximum fraction of about of 0.4, whilst MLOH species decreases from 0.9 to 0.7 at pH = 5.

6.3 Ionic strength dependence

The dependence of the formation constants on the ionic strength for all the Al^{3+}-thiocarboxylate systems was studied, by analysing the experimental stability constant values in a range of ionic strength between 0.1 and 1 mol L^{-1}, by using an extended Debye - Hückel type equation (eq. 3.23). The obtained values of $\log^T\beta$ together with the empirical parameter C for the dependence on ionic strength are reported in Table 6.3.

Some considerations can be made on the C values, which indicate the influence of the cation and anion of supporting electrolyte on the different formation constants.

For Al^{3+}-*tla* and -*mpa* species, calculated C parameters are positive, except for the ML_2OH of the *mpa* system. From the interaction of Al^{3+} with *tma*, the empirical parameter C results negative for all the complex species. Moreover, it is possible to make a comparison with the C values obtained for the carboxylic ligands.

For example, in the case of ML species of Al^{3+}-*mpa* system, *C* corresponds to a value of 0.30, fairly close to those obtained for ML complex of Al^{3+}-*mal* one (*C* = 0.47, see Table 5.4).

Table 6.3 Equilibrium constants for Al^{3+}-*tla*, -*mpa*, -*tma* species at infinite dilution, together with *C* parameter for the ionic strength dependence (eq. (3.23)), at *T* = 298.15 K

Ligand	Species [a)]	$\log^T\beta$	*C*
tla	**MLH**	13.62(5) [b)]	1.18(8) [b)]
	ML	9.77(5)	1.01(8)
	MLOH	5.12(4)	0.31(5)
	ML_2OH	12.89(6)	0.92(9)
mpa	**MLH**	14.03(6)	0.54(9)
	ML	10.26(3)	0.30(4)
	ML_2	18.24(6)	0.50(9)
	ML_2OH	13.17(6)	-0.26(9)
tma	**MLH_2**	19.84(9)	-0.49(6)
	MLH	16.88(8)	-1.13(7)
	ML	12.34(9)	-0.19(8)
	MLOH	8.37 (7)	-1.14 (6)

[a)] According to the reaction (3.16), charges omitted for simplicity; [b)] least-squares errors on the last significant figure are given in parentheses.

6.4 Temperature dependence

By means of calorimetric measurements, the enthalpy changes regarding the acid - base properties of the ligands and the formation of Al^{3+}-thiocarboxylate complexes under study were determined, at *I* = 0.15 mol L^{-1} in NaCl and *T* = 298.15 K. Protonation thermodynamic parameters are reported in Tables 6.4, together with ΔG and $T\Delta S$ values. The enthalpy changes for the complex species, formed in large amounts in the experimental conditions, are shown in Table 6.5. For ML species, the obtained enthalpy change value is weakly endothermic for all the ligands investigated, precisely for *tla*, *mpa* and *tma*, ΔH = 28, 3, 11 kJ mol^{-1}, respectively. This confirms that Al^{3+}-thiocarboxylate interactions can be considered of non-covalent type, considering that aluminium is involved preferably into electrostatic interactions, with hard ligands, such as O-donor one [42]. As it is well known, these type of interactions are featured by positive enthalpy change values and the driving force of the formation reactions is the entropy.

Table 6.4 Protonation thermodynamic parameters of *tla*, *mpa*, *tma* at T = 298.15 K and at I = 0.15 mol L^{-1}in NaCl

Ligand	Species [a]	$-\Delta G$ [b]	ΔH [b]	$T\Delta S$ [b]	Ref.
tla	**LH**	57.2	-23.7	33.5	[119]
	LH_2	77.1	-21.8	55.3	
mpa	**LH**	57.2	-18(1) [c]	39	This thesis, [120]
	LH_2	82.0	-21(2)	61	
tma	**LH**	58.3	-10(2)	48	This thesis, [120]
	LH_2	85.5	-9(3)	76	
	LH_3	105.6	-11(4)	95	

[a] According to the reaction (3.14), charges omitted for simplicity; [b] in kJ mol^{-1}; [c] least-squares errors on the last significant figure are given in parentheses.

Table 6.5 Thermodynamic parameters Al^{3+}-*tla, -mpa, -tma* complex species obtained by titration calorimetry at I = 0.15 mol L^{-1} in NaCl and T = 298.15 K

Ligand	Species [a]	$-\Delta G$ [b]	ΔH [b]	$T\Delta S$ [b]
tla	**MLH**	71.1	-23(5) [c]	48
	ML	47.5	28(2)	75
	ML_2OH	65.2	49(6)	114
mpa	**MLH**	72.5	-59(4)	13
	ML	49.9	3(2)	53
	ML_2	93.5	-69(4)	24
tma	**MLH**	81.6	25(1)	107
	ML	56.3	11(3)	67
	MLOH	34.6	31.0(9)	65.6

[a] According to the reaction (3.16), charges omitted for simplicity; [b] in kJ mol^{-1}; [c] least-squares errors on the last significant figure are given in parentheses.

6.5 UV - Vis spectrophotometry

Similarly to our previous studies on different systems, spectroscopic techniques have been used with the aim to gain more information on the systems under study and to confirm the speciation model obtained by potentiometric investigations [121-125].

It is well known that molecules containing -SH groups absorb in the UV region. UV - Vis spectrophotometric titrations were carried out on Al^{3+}-*mpa* aqueous solutions, at T = 298.15 K and I = 0.15 mol L^{-1} in NaCl.

Before studying the UV properties of the Al^{3+}-*mpa* species, it was necessary to verify that the metal solution did not absorb and to determine the molar absorbance spectra of each protonated and unprotonated ligand form. Ligand UV properties were studied previously by this research group in the spectral range $220 \leq \lambda / nm \leq 280$ [119].

As concerns Al^{3+}-*mpa* interactions, a wide number of spectra were carried out on metal - ligand mixtures, by varying the metal - ligand ratios and the pH values, as shown in the Section 3.3.2, in the spectral range $220 \leq \lambda / nm \leq 280$. Unlike potentiometric measurements, the wider pH range ($2 \leq pH \leq 8.4$), investigated with this technique, is due to the possibility of using lower concentrations of ligand and metal cation. The speciation model for Al^{3+}-*mpa* system, was confirmed by the analysis of spectrophotometric data through the HypSpec software program [75], which allowed to calculate the formation constants and the molar absorption coefficient for each complex. These ones are shown in Fig. 6.4, whilst formation constant values are reported in Table 6.6, together with those obtained by potentiometric investigations. Only the stability constant of the ML species, was determined with a similar value to the one obtained by the potentiometry ($\log\beta_{UV}$ = 8.85 *v.s.* $\log\beta_{ISE\ H^+}$ = 8.756), since it is the predominant in the experimental conditions, as displayed in Fig. 6.2. For this calculation, the formation constant values of the other species, gained by potentiometric titrations, were kept constant.

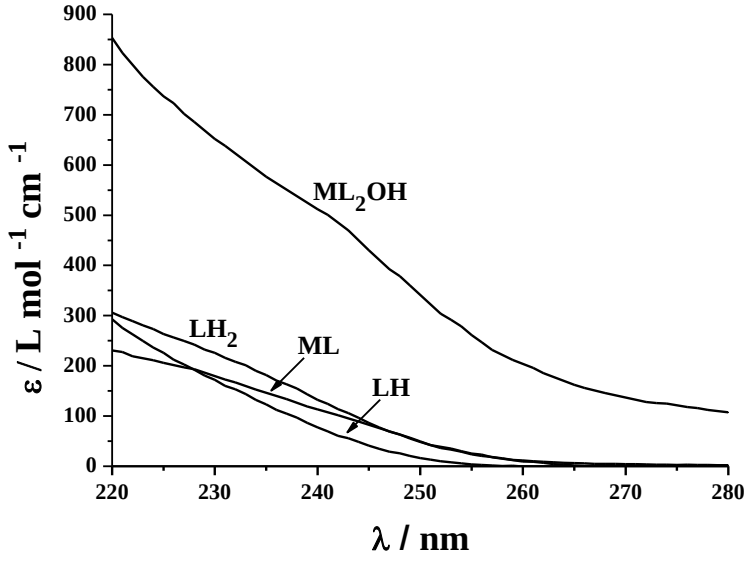

Fig. 6.4 Molar absorbance of Al^{3+}-*mpa* species at I = 0.15 mol L^{-1} in NaCl and T = 298.15 K.

Table 6.6 Comparison between experimental equilibrium constants of Al^{3+}-*mpa* species obtained by spectrophotometry and potentiometry at I = 0.15 mol L^{-1} (NaCl) and T = 298.15 K

Ligand	Species [a)]	$\log\beta_{UV}$	$\log\beta_{ISE\ H^+}$
mpa	**MLH**	12.71	12.71
	ML	8.85(9) [b)]	8.756
	ML_2	16.14	16.14
	ML_2OH	11.47	11.47

[a)] According to the reaction (3.16), charges omitted for simplicity; [b)] least-squares errors on the last significant figure are given in parentheses.

6.6 ^{1}H NMR spectroscopy

For Al^{3+}-*tla* and -*tma* systems, ^{1}H NMR investigations in H_2O/D_2O solutions were carried out, in order to confirm the interaction between Al^{3+} and these molecules containing -SH groups. The spectra of these systems were collected in a small pH range, from pH = 2 up to 5, because of the formation of a sparingly soluble species, which hindered further investigations at higher pH values. The titrations were performed on metal - ligand solutions, which differ for the metal - ligand concentration ratios, as reported in the Section 3.5.2. For both metal-containing systems, all the recorded spectra showed single average resonances related to each kind of proton, suggesting that all the species at equilibrium were involved in a rapid mutual exchange on the NMR time scale. For this reason, it was not possible to distinguish a signal due to the bound ligand with respect to the free one, for both the systems. In general, for all the collected spectra, a slightly shielding of the signals was observed with the increase of the pH values. More in detail, as concerns Al^{3+}-*tla* system, both -CH_3 and -CH- groups were subject to an upfield shift of the signals with respect to those of the metal free ligand solutions. On the contrary, from pH = 4, chemical shift of both metyl and methyne groups were deshielded with respect to the signal of the ligand solution. Al^{3+}-*tma* solution spectra showed an analogous behaviour, even though *tma* is characterized by one more -COOH group with respect to *tla*. In Fig 6.5 a spectrum of Al^{3+}-*tma* solution recorded at pH = 3.2 is shown. In all the investigated pH range, with the increasing of the pH, spectra showed a slightly upfield shift of the proton resonances with respect to the signals of the free-metal ligand. From the collected spectra, it seemed that the high tendency of *tma* to hydrolize played a key role in the formation of the aluminium complex species. Although it was not possible to get more information from the recorded spectra, the obtained chemical shift values of each single species were essential to determine the stability constants of the Al^{3+} complexes for both the systems and to recalculate the average δ values at each experimental pH value. The ^{1}H NMR

data obtained are reported in table 6.7 and 6.8 for Al^{3+} -*tla* and -*tma* species, respectively. The gained results are referred to the formation constants of the predominant species in the experimental conditions, namely MLH and ML for Al^{3+}-*tla* and MLH_2 and MLH for Al^{3+}-*tma*, respectively. These are comparable to those collected by potentiometric titrations, as shown in Table 6.9. The other values, calculated by potentiometric data, were considered in the model and kept constant. The good agreement between experimental and calculated NMR parameters, as displayed in Fig. 6.6, allowed to validate both the speciation models provided by potentiometric investigations.

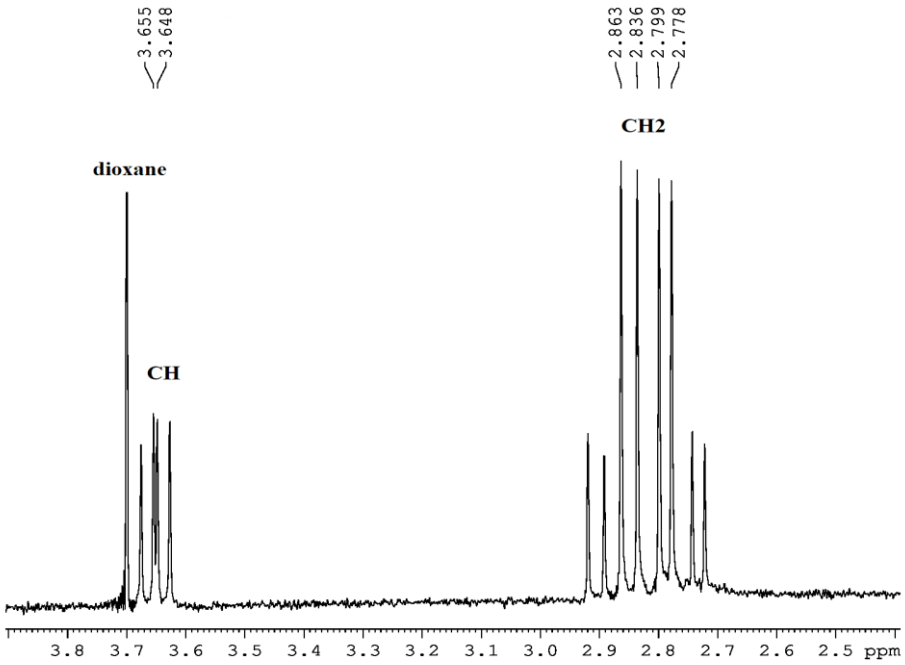

Fig. 6.5 ^{1}H NMR spectrum of *Al^{3+} -tma* system at C_L = 10 mmol L^{-1} and C_M = 5 mmol L^{-1}, pH = 3.2, *T* = 298.15 K and *I* = 0.15 mol L^{-1} in NaCl.

Table 6.7 Protonation constants of *tla*, formation constants and calculated chemical shifts of Al^{3+}-*tla* species obtained by ^{1}H NMR at *I* = 0.15 mol L^{-1} (NaCl) and *T* = 298.15 K

Species [a)]	**logβ**	**δ_{CH3}**	**δ_{CH}**
L		1.252(6) [b)]	3.295(1) [b)]
LH	10.29(1) [b)]	1.379(6)	3.426(1)
LH_2	13.8(1)	1.434(6)	3.592(1)
MLH	12.3 (1)	1.350(7)	3.35(1)
ML	8.4 (3)	1.426(7)	3.51(1)
MLOH	3.62	1.406(7)	3.48(1)
ML_2OH	11.42	1.404(7)	3.48(1)

[a)] According to the reactions (3.14), (3.16), charges omitted for simplicity; [b)] least-squares errors on the last significant figure are given in parentheses.

Table 6.8 Protonation constants of *tma*, formation constants and calculated chemical shifts of Al^{3+}-*tma* species obtained by ^1H NMR at I = 0.15 mol L^{-1} (NaCl) and T = 298.15 K

Species [a]	logβ	δ_{CH}	δ_{CH2}
L		3.458(3) [b]	2.467(7) [b]
LH	10.53 (3) [b]	3.552(3)	2.571(7)
LH_2	15.08(4)	3.602(3)	2.787(7)
LH_3	18.18 (4)	3.766(3)	2.917(7)
MLH_2	17.7 (4)	3.71(2)	2.84(2)
MLH	14.5 (7)	3.54(2)	2.78(2)
ML	9.87	3.87(2)	2.13(2)
MLOH	6.06	3.48(2)	2.86(2)

[a] According to the reactions (3.14), (3.16), charges omitted for simplicity; [b] least-squares errors on the last significant figure are given in parentheses.

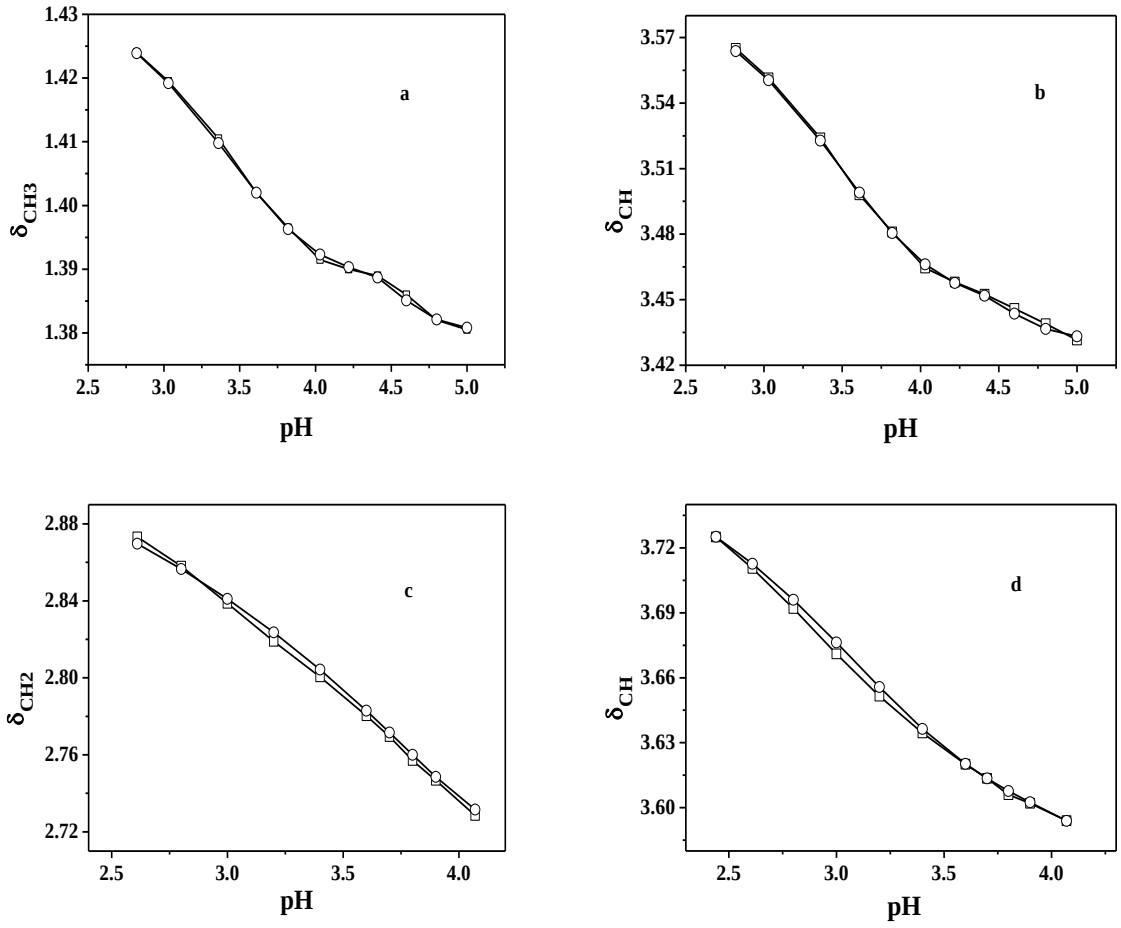

Fig. 6.6 Experimental (□) and calculated (○) values of the chemical shifts of the ligand in Al^{3+}-*tla* (**a**, **b**) and Al^{3+}-*tma* (**c**, **d**) mixtures (C_M = 5 mmol L^{-1}, C_L = 10 mmol L^{-1}).

Table 6.9 Comparison between experimental equilibrium constants of Al^{3+}-*tla, -tma* species obtained by ^1H NMR and potentiometry at I = 0.15 mol L^{-1} (NaCl) and T = 298.15 K

Ligand	Species [a]	$\log\beta_{H\ NMR}$	$\log\beta_{ISE\ H^+}$
tla	**MLH**	12.3(1) [b]	12.462(6) [b]
	ML	8.4(3)	8.33(1)
	MLOH	3.62 [c]	3.62(2)
	ML_2OH	11.42 [c]	11.42(2)
tma	**MLH_2**	17.7(4) [b]	17.57(2) [b]
	MLH	14.5 (7)	14.30(1)
	ML	9.87 [c]	9.87(5)
	MLOH	6.06 [c]	6.06(2)

[a] According to the reaction (3.16), charges omitted for simplicity; [b] least-squares errors on the last significant figure are given in parentheses; [c] potentiometric data kept constant in the calculations.

6.7 Literature comparisons

To the best of our knowledge, the study on the Al^{3+} interaction with thiocarboxylic ligands is not reported in the literature yet. The data here obtained can be compared only with those related to Al^{3+}-carboxylates and -amino acids systems. In particular, for Al^{3+}-*lac* system, reported in the previous chapter, it was asserted that logβ = 2.26 for ML species, at T =298.15 K and I = 0.1 mol L^{-1} (this thesis and [116]). The ML stability for this system results much lower than the one here found for Al^{3+}-*tla* interaction ($\log\beta_{110}$ = 8.33 at T = 298.15 K and I = 0.15 mol L^{-1} in NaCl). Referring to ML species, Berthon *et al.*, in several papers report $\log K_{110}$ = 3.753, 3.788, 4.519, for succinate, tartrate, malate, at physiological conditions (T = 310.15 K and I = 0.15 mol L^{-1} in NaCl) [115, 126, 127]. In the previous chapter the interactions of aluminium with some carboxylic ligands were discussed in the same conditions of temperature and ionic strength, namely T = 298.15 K and I = 0.15 mol L^{-1} in NaCl. In the case of these systems we found log$K$ = 6.40, 4.25, 4.765, 5.87, 5.89, for *mal*, *mala*, *tca*, *btc* and *mlt*, respectively (this thesis and [66]). As amino acids concern, there are some papers which report the stability constants of Al^{3+} species with glycine, serine, threonine, aspartic acid, glutamic acid (log$K$ = 5.91, 5.66, 5.51, 7.87, 7.29, respectively at T = 298.15 K and I = 0.02 mol L^{-1} in KCl) [27, 128]. Furthermore, in the next chapter the results of aluminium speciation with some amino acids, such as glycine (*Gly)* and cysteine (*Cys*), will discuss at T = 298.15 K and I = 0.15 mol L^{-1} in NaCl, where log$K$ = 7.18, 11.91 for *Gly* and *Cys*, respectively (this thesis and [129]). All the data both present in the literature and in this thesis, indicate that formation constant values concerning dicarboxylates,

hydroxycarboxylates and amino acids (except for *Cys*) are lower than those gained for thiocarboxylates under study, namely log*K* = 8.33, 8.756, 9.87 for *tla*, *mpa* and *tma*, respectively.

Chapter 7

Amino acids: results and discussion

The study of the Al^{3+} interaction with amino acids is of great importance, as already pointed out in the Section 2.4, since these small biomolecules containing some potential metal binding sites that may be involved in the uptake and the transport of this metal cation, especially in the gastrointestinal tract. Moreover, amino acids may be also considered as a compound model for the assessment of metal ion binding ability of larger biomolecules, such as proteins, in biological fluids.

In this chapter, a thermodynamic and spectroscopic study concerning the interactions of Al^{3+} with some amino acid ligands, such as glycine (*Gly*), cysteine (*Cys*) and tranexamic acid (*tranex*) was reported. The stability constants of the complex species are determined by the elaboration of potentiometric data, obtained at T = 298.15 K and $0.15 \leq I$ / mol $L^{-1} \leq 1$ in NaCl aqueous solutions. Unfortunately, the pH range investigated, as reported in the section 3.2.2, is limited by the formation of sparingly soluble species, even though complex formation should enhance the Al^{3+} solubility [13]. Calorimetric titrations were also performed at T = 298.15 K and I = 0.15 mol L^{-1} in NaCl, in order to obtain thermodynamic formation parameters for the dependence of stability constants on the temperature. With the aim to confirm the speciation profiles of Al^{3+}-*tranex* and -*Cys* complexes, ^{1}H NMR titrations (at T = 298.15 K and I = 0.15 mol L^{-1} in NaCl) were also carried out for both the systems. In the same conditions of temperature and ionic strength, for Al^{3+}-*Cys*, UV - Vis spectrophotometric investigations were also conducted.

The stability constants of the complex species of the three systems were calculated by taking into account the aluminium hydrolysis reactions, already discussed, and the ligand protonations.

7.1 Ligand protonation constants

Protonation constants of *Gly*, *Cys* and *tranex* were previously determined, but only those related to glycine and cysteine were already published [130, 131]. These data, reported in Table 7.1, were recalculated at the same ionic strength and temperature conditions of the metal - ligand complexes ($0.15 \leq I$ mol $L^{-1} \leq 1$ in NaCl and T = 298.15 K). In addition, for *Cys* and *tranex* these values were confirmed by ^{1}H NMR investigations.

Table 7.1 Protonation constants of *Cys*, *-Gly*, *-tranex* at T = 298.15 K and at different ionic strength (NaCl)

		$\log\beta^{H}$			**Ref.**
Ligand	**Species** [a]	I **= 0.15** [b]	I **= 0.5** [b]	I **= 1** [b]	
Gly	**LH**	9.571	9.562	9.619	[130]
	LH_2	11.933	11.938	12.043	
Cys	**LH**	10.160	10.168	10.215	[131]
	LH_2	18.301	18.327	18.430	
	LH_3	20.325	20.309	20.411	
tranex	**LH**	10.481	10.534	10.654	Unpublished data from this laboratory
	LH_2	14.777	14.845	15.097	

[a] According to the reaction (3.14), charges omitted for simplicity; [b] mol L^{-1}.

7.2 Al^{3+}-amino acid complexes

The study on the Al^{3+}-amino acid systems was performed at different ionic strength values ($0.1 \leq I$ mol $L^{-1} \leq 1$ in NaCl), T = 298.15 K and different metal - ligand concentration ratios, reported in the experimental section 3.2.2, with the purpose to define the speciation models, the stoichiometry and the formation constant values of the species. Al^{3+}-amino acid stability constants are expressed as $\log\beta_{pqr}$, according to the equilibrium reaction (3.16), and are reported in Table 7.2. The speciation models for all the three systems show some differences, since they are characterized by MLH, ML and $M_2L_2(OH)_2$ in the case of *Gly*, ML, M_2L and MLOH for *Cys* and MLH and MLOH for *tranex*. The analysis of potentiometric data allowed to gain for ML species logβ = 7.18, 11.91 for *Gly* and *Cys*, respectively. This clearly means that the additional presence of a -SH group in the cysteine with respect to the glycine, besides -COOH and $-NH_2$ groups, strongly affects the binding ability of this compound and the complex stability. It is known that amines and thiolates have not a good affinity towards hard

metal cations, such as the aluminium, but if amino or thiolate groups are in a chelating position close to a O-donor group, their ability to form stable complexes may further increase [5]. Moreover, for multidentate ligands with O-donor groups, the affinity toward Al^{3+} improves with the increase of the basicity and the number of donor groups [28].

Table 7.2 Experimental formation constants for Al^{3+}-*Gly*, -*Cys*, -*tranex* species (in NaCl) obtained by potentiometry at different ionic strengths and at T = 298.15 K

		logβ		
Ligand	**Species** [a]	***I* = 0.15** [b]	***I* = 0.5** [b]	***I* = 1** [b]
Gly	**MLH**	11.698(7) [c]	11.55(6) [c]	11.694(4) [c]
	ML	7.18(1)	7.212(7)	7.245(5)
	$M_2L_2(OH)_2$	8.62(2)	7.84(5)	8.29(1)
Cys	**ML**	11.91(3)	11.60(5)	11.48(4)
	M_2L	15.17(1)	14.89(1)	14.24(7)
	MLOH	6.96(2)	6.39(4)	6.70(5)
tranex	**MLH**	13.31(1)	13.33(2)	13.26(2)
	MLOH	4.61(1)	4.66(2)	4.52(1)

[a] According to the reaction (3.16), charges omitted for simplicity; [b] mol L^{-1}; [c] least-squares errors on the last significant figure are given in parentheses.

The speciation profiles, presented in Figs. 7.1 - 7.3, show a very small pH experimental window, due to the formation of slowly soluble species for all the systems under study. In the case of Al^{3+}-*Gly* system, whose speciation diagram is drawn in Fig 6.1 at I = 0.15 mol L^{-1}, MLH is the main complex species from pH = 2 up to pH ≈ 4.1, with a metal fraction of about 0.4, which decreases to 0.3 with the increase of ionic strength. ML and $M_2L_2(OH)_2$ are present in lower fractions in a small range of pH between 4 and 4.5. For Al^{3+}-*Cys* system, the complexation starts from pH ≈ 3.5 at I = 0.15 mol L^{-1}, with the predominant M_2L species, with an Al^{3+} maximum fraction equal to 0.6 at pH = 4.2. ML and MLOH species are formed in a limited pH range, with a fraction of almost 0.3 and 0.2 at pH 4.5 and 5, respectively. The increase of the ionic strength from 0.15 to 1 mol L^{-1} brings to a significant lowering of the M_2L species fraction, namely from 0.6 to 0.3 at pH = 4.2. The speciation profile of the Al^{3+}-*tranex* system shows higher metal fraction with respect to the previous ones. At I = 0.15 mol L^{-1}, both MLH and MLOH species reach a maximum fraction of 0.5 at pH = 4 and 4.5,

respectively. With the increase of the ionic strength MLH species undergoes to a decrease of the molar fraction, from 0.5 to 0.4 at pH = 4.

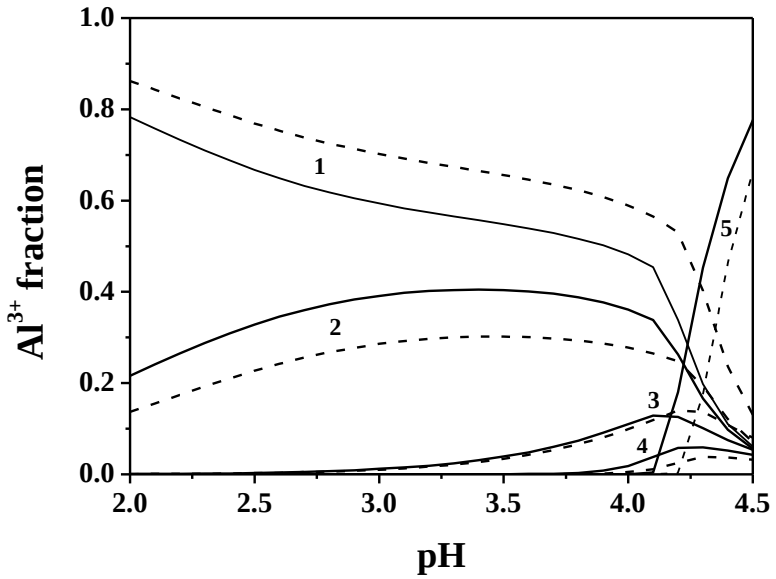

Fig. 7.1 Speciation diagram for Al^{3+}-*Gly* system in NaCl at I = 0.15 mol L^{-1} (solid line) and I = 1 mol L^{-1} (dotted line), T = 298.15 K. Experimental conditions: C_M = 4 mmol L^{-1}; C_L = 8 mmol L^{-1}. Species: **1. M; 2. MLH; 3. ML; 4. $M_2L_2(OH)_2$; 5. $M_{13}(OH)_{32}$.**

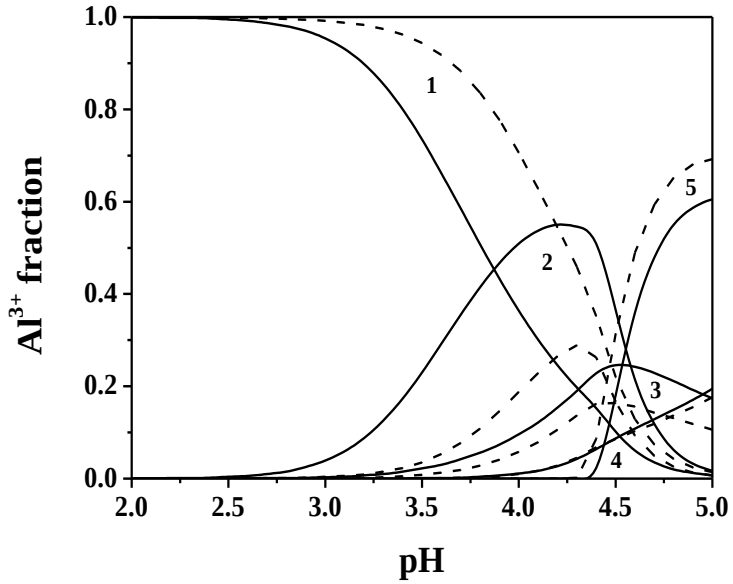

Fig. 7.2 Speciation diagram for Al^{3+}-*Cys* system in NaCl at I = 0.15 mol L^{-1} (solid line) and I = 1 mol L^{-1} (dotted line), T = 298.15 K. Experimental conditions: C_M = 4 mmol L^{-1}; C_L = 8 mmol L^{-1}. Species: **1. M; 2. M_2L; 3. ML; 4. MLOH; 5. $M_{13}(OH)_{32}$.**

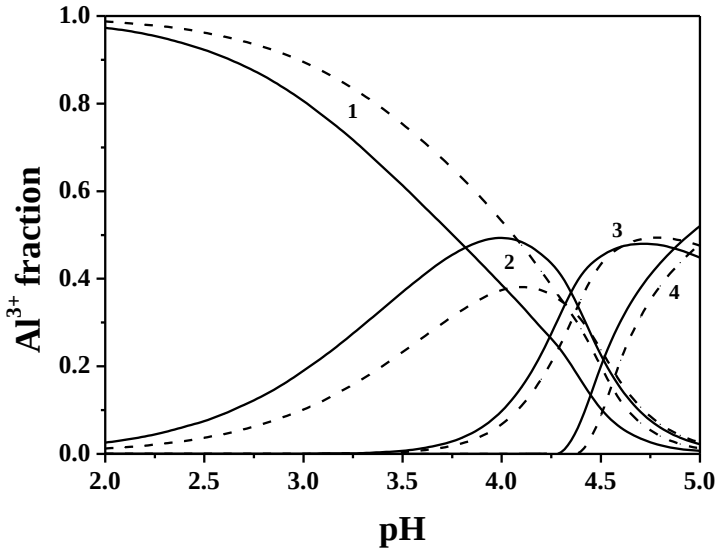

Fig. 7.3 Speciation diagram for Al^{3+}-*tranex* system in NaCl at I = 0.15 mol L^{-1} (solid line) and I = 1 mol L^{-1} (dotted line), T = 298.15 K. Experimental conditions: C_M = 4 mmol L^{-1}; C_L = 8 mmol L^{-1}. Species: **1. M; 2. MLH; 3. MLOH; 4. $M_{13}(OH)_{32}$.**

7.3 Ionic strength dependence

With the aim of evaluating the dependence of the stability constants on ionic strength for all the species of the systems under study, the experimental values obtained in the range of ionic strength between 0.15 and 1 mol L^{-1} were analyzed by means of a Debye - Hückel type equation (3.23), expressed in the Section 3.7.3. The calculations allowed to determine $\log^T\beta$ values for all the species, together with the empirical parameter C for the dependence on ionic strength. These results are reported in Table 7.3. C parameters calculated for all the species, except for M_2L of Al^{3+}-*Cys*, are positive and included in a range between 0.1 and 1. These values, with respect to those of thiocarboxylic ligands, are quite similar to Al^{3+}-*tla* and -*mpa* ones, which are contained within the range between 0.30 and 1.18 (see Table 6.3, except ML_2OH species of Al^{3+}-*mpa* system). On the contrary, for Al^{3+}-*tma* complexes, C parameters are all negative (this thesis and [120]).

For ML species of Al^{3+}-*mal* system, C, with a value of 0.47, is comparable to the one obtained for Al^{3+}-*Gly* and -*Cys*, where it is 0.6 for both (this thesis and [66]).

As already pointed out, the knowledge of the thermodynamic constants and C parameters for each species is useful to calculate the stability constants at any ionic strength over all the investigated range.

Table 7.3 Formation constants for Al^{3+}-*Gly*, -*Cys*, -*tranex* species at infinite dilution, together with *C* parameter of eq. (3.23) in NaCl, at T = 298.15 K

Ligand	Species [a]	$\log^T\beta$	*C*
Gly	**MLH**	11.9(2) [b]	0.2(3) [b]
	ML	7.9(2)	0.6(3)
	$\mathbf{M_2L_2(OH)_2}$	10.1(2)	1.0(3)
Cys	**ML**	13.31(7)	0.6(1)
	$\mathbf{M_2L}$	16.0(1)	-0.6(1)
	MLOH	8.2(1)	0.9(2)
tranex	**MLH**	13.57(8)	0.1(1)
	MLOH	5.6(1)	0.6(2)

[a] According to the reaction (3.16), charges omitted for simplicity; [b] least-squares errors on the last significant figure are given in parentheses.

7.4 Temperature dependence

The determination of the enthalpy changes for the systems under study is of fundamental importance, in order to complete the framework of the thermodynamic parameters.

The enthalpy changes of the complex species were gained by means of calorimetric titrations, carried out at T = 298.15 K and I = 0.15 mol L^{-1} in NaCl. In addition, for tranexamic acid ΔH protonation values were obtained under the same experimental conditions of ionic strength and temperature employed for the complex study. These values were here reported for the first time in Table 7.4, together with the enthalpy protonation values of glycine and cysteine. The enthalpy changes for the Al^{3+}-*Gly*, -*Cys*, -*tranex* complex species, were collected in Table 7.5, together with ΔG and $T\Delta S$ values. As expected for hard-hard interactions, also in this case, the contribution to the Gibbs free energy is mainly entropic in nature. In fact, for ML species of Al^{3+}-*Cys*, ΔH = 35 kJ mol^{-1} and $T\Delta S$ = 103 kJ mol^{-1}. The enthalpy change of this species is quite similar to the one found for ML of Al^{3+}-*tla* system (ΔH = 28 kJ mol^{-1}) (this thesis and [120]). Moreover, by considering the MLH species of *Gly* and *tranex*, according to the reaction (3.17), ΔH = 16, 43 kJ mol^{-1} and $T\Delta S$ = 3.8, 27 kJ mol^{-1}, respectively.

The enthalpy change values, here reported at T = 298.15 K, are useful to calculate the formation constants of the complex species at any other temperature value, by means of the Van't Hoff equation (3.24), for example at physiological value (T = 310.15 K), thus evaluating the temperature effect on the speciation.

Table 7.4 Thermodynamic protonation parameters of *Gly*, *Cys* and *tranex* obtained by titration calorimetry at I = 0.15 mol L^{-1} in NaCl and T = 298.15 K

Ligand	Species [a]	$-\Delta G$ [b]	ΔH [b]	$T\Delta S$ [b]	Ref.
Gly	**LH**	54.8	-44.8	10	
	LH_2	68.2	-48.9	19.3	[130]
Cys	**LH**	58.0	-42	16	
	LH_2	104.5	-77	27.5	[131]
	LH_3	116.0	-81	35	
tranex	**LH**	59.8	-52.0(5) [c]	7.8	This thesis
	LH_2	84.3	-49.8(8)	34.5	

[a] According to the reaction (3.14), charges omitted for simplicity; [b] in kJ mol^{-1}; [c] least-squares errors on the last significant figure are given in parentheses.

Table 7.5 Thermodynamic formation parameters of Al^{3+}-*Gly* -*Cys*, -*Tranex* species obtained by titration calorimetry at I = 0.15 mol L^{-1} in NaCl and T = 298.15 K

Ligand	Species [a]	$-\Delta G$ [b]	ΔH [b]	$T\Delta S$ [b]
Gly	**MLH**	66.8	-41(5) [c]	26
Cys	**ML**	68.0	35(3)	103
	M_2L	86.6	-11(1)	76
	MLOH	39.7	52(3)	92
tranex	**MLH**	76.0	-25(3)	51
	MLOH	26.3	-51(1)	-25

[a] According to the reaction (3.16), charges omitted for simplicity; [b] in kJ mol^{-1}; [c] least-squares errors on the last significant figure are given in parentheses.

7.5 UV - Vis spectrophotometry

For Al^{3+}-*Cys* system, UV - Vis spectrophotometric titrations were carried out at T = 298.15 K and I = 0.15 mol L^{-1} in NaCl aqueous solutions, in order to investigate the UV properties of the complexes and to confirm the speciation model obtained by potentiometry. A wide number of spectra were collected in the pH range between 2.4 and 7.0, by varying metal - ligand concentration ratios. The study on a wider range of pH was possible since lower concentrations of the metal cation and ligands were used with respect to those employed in the potentiometric titrations. Some experimental spectra are shown in Fig. 7.4, where the absorbance increases with the increasing of the pH.

The obtained results were reported in Table 7.6, where the formation constant values of the ML and MLOH species were shown. M_2L formation constant value, obtained by potentiometry, was kept constant in the elaboration of the spectrophotometric data. ML and MLOH stability constants (logβ =12.20, 6.93) are very close to the ones already obtained by the potentiometric study, in particular MLOH value.

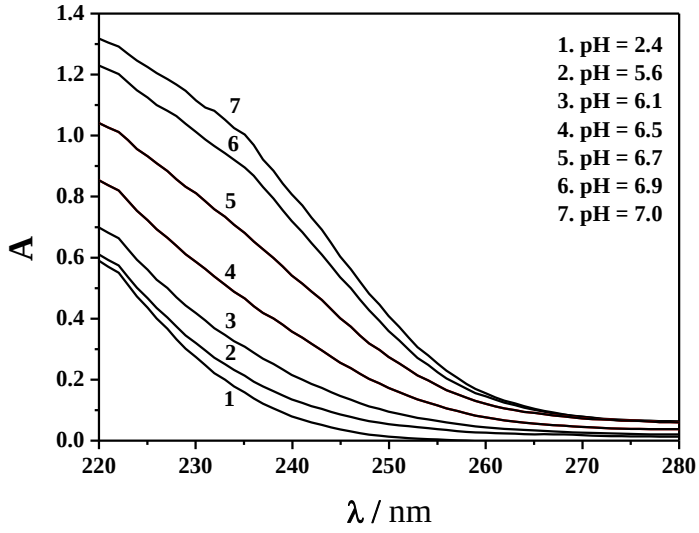

Fig. 7.4 Experimental spectra of Al^{3+}-*Cys* solutions at different pH values, I = 0.15 mol L^{-1} (NaCl), T = 298.15 K. Experimental conditions: C_M = 1 mmol L^{-1}; C_L = 4 mmol L^{-1}.

Table 7.6 Experimental formation constants of Al^{3+}-*Cys* species obtained by spectrophotometry at I = 0.15 mol L^{-1} (NaCl) and T = 298.15 K

Species [a)]	**logβ_{UV}**
ML	12.20(4) [b)]
M_2L	15.17
MLOH	6.93(4)

[a)] According to the reaction (3.16), charges omitted for simplicity; [b)] least-squares errors on the last significant figure are given in parentheses.

7.6 ^{1}H NMR spectroscopy

^{1}H NMR titrations were performed for *Cys*, *tranex*, Al^{3+}-*Cys* and -*tranex* systems, in D_2O/H_2O solutions at T = 298.15 K and I = 0.15 mol L^{-1} in NaCl. As far as metal free *Cys* solutions concerned, whose spectrum is shown in Fig. 7.5, an upfield shift of the methyne group signal, from 4.1 to 3.9 ppm, was observed at low pH. This indicated that the deprotonation of the carboxylic group occurred below pH = 3.5, as already pointed out in previous studies [108, 132, 133]. In the pH range between 3.5 and 7, where LH_2 appeared to be the most abundant species, CH signal remained unaltered. After neutral pH, this signal started to decrease up to a value of 3.2 ppm at pH = 11. In addition, with the increase of the pH a deshielding of the CH_2 resonance was observed, even though less pronounced.

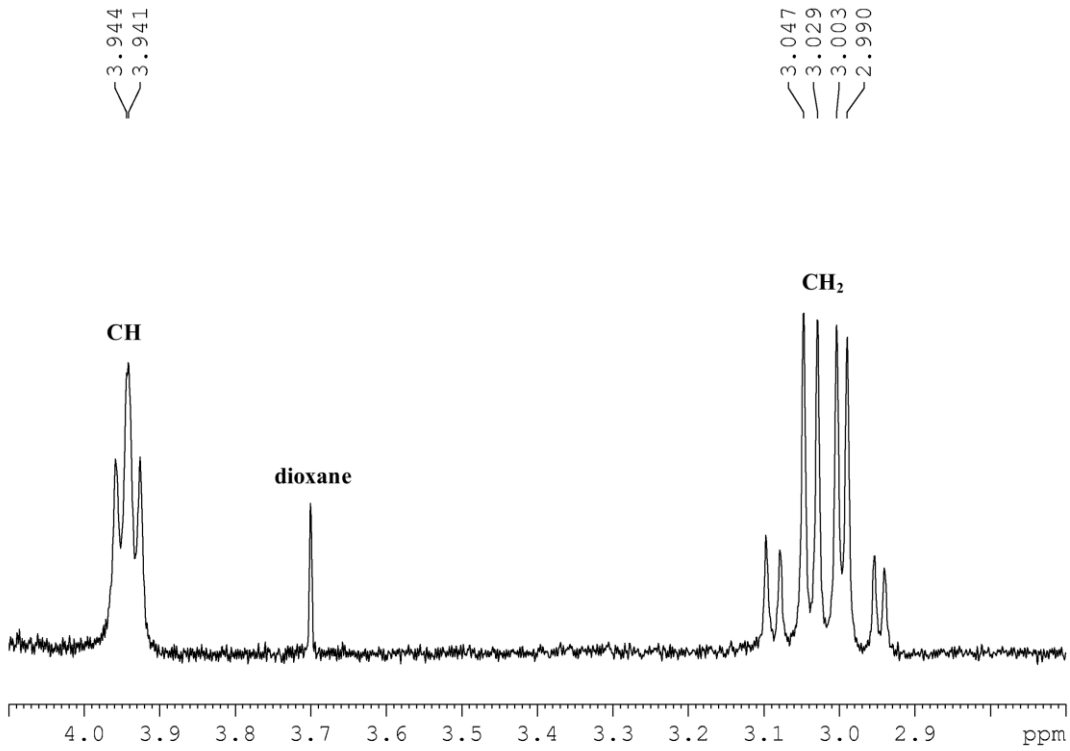

Fig. 7.5 ^{1}H NMR spectrum of *Cys* at C = 8 mmol L^{-1}, pH = 4.0, T = 298.15 K and I = 0.15 mol L^{-1} in NaCl.

The investigations on the Al^{3+}-*Cys* solutions were carried out in a small pH range, since the formation of a sparingly soluble species occurred as well as in potentiometric titrations. The presence of the metal in these solutions left almost unchanged the chemical shift of both methyne and methylene resonances, unlike other metal-*Cys* studied systems, where the strong affinity of the metal cation towards S-donor ligands was evident from the analysis of the NMR spectra [108, 109, 132]. The only visible difference in the spectra of the Al^{3+} containing

solutions was a slightly deshielding of the CH signal, with respect to the one related to the *Cys* alone.

As *tranex* solutions concerns, the spectra collected showed an upfield shift of the signals of the methyne and methylenic groups at pH < 6, which are those close to the carboxylic moiety, as displayed in Fig 7.6, together with a metal free *tranex* spectra. In particular, CH(1) showed a shielding quite pronounced with respect to the other ones, precisely from 2.3 to 2.08 ppm. A similar trend is observed from the cycloaliphatic CH_2 signals, namely CH_2(2,6) and CH_2(3,5), whose resonances shifted to lower ppm. With the increasing of the pH, all these signals remained unaltered up to pH = 8.5, after that they shifted to higher fields. On the contrary, the peaks related to the CH(4) and CH_2(7) close to the amino group were subject to a constant shielding effect up to 1.6 and 2.83 ppm, respectively, at pH = 8.5. After this pH value, these signals started to shift towards lower fields, because of the deprotonation of the $-NH_3^+$ group.

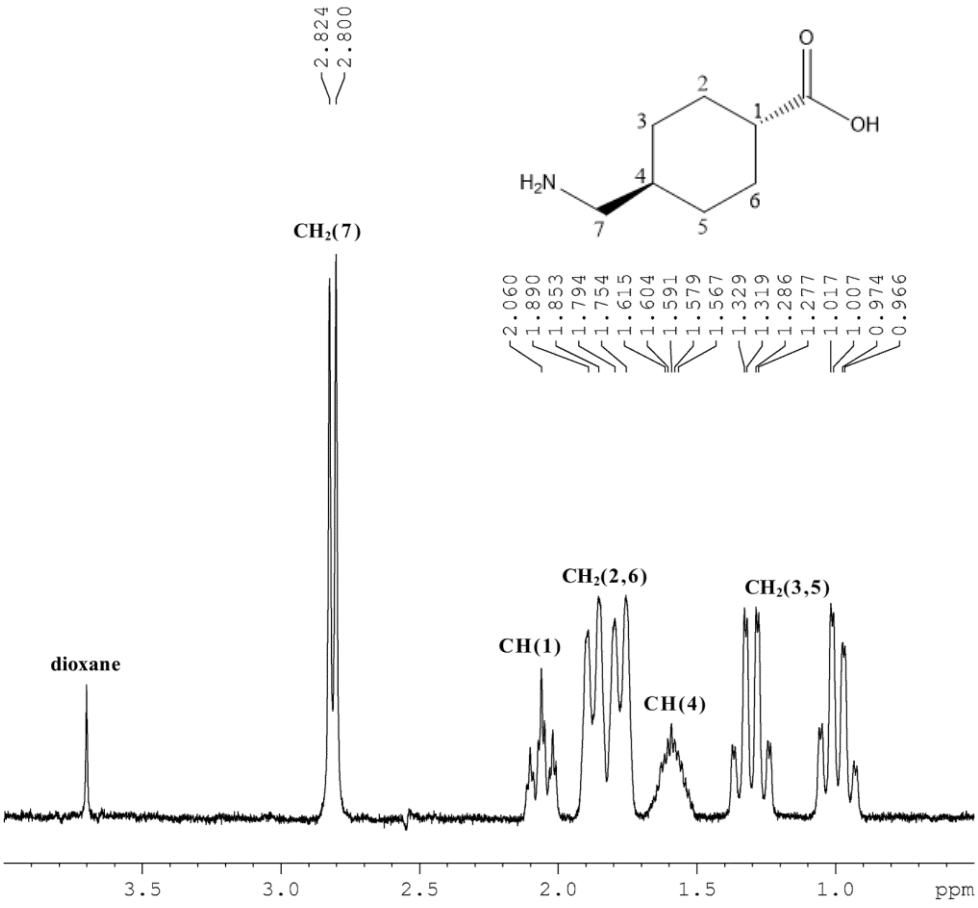

Fig. 7.6 ^{1}H NMR spectrum of *tranex* at C = 8 mmol L^{-1}, pH = 7.07, *T* = 298.15 K and *I* = 0.15 mol L^{-1} in NaCl.

As already discussed for Al^{3+}-*Cys* system, the presence of the metal in the case of the Al^{3+}-*tranex* solutions, did not implicate significant changes in the spectra. For this reasons, it was

not possible to distinguish free and bound ligand directly from the analysis of the data collected, as all the species present at equilibria were involved in a rapid mutual exchange on the NMR time scale. Despite this, the formation constants of the complexes for both the systems, the ligand protonation constants and the average chemical shifts of each species were calculated and reported in Tables 7.7 and 7.8. The ML constant value (obtained by potentiometry) of the Al^{3+}-*Cys* system, was kept constant in the data processing.

Table 7.7 Formation constants and calculated chemical shifts of Al^{3+}-*Cys* species obtained by ^1H NMR at I = 0.15 mol L^{-1} (NaCl) and T = 298.15 K

Species [a)]	**logβ**	**δ_{CH}**	**δ_{CH_2}**
L		3.020(1) [b)]	2.613(1) [b)]
LH	10.61(2) [b)]	3.516(1)	2.831(1)
LH_2	18.91(2)	3.939(1)	3.017(1)
LH_3	20.80(4)	4.307(3)	3.113(1)
ML	11.91	3.913(3)	3.00(2)
M_2L	15.0(4)	3.969(3)	3.03(2)
MLOH	7.0(5)	3.926(3)	3.01(2)

[a)] According to the reactions (3.14), (3.16), charges omitted for simplicity; [b)] least-squares errors on the last significant figure are given in parentheses.

Table 7.8 Formation constants and calculated chemical shifts of Al^{3+}-*tranex* species obtained by ^1H NMR at I = 0.15 mol L^{-1} (NaCl) and T = 298.15 K

Species [a)]	**logβ**	**$\delta_{CH_2(7)}$**	**$\delta_{CH(4)}$**	**$\delta_{CH(1)}$**	**$\delta_{CH_2(2,6)'}$**
L		2.353(2)[b)]	1.238(2)[b)]	2.024(2)[b)]	1.818(2)[b)]
LH	10.72(2)[b)]	2.814(2)	1.592(2)	2.059(2)	1.872(2)
LH_2	15.15(4)	2.829(2)	1.614(2)	2.305(2)	1.974(2)
MLH	13.31(6)	2.831(2)	1.620(2)	2.317(2)	1.978(2)
MLOH	5.39(5)	2.824(2)	1.603(2)	2.183(2)	1.931(2)

Species [a)]	**$\delta_{CH_2(2,6)''}$**	**$\delta_{CH_2(3,5)'}$**	**$\delta_{CH_2(3,5)''}$**
L	1.737(8)[b)]	1.267(5)[b)]	0.852(4)[b)]
LH	1.775(8)	1.303(5)	0.992(4)
LH_2	1.811(8)	1.366(5)	1.029(4)
MLH	1.812(8)	1.366(5)	1.030(4)
MLOH	1.795(8)	1.339(5)	1.009(4)

[a)] According to the reactions (3.14) (3.16), charges omitted for simplicity; [b)] least-squares errors on the last significant figure are given in parentheses.

The results here collected are in good agreement with the potentiometric findings and confirm the speciation profile of both systems, as shown in Table 7.9. In particular, in the case of Al^{3+}-*Cys* system, a comparison between the formation constants of the species, obtained by ^1H NMR spectroscopic, UV spectrophotometric and potentiometric titrations is reported. Moreover, it is also proved by the excellent accordance between the observed and calculated chemical shifts for CH and CH_2 resonances of Al^{3+}-*Cys* system, as shown in Fig 7.7.

Table 7.9 Comparison between experimental equilibrium constants of Al^{3+}-*Cys* species obtained by ^1H NMR, UV spectrophotometry and potentiometry at I = 0.15 mol L^{-1} (NaCl) and T = 298.15 K

Ligand	Species [a]	$\log\beta_{H\ NMR}$	$\log\beta_{UV}$	$\log\beta_{ISE\ H^+}$
Cys	**ML**	11.91 [c]	12.20 (4) [b]	11.91(3) [b]
	M_2L	15.0(4) [b]	15.17 [c]	15.17(1)
	MLOH	7.0(5)	6.93(4)	6.96(2)
tranex	**ML**	13.31(6) [b]	—	13.31(1)
	MLOH	5.39(5)	—	4.61(1)

[a] According to the reaction (3.16), charges omitted for simplicity; [b] least-squares errors on the last significant figure are given in parentheses; [c] potentiometric data kept constant in the calculations.

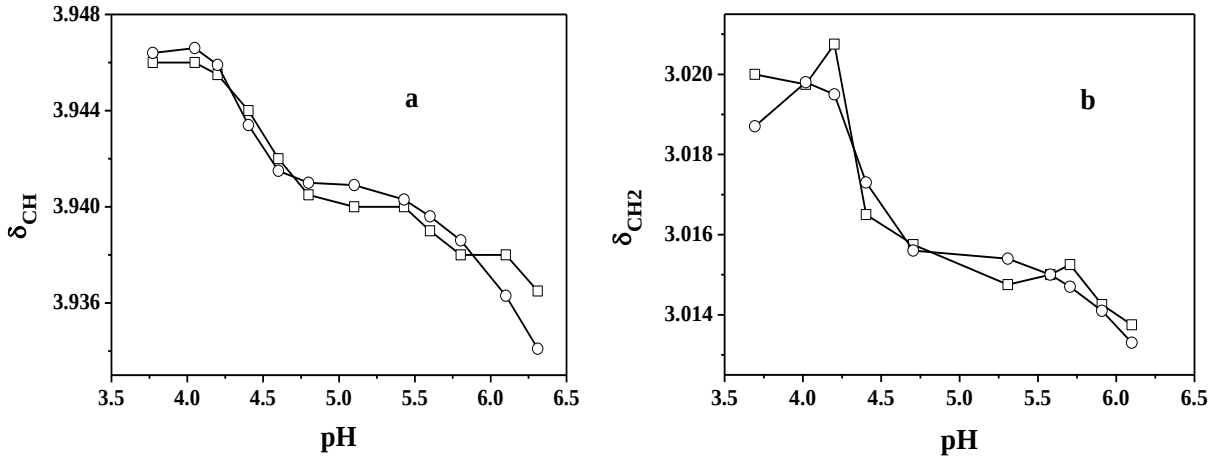

Fig. 7.7 Experimental (□) and calculated (○) values of the chemical shifts for CH (a) and CH_2 (b) of the ligand in Al^{3+}-*Cys* mixtures at C_M = 6 mmol L^{-1}, C_L = 10 mmol L^{-1} (a), C_M = 8 mmol L^{-1}, C_L = 10 mmol L^{-1} (b) and T = 298.15 K.

7.7 Literature comparisons

In the literature, few data are reported about Al^{3+}-amino acids complex species [5, 15, 27, 134-136], as shown in Table 7.10. As far as Al^{3+}-*Gly* interaction concerns, Daydè *et al*. provided a speciation model at T = 310.15 K and I = 0.15 mol L^{-1} in NaCl with only one species, namely $M_2L(OH)_2$, different from the one here reported (MLH, ML and $M_2L_2(OH)_2$). Kiss and other coworkers proposed the formation of three species, ML, MLOH and M_2LOH, with logβ = 5.91, 1.08, 4.35, respectively, at T = 298.15 K and I = 0.2 mol L^{-1} in KCl [27]. The only common species, ML, shows a quite different stability constant (logβ = 5.91) with respect to the one here reported (logβ = 7.18). These difference may be attributed to the different concentrations and metal - ligand ratios employed by Kiss (C_M = 20 - 40 mmol L^{-1} and M:L = 1:10 - 1:40 against C_M = 2 - 6 and M:L = 1:1 - 1:4 here reported). A similar condition occurred in the case of the Al^{3+}-*mala* discussed in the Section 5.6 in comparison with literature data provided by Venturini-Soriano and Berthon [66, 115]. Moreover, in the review of Rubini *et al.*, a logK = 5.8 - 5.9 was estimated by using LFER approach [15].
Referring to the Al^{3+}-*Cys* system, Bohrer *et al*, proposed a speciation model quite similar to the one found in this study, with ML and MLOH as common species [134]. In addition, the study reported the formation of two hydrolytic mixed species, namely $ML(OH)_2$ and $ML(OH)_3$, since the investigations were performed in a range of pH between 4.0 and 11.0, even though the authors admit the presence of a "slight turbidity" starting from pH = 4.6. Despite this, for ML and MLOH species they found logβ = 6.45 and logβ = 6.15, respectively at T = 298.15 K and I = 0.1 mol L^{-1}. These results showed that ML formation constant value is different from the one here obtained (logβ = 11.91 at T = 298.15 K and I = 0.1 mol L^{-1} in NaCl), whilst MLOH, with a logβ = 6.96, is rather comparable.

Table 7.10 Literature data on Al^{3+}-amino acid systems

			logβ [a]		**Ref.**
***T*/K**	***I*/mol L^{-1}**	**Ligand**	**ML**	**MLOH**	
298.15	0.2 [b]	*Gly*	5.91	—	[27]
	—		5.8 - 5.9 [c]	—	[15]
298.15	0.1	*Cys*	6.45	6.15	[134]

[a] According to the reactions (3.16), charges omitted for simplicity; [b] in KCl; [c] by LFER approach.

Chapter 8

Oligophosphate ligands: results and discussion

As already pointed out in the dedicated Section 2.5, phosphate ligands are of great interest in the speciation field, since they play a key role in many natural fluids. The study of Al^{3+} interaction with this class of compounds is of great significance, since these molecules are naturally present in the human body and can be considered as model compounds for other phosphate bearing molecules, such as sugarphosphates, adenosinephosphate and phosphorylated amino acids. Furthermore, as aluminium is a typical hard metal cation, it can strongly interact with organic and inorganic ligands containing O-donor groups, especially carboxylates and phosphates [8, 13, 64]. Consequently, its interaction with biomolecules containing phosphate may affect its intake and transport in living organisms.

In this chapter, particular attention was focused on four phosphate ligands, namely PO_4^{3-}, *PP*, *TPP* and *HMP*. The Al^{3+} interaction with these compounds was studied by means of potentiometric and calorimetric titrations at T = 298.15 K and ionic strength between 0.15 and 1 mol L^{-1} in NaCl or $NaNO_3$, in the case of *HMP*. Potentiometric investigations were performed also at I = 0.5 and 1 mol L^{-1} in NaCl or $NaNO_3$, except for PO_4^{3-}, whose solutions at higher ionic strength showed a poorly soluble species at lower pH values. Both the analysis techniques were carried out in order to obtain the best speciation model, the stability constants and the thermodynamic formation parameters of the different complex species. In addition to these investigations, ^{31}P -{^{1}H}NMR titrations on Al^{3+}-*TPP* solutions and laser desorption mass spectrometry for Al^{3+}-*PP*, -*TPP*, -*HMP* systems were performed, with the aim to confirm the speciation models and formation constants and to obtain more information about the composition and the structure of the complex species. Before to study the interaction between the metal cation and these compounds, ligand acid - base properties (reported in the next paragraph) and metal hydrolysis equilibria (previously discussed in the Chapter 4) were evaluated in the same experimental conditions used for the systems under study.

8.1 Ligand protonation constants

Protonation constants of PO_4^{3-}, *PP*, *TPP* and *HMP*, were previously studied by the research group, but only PO_4^{3-}, *PP*, *TPP* data were already published [137, 138].
These values, reported in Table 8.1, were recalculated at the same ionic strength and temperature conditions of the metal - ligand complexes (T = 298.15 K, $0.15 \leq I$ mol $L^{-1} \leq 1$ in NaCl and $NaNO_3$ only for *HMP*). Moreover, *TPP* protonation constants were confirmed by ^{31}P -{^1H} NMR investigations.

Table 8.1. Protonation constants of PO_4^{3-}, *PP*, *TPP*, *HMP* at T = 298.15 K and at different ionic strength (NaCl)

		$\log\beta^H$			Ref.
Ligand	**Species** [a]	I **= 0.15** [b]	I **= 0.5** [b]	I **= 1** [b]	
PO_4^{3-}	**LH**	11.49	—	—	[137]
	LH_2	18.14	—	—	
	LH_3	20.01	—	—	
PP	**LH**	8.04	7.61	7.36	[138]
	LH_2	13.88	13.17	12.83	
	LH_3	15.63	14.68	14.59	
	LH_4	16.35	15.40	15.92	
TPP	**LH**	7.48	7.10	7.05	[138]
	LH_2	12.68	12.01	12.08	
	LH_3	14.43	13.34	13.42	
	LH_4	15.50	14.26	14.56	
	LH_5	15.97	14.64	15.26	
HMP [c),d)]	**LH**	6.42	6.00	5.63	Unpublished data from this laboratory
	LH_2	8.69	7.94	7.31	
	LH_3	10.85	9.68	8.62	

[a] According to the reaction (3.14), charges omitted for simplicity; [b] mol L^{-1}; [c] in $NaNO_3$; [d] unpublished data from this laboratory.

8.2 Al^{3+}-oligophosphate complexes

In order to define the speciation model and the formation constants of the different species of the systems under study, the Al^{3+} interaction with oligophosphates was firstly assessed by performing potentiometric titrations at different ionic strength values ($0.1 \leq I$ / mol $L^{-1} \leq 1$ in NaCl, except for PO_4^{3-} and in $NaNO_3$ for Al^{3+}-*HMP* system), different metal - ligand ratios, reported in the experimental section 3.2.2, and T = 298.15 K. The results, shown in Table 8.2, are expressed as $\log\beta_{pqr}$, according to the equilibrium reaction (3.16).

Table 8.2 Experimental formation constants for Al^{3+}- PO_4^{3-}, -*PP,* -*TPP,* -*HMP* species (in NaCl), obtained by potentiometry at 298.15 K

		logβ		
Ligand	**Species** [a]	***I* = 0.15** [b]	***I* = 0.5** [b]	***I* = 1** [b]
PO_4^{3-}	**MLH**	17.00(2) [c]		
	ML	14.07(1)		
PP	**ML_2H**	25.17(3)	23.34 (4) [c]	22.95 (2) [c]
	MLH	16.81(4)	15.18(4)	15.06(3)
	ML	13.53(3)	12.16(4)	12.02(3)
	ML_2	19.29(2)	17.99(2)	17.68(2)
	MLOH	6.69(6)	6.47(3)	6.07(2)
TPP	**MLH_2**	19.84(5)	18.50(7)	17.38(5)
	MLH	17.79(4)	16.46(6)	15.42(4)
	ML	14.11(3)	12.76(4)	11.93(3)
	ML_2	17.95(2)	17.06(3)	16.75(3)
	MLOH	6.64(3)	6.31(2)	5.85(2)
HMP [d]	**MLH**	11.10(2)	11.42(1)	12.69(2)
	ML	9.04(2)	8.82(2)	9.19(2)
	MLOH	3.87(2)	3.15(1)	2.65(1)

[a] According to the reaction (3.16), charges omitted for simplicity; [b] mol L^{-1}; [c] least-squares errors on the last significant figure are given in parentheses; [d] in $NaNO_3$.

As reported in the previous Table, the speciation models are featured by the formation of two common species, MLH and ML ones, which are characterized by different stability values. For example, $\log\beta_{110}$ = 14.07, 13.53, 14.11, 9.04 for Al^{3+}-PO_4^{3-}, -*PP*, -*TPP*, -*HMP* systems, respectively, at I = 0.15 mol L^{-1} and T = 298.15 K. This indicates that the stability of ML species is quite similar for PO_4^{3-}, *PP* and *TPP* and follows the trend: *HMP* << *PP* < PO_4^{3-} ≈ *TPP*.

In addition, the formation of ML_2H, ML_2 and MLOH was observed for Al^{3+}-*PP*, MLH_2, ML_2 and MLOH for Al^{3+}-*TPP* and, lastly MLOH for Al^{3+}-*HMP*.

For each system, the pH range investigated was limited by the formation of a precipitate, ascribable to the sparingly soluble hydrolytic $Al(OH)_{3(s)}$ species. For this reason, it was not possible to study Al^{3+} interaction with PO_4^{3-} at higher ionic strength values. Moreover, in the Al^{3+}-PO_4^{3-} speciation diagram, shown in Fig. 8.1, high free metal fractions are present up to pH = 3, whilst MLH and ML species reach maximum fractions of about 0.2 and 0.95, respectively at pH ≈ 3.2 and 4.25. At pH ≥ 4.4, a shaded zone indicates the presence of the precipitate.

Speciation curves for the other systems under study, drawn in Figs. 8.2 - 8.4, denote the possibility of investigating Al^{3+}-*PP*, -*TPP*, -*HMP* systems up to pH = 6.75, 7.3, 5.5, respectively.

For Al^{3+}-*PP* system, shown in Fig. 8.2, the complexation is significant already from pH = 2 with the formation of the MLH species, which achieves a maximum fraction of over 0.9 at I = 0.15 mol L^{-1} between pH = 2 and 2.5. At pH = 4.5, ML is the main species with very high metal fraction of about 0.9. ML_2 is present in a limited pH range with a maximum fraction of 0.6 at pH ≈ 6.75, and its formation is hindered by the presence of $Al(OH)_{3(s)}$ (shaded zone). On the contrary, ML_2H, and MLOH are formed in lower amounts, with fraction of 0.2 and 0.1 at pH = 5.5 and 6.75, respectively. The increasing of the ionic strength from 0.15 to 1 mol L^{-1} does not cause very significant changes, the maximum molar fraction of all the complex decreases, except for the MLOH one, which increases from 0.1 to ~ 0.3 at pH = 6.75. Moreover, all the distribution curves are shifted to lower pH values.

For Al^{3+}-*TPP* system, depicted in Fig. 8.3, starting from pH = 2, Al^{3+} is completely complexed with the formation of MLH_2 and MLH protonated species. The latter achieves a maximum molar fraction of over 0.75 at pH = 3 and I = 0.15 mol L^{-1}. ML is the main species in a wide pH range, between 4 and 7, with a maximum fraction of over 0.95 at pH ≈ 5.5 and I = 0.15 mol L^{-1}. ML_2 and MLOH species are formed in lower fractions, namely 0.35 and 0.25 at pH ≈ 7.25, where the shaded zone begins. By increasing the ionic strength, the maximum formation of all the species is shifted to lower pH values and ML_2 and MLOH molar fractions significantly increase.

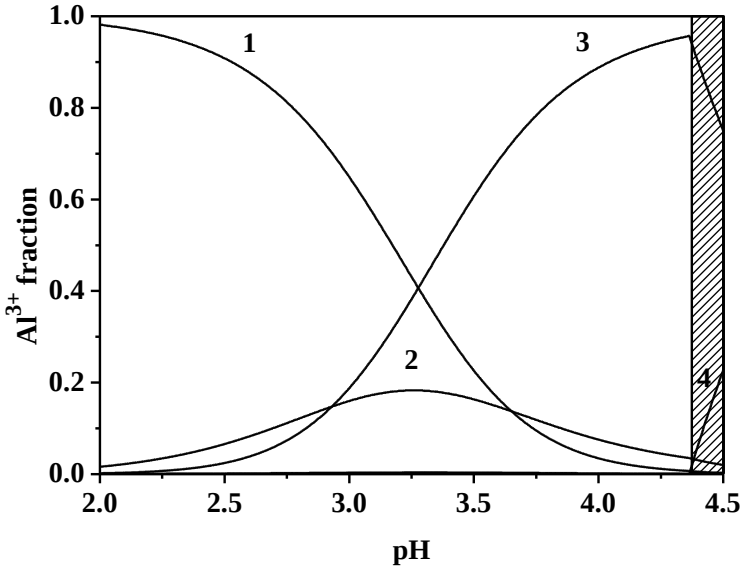

Fig. 8.1 Speciation diagram for Al^{3+}-PO_4^{3-} system in NaCl at I = 0.15 mol L^{-1}, T = 298.15 K. Experimental conditions: C_M = 1 mmol L^{-1}; C_L = 4 mmol L^{-1}. Species: **1. M; 2. MLH; 3. ML; 4. $M(OH)_{3(s)}$**. The shaded zone indicates the presence of a sparingly soluble species.

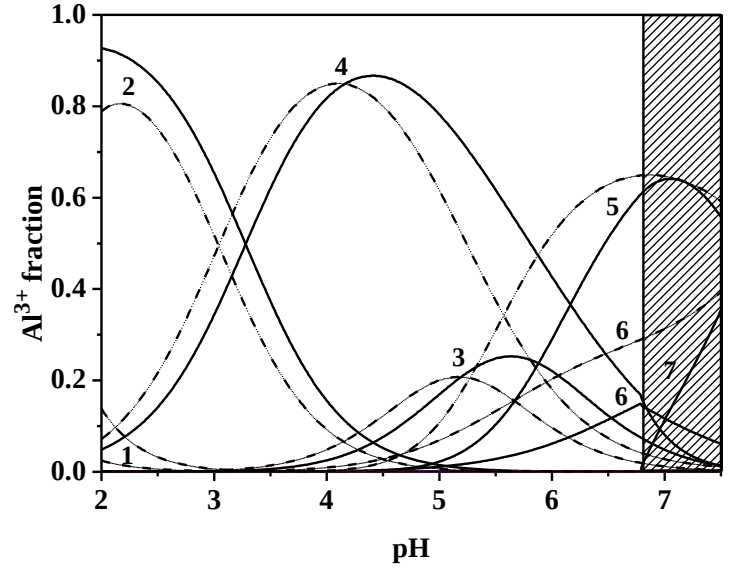

Fig. 8.2 Speciation diagram for Al^{3+}-*PP* system in NaCl at I = 0.15 mol L^{-1} (solid line) and I = 1 mol L^{-1} (dotted line), T = 298.15 K. Experimental conditions: C_M = 0.5 mmol L^{-1}; C_L = 1 mmol L^{-1}. Species: **1. M; 2. MLH; 3. ML_2H; 4. ML; 5. ML_2; 6. MLOH; 7. $M(OH)_{3(s)}$**. The shaded zone indicates the presence of a sparingly soluble species.

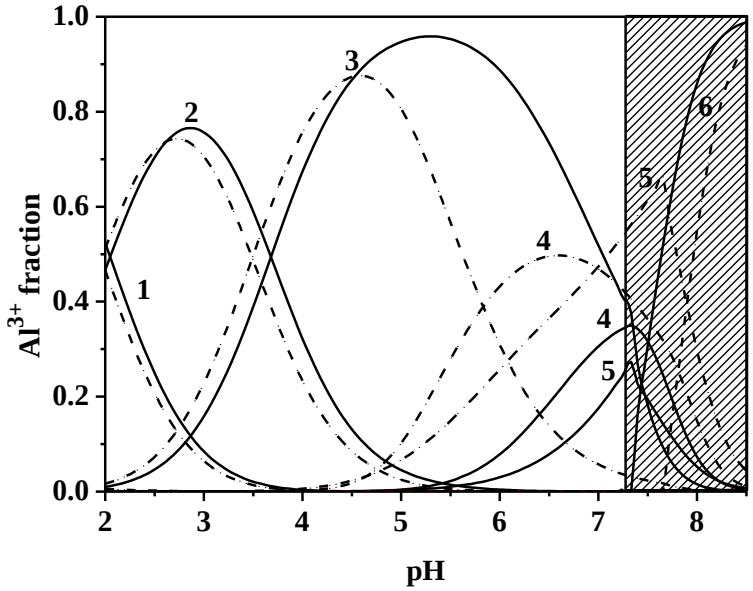

Fig. 8.3 Speciation diagram for Al^{3+}-*TPP* system in NaCl at I = 0.15 mol L^{-1} (solid line) and I = 1 mol L^{-1} (dotted line), T = 298.15 K. Experimental conditions: C_M = 0.5 mmol L^{-1}; C_L = 1 mmol L^{-1}. Species: **1. MLH_2; 2. MLH; 3. ML; 4. ML_2; 5. MLOH; 6. $M(OH)_{3(s)}$**. The shaded zone indicates the presence of a sparingly soluble species.

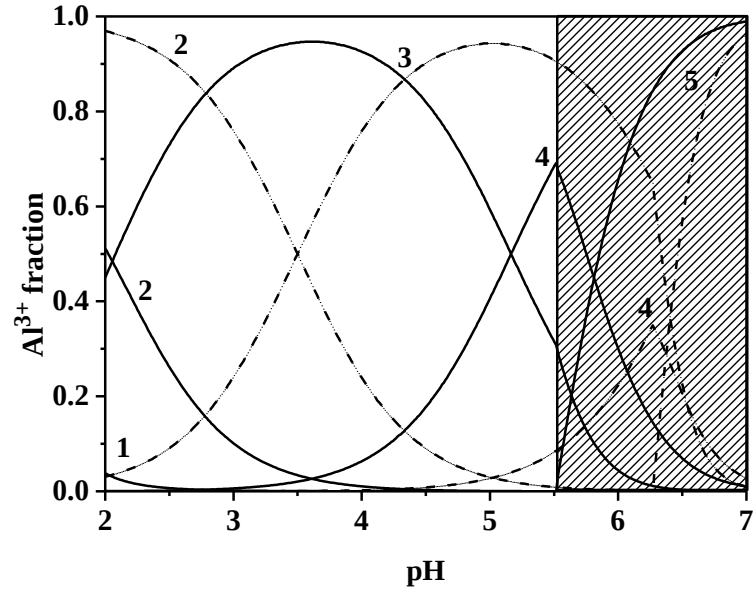

Fig. 8.4. Speciation diagram for Al^{3+}-*HMP* system in $NaNO_3$ at I = 0.15 mol L^{-1} (solid line) and I = 1 mol L^{-1} (dotted line), T = 298.15 K. Experimental conditions: C_M = 1.5 mmol L^{-1}; C_L = 3 mmol L^{-1}. Species: **1. M; 2. MLH; 3. ML; 4. MLOH; 5. $M(OH)_{3(s)}$**. The shaded zone indicates the presence of a sparingly soluble species.

In the Al^{3+}-*HMP* speciation profile, shown in Fig. 8.4, ML appears the main species with a maximum molar fraction of over 0.95 in a wide pH range, from 2.5 to 5, at I = 0.15 mol L^{-1}. MLH and MLOH species are formed with lower fractions (0.5 and 0.7 at pH = 2 and 5.5 respectively), even though very significant at I = 0.15 mol L^{-1}. With the increase of the ionic strength from I = 0.15 to 1 mol L^{-1}, MLH protonated species achieves a fraction of over 0.95 at pH = 2, whilst MLOH significantly decreases from 0.7 to 0.1 at pH = 5.5 and its formation is hindered by the presence of the poorly soluble metal hydrolytic species. In addition, MLH and ML distribution curves are shifted to higher pH values.

8.3 Ionic strength dependence

For all the investigated systems, except for Al^{3+}-PO_4^{3-}, the dependence of the formation constants on ionic strength was evaluated, by using the Debye - Hückel type equation (3.23), expressed in the Section 3.7.3. The $\log^T\beta$ values for all the species together with the empirical parameter C for the dependence on ionic strength are listed in Table 8.3.

Table 8.3. Formation constants for Al^{3+}-*PP* -*TPP*, -*HMP* species at infinite dilution, together with C parameter of eq. (3.23) in NaCl, at T = 298.15 K

Species [a]	Ligand	$\log^T\beta$	C
ML_2H	*PP*	28.4(3) [b]	-0.3(5) [b]
MLH		20.0(3)	0.3(5)
ML		16.4(3)	0.4(4)
ML_2		21.3(3)	-0.5(4)
MLOH		9.2(3)	1.0(4)
MLH_2	*TPP*	24.5(1)	0.1(2)
MLH		22.2(1)	0.1(2)
ML		18.01(6)	-0.1(1)
ML_2		19.3(2)	-0.6(2)
MLOH		9.7(2)	1.1(3)
MLH	*HMP* [c]	14.93(6)	10.4(1)
ML		12.55(4)	7.44(8)
MLOH		6.84(1)	4.21(3)

[a] According to the reaction (3.16), charges omitted for simplicity; [b] least-squares errors on the last significant figure are given in parentheses; [c] in $NaNO_3$.

It is well known that oligophosphate ligands can interact with the ionic medium cation Na^+, employed for the investigations [137, 138]. These Na^+-oligophosphate complexes are not weak, but those with Al^{3+} are strongest. For this reason, their formation is neglected in the calculations. *C* parameter values for each system are all positive, except for ML_2H and ML_2 species of *PP* and ML and ML_2 of *TPP*. The values obtained are comparable with those of Al^{3+}-*tla, -mpa, -Gly, - Cys,* and -*tranex* systems, which are included in a range between 0.1 and 1.0 (except for M_2L of *Cys* and MLOH of *mpa* (this thesis and [120, 129]). Moreover, as far as *C* parameter value concerns, related to the ML species of Al^{3+}-*PP*, it seems to be similar to the one obtained for Al^{3+}-*mal* and -*mpa* systems, with values of 0.47 and 0.30 respectively (this thesis and [66, 120]).

8.4 Temperature dependence

For all the investigated systems, enthalpy changes were obtained by means of calorimetric titrations, at T = 298.15 K and I = 0.15 mol L^{-1}. Before to study the enthalpy changes of Al^{3+}-oligophosphate complexes, ΔH values of ligand protonation were previously determined under the same experimental conditions of solution containing also the metal cation. They are previously determined by the research group, except for *HMP* ones, which are reported here for the first time. Enthalpy changes, together with ΔG and $T\Delta S$ values of the protonated species, are listed in Table 8.4. Thermodynamic formation parameters referring to the most abundant species of Al^{3+}-PO_4^{3-}, -*PP, -TPP* and -*HMP* systems are provided in Table 8.5.
Also in the case of these systems, as expected for hard-hard interactions, the contribution to the standard free energy is mainly due to the entropy and the interaction between Al^{3+} and oligophosphate ligands can be considered of non-covalent type, such as electrostatic one. For example, referring to the ML species of Al^{3+}-PO_4^{3-}, -*PP, -TPP* and -*HMP* systems, ΔH = 9.2, 18, 27.8, 44.4 kJ mol^{-1}, whilst $T\Delta S$ = 89.5, 95, 108.3, 96 kJ mol^{-1}. Moreover, the enthalpy changes related to the ML species regarding Al^{3+}-PO_4^{3-}, -*PP, -TPP* interactions, are fairly similar to those obtained for Al^{3+}-*mal, -tca, -btc* sytems, namely ΔH_{110}= 21, 15, 19 kJ mol^{-1} (this thesis and [66]). In addition to these considerations, from the gained results, it appears that the enthalpy changes increase with the increasing of the number of phosphate groups with a good regularity. This trend, shown in Fig. 8.5, is governed by the following relationship:

$$\Delta H \text{ / kJ mol}^{-1} = 8.99(\pm 0.09)\ n_{PO4}$$

where R^2 = 0.999 and the value of n_{PO4} groups for the *HMP* molecule was forced to 5. From this equation, it would seem that in the *HMP* molecule one terminal phosphate group does not participate in the Al^{3+} complexation.

Table 8.4 Thermodynamic protonation parameters of PO_4^{3-}, *PP, TPP* and *HMP* obtained by titration calorimetry at I = 0.15 mol L^{-1} in NaCl and T = 298.15 K

Species [a]	Ligand	$-\Delta G$ [b]	ΔH [b]	$T\Delta S$ [b]	Ref.
LH	PO_4^{3-}	65.6	-31	34.6	
LH_2		103.5	-35.8	67.7	[137]
LH_3		114.2	-29.8	84.4	
LH	*PP*	46.5	-7	39	
LH_2		79.0	-9	70	[138]
LH_3		87.5	5	82	
LH_4		89.8	14	76	
LH	*TPP*	42.7	-2	41	
LH_2		72.3	-1	71	
LH_3		82.3	11	93	[138]
LH_4		88.4	16	104	
LH_5		91.1	26	117	
LH	*HMP* [c)]	36.6	4.7(4) [d]	41.3	
LH_2		49.6	15.1(8)	64.7	This thesis
LH_3		61.9	17.4(6)	79.3	and [139]

[a] According to the reaction (3.14), charges omitted for simplicity; [b] in kJ mol^{-1}; [c] in $NaNO_3$; [d] least-squares errors on the last significant figure are given in parentheses.

Table 8.5 Thermodynamic parameters of Al^{3+} -PO_4^{3-}, -*PP*, -*TPP*, -*HMP* species obtained by titration calorimetry at I = 0.15 mol L^{-1} in NaCl and T = 298.15 K

Species [a]	Ligand	$-\Delta G$ [b]	ΔH [b]	$T\Delta S$ [b]
ML	PO_4^{3-}	80.3	9.2(8) [c]	89.5
MLH		95.9	18.4(4)	114.3
ML	*PP*	77.2	18(1)	95
ML_2		110.0	30(5)	140
MLH_2	*TPP*	113.2	4(5)	117
MLH		101.5	31.0(8)	132.5
ML		80.5	27.8(8)	108.3
MLOH		37.9	13(3)	51
ML	*HMP* [d]	51.6	44.4(9)	96
MLOH		22.1	69(2)	91

[a] According to the reaction (3.16), charges omitted for simplicity; [b] in kJ mol^{-1}; [c] least-squares errors on the last significant figure are given in parentheses; [d] in $NaNO_3$.

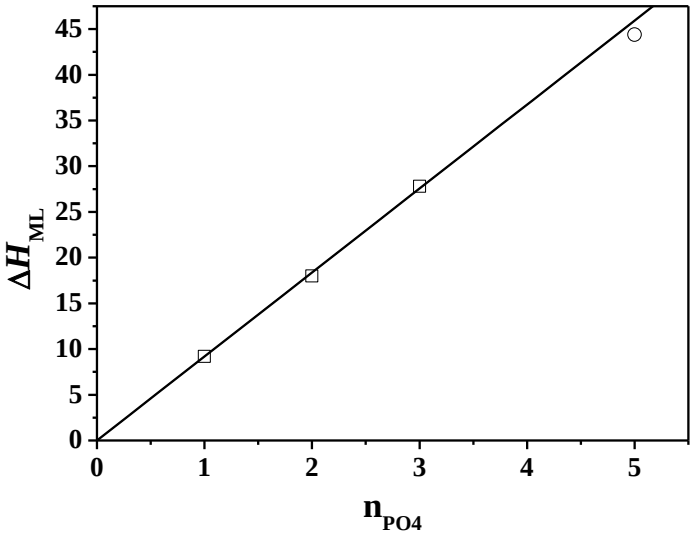

Fig. 8.5 Enthalpy change values (in kJ mol^{-1}) *vs.* number of phosphate groups for ML species of Al^{3+}-PO_4^{3-}(□), -*PP* (□), -*TPP* (□), -*HMP* (○) systems.

8.5 ^{31}P -{^{1}H} NMR spectroscopy

Before investigating the Al^{3+}-*TPP* interactions by means of ^{31}P -{^{1}H} NMR titrations in H_2O/D_2O solutions, at T = 298.15 K and I = 0.15 mol L^{-1} in NaCl, the spectroscopic protonation behavior of the *TPP* ligand in the same experimental conditions of ionic strength and temperature was studied. *TPP* signals appeared as a single set of two average resonances, precisely a doublet and a triplet corresponding to the ending phosphorus (P_e) and the middle phosphorus (P_m). This multiplicity was due to the coupling with the neighboring ^{31}P active nuclei. The only presence of these two resonances was ascribable to a symmetry center in the molecule structure. From the collected spectra, with the increasing of the pH, a general shift of the peaks towards upfields was detected. For example, P_e resonances decreased from -10.2 ppm to -9.6 ppm at pH between 1.67 and 4.5, reaching a value of -5 ppm at pH = 10.2. The P_m signals showed a similar behavior, even though less pronounced, shifting from -22.5 to -19.6 ppm during the whole titration. The presence of a single set of resonance indicated that the protonated species of the ligand present at the equilibrium were involved in a rapid exchange on the NMR time scale. The protonation constants together with the individual chemical shift of each single species were provided in Table 8.6. The obtained results are in good accordance with the ones gained by potentiometry. Furthermore, the excellent agreement between the observed and calculated chemical shift of the different protonated species, shown in Fig. 8.6, confirmed the reliability of the potentiometric findings.

The protonation *TPP* behavior was also recently studied by Maki *et al.* in different experimental conditions with respect to those here found [140]. They provided comparable

values of the calculated chemical shifts for each protonated species with respect to the ones reported in this thesis.

Table 8.6 Protonation constants and calculated chemical shifts of *TPP* species obtained by ^{31}P -{^{1}H} NMR at I = 0.15 mol L^{-1} (NaCl) and T = 298.15 K

Species[a)]	logβ	δ_{Pe}	δ_{Pm}
L	—	-4.97(1) [b)]	-19.65(3) [b)]
LH	7.84(2) [b)]	-7.48(1)	-21.38(3)
LH_2	13.27(3)	-9.95(1)	-22.37(3)
LH_3	15.1(1)	-10.39(1)	-22.96(4)

[a)] According to the reaction (3.14), charges omitted for simplicity; [b)] least-squares errors on the last significant figure are given in parentheses.

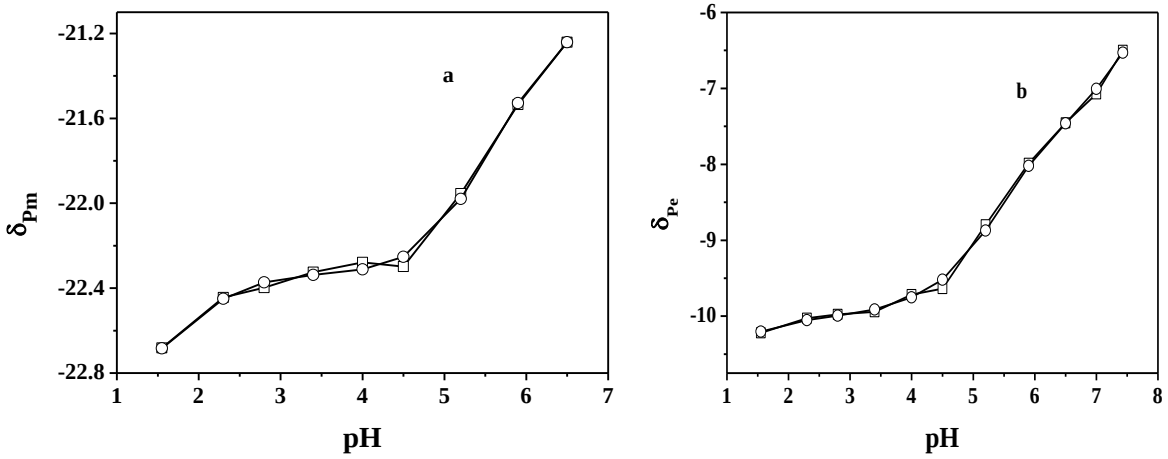

Fig. 8.6 Experimental (□) and calculated (○) values of the chemical shifts for P_m (a), P_e (b), of the *TPP* ligand at C_L = 10 mmol L^{-1}, I = 0.15 mol L^{-1} and T = 298.15 K.

As far Al^{3+}-*TPP* system concerns, all the registered spectra below pH = 7, regardless metal - ligand concentration ratios, showed four main signals, *i.e.* a doublet and a triplet related to the free ligand and other two broad signals due to the interaction of aluminium with *TPP*, referred as P_{ebound} and P_{mbound} along the discussion. This signal splitting were also found by Kiss *et al.* [141], according to which the free and bound ligands were involved in a slow mutual exchange in the NMR time scale, thus providing distinct signals. More in detail, for metal ligand solutions, having concentration ratios of 1:1, as expected by considering the speciation diagrams, the disappearance of the resonances due to the free ligand occurred even at lower pH. P_{mbound} resonances were deshielded with the respect to the one of the metal free ligand in the whole pH range. In addition, this broad signal, which is due to the central coordinated

phosphorus, shifted toward upfield from -19.9 to -17.5 ppm in the pH range between 1.6 and 5.2, whereas its chemical shift did not change to a great extent up to pH = 8. On the contrary, P_{ebound} resonances showed an upfield shift with respect to the corresponding P_e due to the free ligand, as already observed [141]. This signal, at the same time, was featured by a continuous shift towards higher ppm (from -12.9 up to -8.7 ppm), over the whole investigated pH range.

The formation constants of the main species, namely MLH, ML and ML_2, were calculated and listed in Tables 8.7. MLH_2 and MLOH stability constants, obtained by potentiometry, were kept constant in the calculations. The gained data were in good agreement with the potentiometric ones, thus confirming, once again, the selected speciation model, as shown in Table 8.8. In addition, starting from the average observed chemical shifts referred to P_{ebound} and P_{mbound}, the individual δ for each single complex was calculated and reported in Table 8.7 as well.

The good agreement between the observed and the recalculated average chemical shifts (Fig. 8.6), found for both P_{ebound} and P_{mbound}, together with the data listed in Table 8.7, as well as confirming the potentiometric findings, suggest that *TPP* ligand interacts with Al^{3+} through two adjacent phosphate oxygens to form a stable six membered ring, as already suggested by Kiss [141].

Table 8.7 Formation constants and calculated chemical shifts of Al^{3+}-*TPP* species obtained by ^{31}P -{^{1}H} NMR at I = 0.15 mol L^{-1} (NaCl) and T = 298.15 K

Species [a)]	**logβ**	**$\delta_{Pebound}$**	**$\delta_{Pmbound}$**
MLH_2	19.84	-13.563(7) [b)]	-24.95(7) [b)]
MLH	17.5(3) [b)]	-13.695(7)	-20.71(7)
ML	13.6(4)	-10.285(7)	-17.50(7)
ML_2	18.1(3)	-8.819(7)	-17.36(7)
MLOH	6.64	-7.882(7)	-17.60(7)

[a)] According to the reaction (3.16), charges omitted for simplicity; [b)] least-squares errors on the last significant figure are given in parentheses.

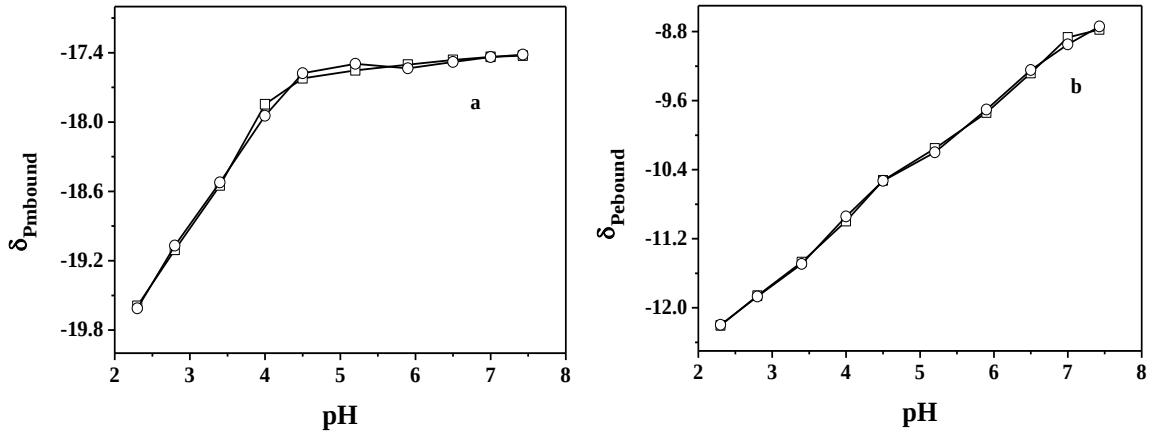

Fig. 8.6. Experimental (□) and calculated (○) values of the chemical shifts for P_{mbound} (a), P_{ebound} (b) of the ligand in Al^{3+}-*TPP* mixtures at C_M = 5 mmol L^{-1}, C_L = 10 mmol L^{-1}, I = 0.15 mol L^{-1} and T = 298.15 K.

Table 8.8 Comparison between experimental equilibrium constants of Al^{3+}-*TPP* species obtained by ^{31}P -{^{1}H} NMR and potentiometry at I = 0.15 mol L^{-1} (NaCl) and T = 298.15 K

Ligand	Species [a]	$\log\beta_{H\ NMR}$	$\log\beta_{ISE\ H^+}$
TPP	**MLH_2**	19.84 [c]	19.84(5) [b]
	MLH	17.5(3) [b]	17.79(4)
	ML	13.6(4)	14.11(3)
	ML_2	18.1(3)	17.95(2)
	MLOH	6.64 [c]	6.64(3)

[a] According to the reaction (3.16), charges omitted for simplicity; [b] least-squares errors on the last significant figure are given in parentheses; [c] potentiometric data kept constant in the calculations.

8.6 Mass spectrometry

MALDI LD-MS and MS/MS spectrometry were used to investigate the interactions between Al^{3+} and *PP*, *TPP* and *HMP* ligands, in order to obtain some evidences on the structure of the complex species, as previously done for several other systems [107, 142, 143].

As far as Al^{3+}-*PP* system concerns, the LD-MS spectrum provides structural information on the $[ML_{2PP}]^+$ ion, which indicates that the ML_2 is the predominant species at pH = 6.5, with m/z 380.85, $[H_6O_{14}AlP_4]^+$, Δppm = 4.7 and DBE = 0.50. On the contrary, ML_{PP} denotes a little portion of the total ion current, with m/z 202.91, $[H_2O_7AlP_2]^+$ and Δppm = 5.6. The results suggest that the formation of the complexes is affected by the increasing of pH values.

Moreover, the fragmentation pattern of the $[ML_{2PP}]^+$ ion leads to the species $[L_{PP}]^+$ and $[ML_{PP}]^+$ with m/z 161.9, $[H_3O_6P_2]^+$, and m/z 202.9, $[AlH_2O_7P_2]^+$, respectively. $[ML_{PP}]^+$ species, in turn, undergoes dissociation giving rise to a specific ion fragment, $[AlHO_4P]^+$, with m/z 122.9.

The LD-MS spectrum, obtained for Al^{3+}-*TPP* system at pH = 3.5 and 6.5, shows the formation of the $[ML_{TPP}]^+$ ion, with m/z 282.88, Δppm = 4.4, $[H_3O_{10}AlP_3]^+$ and DBE = 1.50. The assumed composition of this ion suggests that *TPP* interacts with aluminium through two adjacent phosphate oxygens, leading to a six membered ring structure, as indicated from NMR findings. In addition, the MS/MS investigations on this ion $[ML_{TPP}]^+$ produce some fragments that derive from the phosphate group, consolidating the previous statement. The first event is, in fact, the Al^{3+}-diphosphate and phosphate release, with the following signals: m/z 99.0 $[H_4O_4P]^+$, m/z 83.0 $[H_4O_3P]^+$ for the first one and m/z 203.0 $[H_2O_5AlP_2]^+$, m/z 187.0 $[H_2O_6AlP_2]^+$ for the second one. Moreover, Al^{3+}-phosphate ion undergoes to a further fragmentation, providing two species, $[AlHO_3P]^+$ (m/z 106.9) and $[AlH_2O_2]^+$ (m/z 60.9), deriving from Al^{3+}-diphosphate cross ring fragmentation, as shown in the Fig. 8.7.

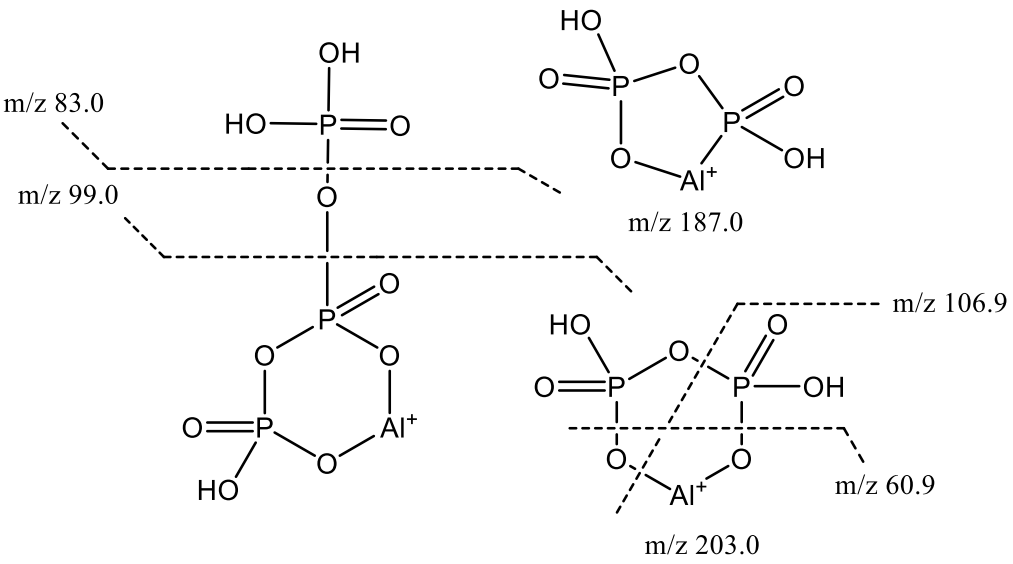

Fig. 8.7 LD MS/MS fragmentation pathways of Al^{3+}-*TPP* system.

From the LD mass spectra of Al^{3+}-*HMP* system, the formation of some fragments due to the partial decomposition of the complexes was found. These ions are reported in Table 8.9 with the corresponding m/z signals. In accordance with the speciation profile of Al^{3+}-*HMP* system, which shows that ML is the predominant species in solution at pH = 3.5, the formation of higher molecular weight species is not observed. The LD-MS investigations suggest that *HMP* acts as a bidentate ligand providing a six membered ring, as in the case of the previous described system. Since *HMP* is a complex mixture of polyphosphates, as already pointed out

in the Section 2.5, DBE values for the $[ML]^+$ ion, reported in Table 8.9, and the deduced elemental composition show that all the *HMP* isomers are able to chelate Al^{3+}. On the LD-MS interface, a partial decomposition of the complex occurs. This can be evaluated by the detection of the signals with m/z 412.79, 380.85 and 346.83 related to the ion peaks, which derive from the loss of a diphosphate group. These m/z values together with the formation of Al^{3+}-diphosphates with m/z 310.85 and 282.88, indicate that the solution contains isomeric species, which bound Al^{3+} through two adjacent phosphates, as in the case of Al^{3+}-*TPP* system. The MS/MS analysis of $[ML_{HexaP}]^+$ ion with m/z 522.78 leads to daughter ions deriving from the consecutive cleavage of phosphate bonds with the charge retention on Al^{3+}. The formation of these ions ($[H_4O_{18}AlP_6]^+$, $[H_5O_{16}AlP_5]^+$, $[H_4O_{13}AlP_4]^+$, $[H_5O_{16}AlP_3]^+$, $[H_4O_7AlP_2]^+$ and $[H_3O_4AlP]^+$, with m/z 504.8, 442.8, 362.8, 380.9, 204.9, 124.9, respectively) shows that the ion species involve linear *HMP* isomers and two adjacent terminal phosphate units probably provide the metal coordination.

Table 8.9 LD MS of Al^{3+}-*HMP* systems

Species	m/z	Error (ppm)	DBE [a)]	Formula
$[ML_{HexaP}]^+$	550.74	4.7	1.50	$[H_4O_{18}Na_2AlP_6]^+$
$[ML_{HexaP}]^+$	522.78	4.6	1.50	$[H_6O_{19}AlP_6]^+$
$[ML_{HexaP}]^+$	504.76	4.8	2.5	$[H_4O_{18}AlP_6]+$
$[ML_{HexaP}]^+$	494.76	4.7	2.50	$[H_3O_{16}NaAlP_6]^+$
$[ML_{HexaP}]^+$	488.77	4.2	2.50	$[H_4O_{17}AlP_6]^+$
$[ML_{TetraP}]^+$	412.79	4.9	1.50	$[HO_{12}Na_3AlP_4]^+$
$[ML_{TetraP}]^+$	380.85	4.7	0.50	$[H_6O_{14}AlP_4]^+$
$[ML_{TetraP}]^+$	346.83	5.2	1.50	$[H_4O_{12}AlP_4]^+$
$[ML_{DiP}]^+$	310.85	4.8	1.50	$[O_{11}Na_2AlP_2]^+$
$[ML_{DiP}]^+$	282.88	4.4	1.50	$[H_2O_{12}AlP_2]^+$

[a)] DBE, double bound equivalent.

8.7 Literature comparisons

In the literature there are some data regarding Al^{3+}-PO_4^{3-}, -*PP,* -*TPP* systems, as reported in Table 8.10. As Al^{3+}-PO_4^{3-} interaction concerns, a review of Rubini *et al.* [15] reports the formation constant values of MLH, ML and MLOH, namely logβ = 17.6, 13.5, 7.2, respectively, at I = 0.2 mol L^{-1} in KCl and T = 298.15 K, as already provided in a paper of Atkari *et al*. [141]. These data are fairly close to those here obtained, even though the

experimental conditions of ionic strength are different (logβ = 17.0, 14.07 for MLH and ML respectively, at I = 0.15 mol L^{-1} in NaCl and T = 298.15 K). Owing to the formation of a sparingly soluble species at pH > 4, as underlined in this thesis and already pointed out by Kiss [64], Harris, provided a $\log\beta_{110}$ = 14.10, calculated by means of the LFER relation (Linear free Energy Relation of log stability constants against ligand basicity values) [144]. Atkari *et al*. also used LFER for different organic monophosphate and phosphonate ligands, obtaining for Al^{3+}-PO_4^{3} interaction a $\log\beta_{111}$ = 17.60 at I = 0.2 mol L^{-1} in KCl and T = 298.15 K [141]. The results obtained by Atkari, Harris and other co-workers by means of LFER calculations are in good agreement to those here reported.

For Al^{3+}-*PP* interactions, Atkari and coauthors report the same speciation model with an additional species, namely MLH_2. More in detail, they found logβ = 17.03, 13.74, 7.41, 25.64, 19.77 for MLH, ML, MLOH, ML_2H, ML_2, respectively, at T = 298.15 K and I = 0.2 mol L^{-1} in KCl [141]. These values are fairly higher than the ones here reported (logβ = 16.81, 13.53, 6.69, 25.17, 19.29, for MLH, ML, MLOH, ML_2H, ML_2, respectively, at I = 0.15 mol L^{1} in NaCl and T = 298.15 K).

For Al^{3+}-*TPP*, Atkari provided the same speciation pattern already proposed for Al^{3+}-*PP* systems, with six species [141]. The complexes here obtained are the same (except for the ML_2H) and the relative stability constants, in some cases, are higher than an order of magnitude.

Table 8.10 Literature data on Al^{3+}-oligophosphate systems

			logβ [a]				**Ref.**
***T*/K**	***I*/mol L^{-1}**	**Ligand**	**MLH**	**ML**	**ML_2**	**MLOH**	
298.15	0.2 [b]	PO_4^{3-}	17.6	13.5		7.2	[15, 141]
	—		—	14.10 [c]			[64]
298.15	0.2 [b]	*PP*	17.03	13.74	19.77	7.41	[141]
	0.2 [b]	*TPP*	16.65	13.15	19.14	6.53	[141]

[a] According to the reactions (3.16), charges omitted for simplicity; [b] in KCl; [c] by LFER approach.

Chapter 9

Other inorganic ligands: results and discussion

Beside the previous classes of compounds, the attention was also focused on other two ligands of inorganic nature, namely carbonate and fluoride.

Because of the environmental and biological importance of the carbonate, as pH buffer in biological and natural systems and being the fluoride ion one of the major components of natural waters, it was considered interesting to study their behavior in aqueous solution in presence of the aluminium cation. Moreover, the fluoride interaction with Al^{3+} and lactic acid at the same time in aqueous solution was assessed, in order to check the formation of different ternary mixed complexes.

The aluminium speciation with these inorganic ligands was studied by means of potentiometric titrations at T = 298.15 K and different ionic strength values, namely $0.1 \leq I$ mol $L^{-1} \leq 1$ in NaCl. The stability constants of the complex species were determined by taking into account the aluminium hydrolysis reactions, already discussed in the Chapter 4, and ligand protonations, argued in the next paragraph.

9.1 Ligand protonation constants

Protonation constants of CO_3^{2-} were previously determined by the research group and published in a paper of Crea *et al.* [145]. For the study of the Al^{3+}-CO_3^{2-} complexes, protonation smoothed values at 0.5 and 1.0 mol L^{-1} were used, whilst those at 0.15 mol L^{-1} were recalculated by using $\log^{T}\beta^{H}$ values at infinite dilution and the empirical parameter C for the dependence on ionic strength reported in the already mentioned paper, by means of the Debye - Hückel type equation 3.23. These results are listed in Table 9.1 at T = 298.15 K and I = 0.15, 0.5 and 1 mol L^{-1} in NaCl. As *lac* concerns, the acid - base properties are already discussed in the previous Paragraph 5.1.

Table 9.1 Protonation constants of CO_3^{2-} at different ionic strength in NaCl

		logβ			Ref.
Ligand	**Species** [a)]	***I* = 0.15** [b)]	***I* = 0.5** [b)]	***I* = 1** [b)]	
CO_3^{2-}	**LH**	10.02	9.589	9.476	[145]
	LH_2	13.52	15.588	15.435	

[a)] According to the reaction (3.14), charges omitted for simplicity; [b)] in mol L^{-1}.

9.2 Al^{3+}-CO_3^{2-}, -F^- and -F^-/*lac* complexes

The Al^{3+}-CO_3^{2-} system was studied by means of potentiometric investigations at T = 298.15 K, different ionic strengths (0.15, 0.5 and 1 mol L^{-1} in NaCl) and metal - ligand concentration ratios, reported in the Section 3.2.2. In this system, the formation of three species, MLH, ML_3 and M_2L_3 in the range of pH 2.0 - 5.0 was observed. The speciation profile, shown in Fig. 9.1, indicates that MLH is the most abundant species formed in a wide pH range (from 2.5 to 4.5), with an Al^{3+} maximum fraction of about 0.3 at pH ≈ 3.6. The other two minor species, ML_3 and M_2L_3, are observed only in particular conditions of concentration ratios (c_M:c_L > 1:6) over pH ~ 4.5, where the sparingly soluble species of aluminium is formed, hindering the rise of these two complexes. For these reasons, in the speciation model only the MLH species was considered and its stability constant value was reported in Table 9.2, at different ionic strengths. Furthermore, comparing the MLH formation constant values of the Al^{3+}-CO_3^{2-} ($\log K_{111}$ = 4.25) with the one of another inorganic ligand, PO_4^{3-}($\log K_{111}$ = 5.51), both at I = 0.15 mol L^{-1} in NaCl and T = 298.15 K, by taking into account the reaction (3.17), it is evident that the aluminium interaction with the phosphate ligand is stronger.

As Al^{3+}-F^- concerns, the results reported in Table 9.2 at T = 298.15 K and I = 0.15 and 1 mol L^{-1} in NaCl, were obtained by a critical analysis of literature data reported in the papers of Martell *et al.* and Cordillon *et al.* at different temperature and ionic strength values [84, 146]. Speciation models, indicated by these authors, are both in agreement between them, including ML, ML_2, ML_3, ML_4 and a poorly soluble species, $ML_2OH_{(s)}$.

As a further investigation, mixed Al^{3+}-F^-/*lac* system were studied at T = 298.15 K and different ionic strengths (0.1, 0.5 and 1 mol L^{-1} in NaCl). The determination of the best speciation model was achieved by taking into account the simple binary Al^{3+}-*lac* and Al^{3+}-F^- species previously studied in the same conditions of ionic strength and temperature. The only possible species with significant formation percentages for this ternary system was the M(l*ac)*F^-, whose stability constant is reported in Table 9.2. This species, as shown in the distribution diagram (Fig. 9.2), reaches significant aluminium fraction in the whole pH range investigated (about 0.5 at pH = 4.0).

Table 9.2 Experimental formation constants for Al^{3+}-CO_3^{2-}, -F^-,-F^-/*lac* species (in NaCl), obtained by potentiometry at T = 298.15 K

		logβ				Ref.
Ligand	**Species** [a]	I = **0.1** [b]	I = **0.15** [b]	I = **0.5** [b]	I = **1** [b]	
CO_3^{2-}	**MLH**	—	14.27 (1) [c]	13.66 (1) [c]	13.20 (1) [c]	
F^-	**ML**	—	6.33 (1)	—	6.12 (1)	
	ML_2	—	11.45 (2)	—	11.05 (3)	
	ML_3	—	15.33(1)	—	14.80 (2)	[84, 146]
	ML_4	—	17.98(1)	—	17.36 (3)	
	$ML_2OH_{(s)}$ [d]	—	-12.88 (4)	—	-12.66 (4)	
F^-/*lac*	**M(*lac*)F^-**	8.96 (2)	—	7.98 (5)	8.34 (1)	

[a] According to the reaction (3.16), charges omitted for simplicity; [b] in mol L^{-1}; [c] least-squares errors on the last significant figure are given in parentheses; [d] according to the reaction: $ML_2OH(s) = MOH + 2L$.

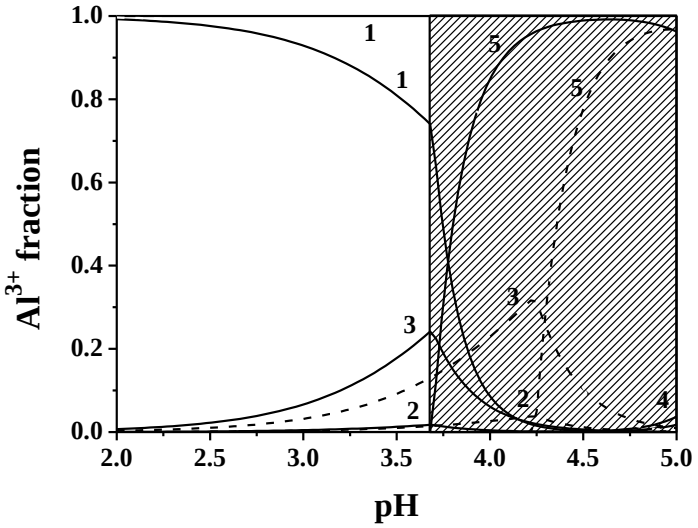

Fig. 9.1 Speciation diagram for Al^{3+}- CO_3^{2-} system in NaCl at I = 0.15 mol L^{-1} (solid line) and I = 1 mol L^{-1} (dotted line), T = 298.15 K. Experimental conditions: C_M = 1 mmol L^{-1}; C_L = 4 mmol L^{-1}. Species: **1. M; 2. MOH; 3. MLH; 4. ML_3; 5. $M(OH)_{3(s)}$.** The shaded zone indicates the presence of a sparingly soluble species.

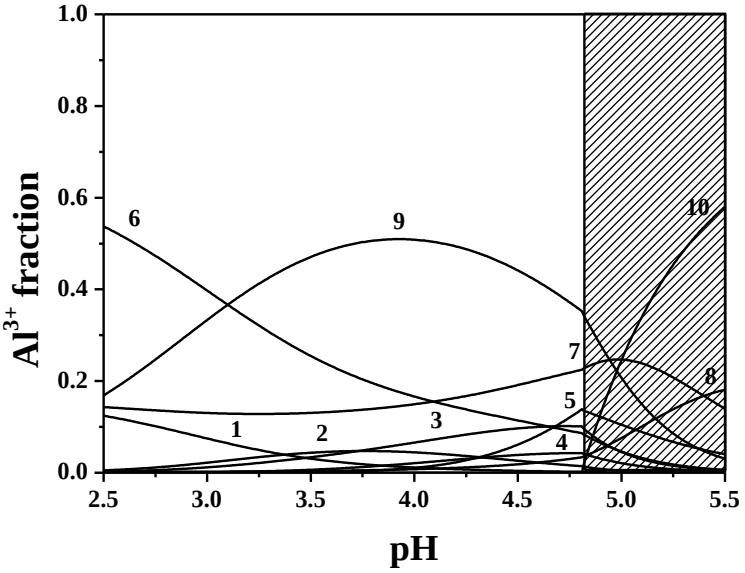

Fig. 9.2 Speciation diagram for Al^{3+}- F^-/*lac* system in NaCl at I = 0.15 mol L^{-1} and T = 298.15 K. Experimental conditions: C_M = 2 mmol L^{-1}; C_{F^-} = 2 mmol L^{-1} and C_{lac} = 12 mmol L^{-1}. Species: **1. M; 2. M*(lac)*$_2$; 3. M*(lac)*OH; 4. M*(lac)*$_2$OH; 5. M*(lac)*$_2$(OH)$_2$; 6. MF; 7. MF$_2$; 8. MF$_3$; 9. M*(lac)F*$^-$; 10. M(OH)$_{3(s)}$**. The shaded zone indicates the presence of a sparingly soluble species.

9.3 Ionic strength and temperature dependence

For all the investigated systems, the dependence of the formation constants of the different species on ionic strength was evaluated, by the Debye - Hückel type equation (3.23) for Al^{3+}-CO_3^{2-} and Al^{3+}-F^-/*lac* complexes and by the eq. 3.28, which takes also into account the dependence on the temperature with the *P(T)* term, for Al^{3+}-F^- system. The gained results are reported in Table 9.3. As far as formation constant dependence on the temperature concerns, also in this case, as expected, for Al^{3+}-F^- system the contribution to the standard free energy is mainly entropic in nature.

Table 9.3. Thermodynamic parameters at infinite dilution of Al^{3+}-CO_3^{2-},-F^-,-F^-/*lac* species, in NaCl, at T = 298.15 K

Species [a]	**Ligand**	**log^{T}β**	***C***	**-Δ*G*** [b]	**Δ*H*** [b]	**TΔ*S*** [b]	***C*$_T$** [c]
MLH	CO_3^{2-}	15.54 (2) [d]	-0.34 (6) [d]	—	—	—	—
ML	F^-	7.03 (2)	0.31 (4)	40.1 (1) [d]	6.3 (2) [d]	46.4 (2) [d]	-1.02 (2) [d]
ML$_2$		12.63 (2)	0.46 (4)	72.1 (1)	10.9 (4)	83.0 (4)	-1.70 (3)
ML$_3$		16.75 (2)	0.50 (4)	95.6 (1)	13.2 (6)	108.8 (6)	-2.04 (4)
ML$_4$		19.42 (4)	0.39(5)	110.8 (2)	15.1 (8)	125.9 (8)	-2.04 (4)
ML$_2$OH [e]		-13.6 (1)	-0.3 (1)	—	—	—	—
M(*lac*)*F*$^-$	F^- /*lac*	9.52 (3)	0.97 (1)	—	—	—	—

[a] According to the reaction (3.16), charges omitted for simplicity; [b] in kJ mol^{-1}; [c] parameter for the dependence of Δ*H*/kJ mol^{-1}on the ionic strength (eq. 3.28); [d] least-squares errors on the last significant figure are given in parentheses; [e] according to the reaction: $AlL_2OH(s) = MOH + 2L$.

9.4 Literature comparisons

To the best of our knowledge, only a paper concerning the Al^{3+}-CO_3^{2-} system was published, whilst the study on the Al^{3+} interaction with both fluoride and lactate is reported here for the first time. As far as Al^{3+}-CO_3^{2-} system concerns, Hedlund and co-workers, employing high concentration of aluminium (up to 0.02 mol L^{-1}), provide a speciation model featured by MLH, $M_2L(OH)_4$ and $M_3L(OH)_5$ species, with a $\log\beta_{111}$ = 16.68 at T = 298.15 K and I = 3 mol L^{-1} in NaCl [88]. By considering the different experimental conditions in metal concentration and high strength values, the MLH formation constant reported by Hedlund can be considered comparable with the one here obtained ($\log\beta_{111}$ = 13.20 at T = 298.15 K and I = 1 mol L^{-1} in NaCl).

Chapter 10

Nucleotides: results and discussion

The study of aluminium interactions with nucleotides, building blocks of nucleic acids (DNA and RNA), is essential for the knowledge of the effect of this metal cation in biological systems. In general, the Al^{3+} coordination to these biomolecules might induce important dysfunctions in fundamental biological processes, since nucleotides are involved in most enzymatic routes. In many cases, their interaction with toxic metal cations can lead to a competition with the essential ions, which act as catalysts, giving rise to some disorders.
In this chapter, particular attention was focused on three nucleotides, namely *AMP*, *ADP* and *ATP*. They contain three different aluminium - binding sites: an amino group in the nucleic base, alcoholic or hydroxyl functions in the sugar side and phosphate groups in the mono-, di- or tri-phosphate moieties. Their solution chemistry is closely related to the binding capacity of the phosphate group, in particular the terminal one. In addition, the pentose hydroxyl functions and the amino group present on the purine base could play a key role in the interaction with several ions.
The Al^{3+} complexation with these molecules was discussed on the basis of potentiometric data obtained at T = 298.15 K and ionic strength between 0.1 and 1 mol L^{-1} in NaCl. In the case of Al^{3+}-*ATP* system, calorimetric and ^{1}H NMR investigations were also performed at I = 0.1 mol L^{-1} in NaCl and T = 298.15 K. Before to study the interaction between the metal cation and these compounds, metal and ligands acid - base properties were evaluated in the same experimental conditions used for the complex systems under study.

10.1 Ligand protonation constants

Ligand protonation constants were reported in Table 10.1 at T = 298.15 K and $0.1 < I$ / mol $L^{-1} < 1$ in NaCl. For *AMP* and *ADP*, these values were experimentally determined by potentiometry at T = 298.15 K and I = 0.15 mol L^{-1} in NaCl. In the case of *ATP*, protonation constants were recalculated at the same ionic strength and temperature conditions of the metal - ligand complexes, by considering literature data previously published by this research group [147]. Moreover, only for *ATP*, the first two protonation

constants values were confirmed by ^{1}H NMR investigations and the third one was also obtained.

Table 10.1. Protonation constants of *AMP, ADP, ATP* at T = 298.15 K and at different ionic strength (NaCl)

				$\log\beta^{H}$		Ref.
Ligand	**Species** [a]	I **= 0.1** [b]	I **= 0.15** [b]	I **= 0.5** [b]	I **= 1** [b]	
AMP	**LH**	—	6.216 (5)	—	—	This Thesis
	LH_2	—	10.07 (1)	—	—	
ADP	**LH**	—	6.274 (5)	—	—	This Thesis
	LH_2	—	10.095 (9)	—	—	
ATP	**LH**	6.467	—	5.991	5.820	[147]
	LH_2	10.471	—	9.903	9.810	
	LH_3 [c]	12.9 (3)	—	—	—	This Thesis

[a] According to the reaction (3.14), charges omitted for simplicity; [b] mol L^{-1}; [c] obtained by ^{1}H NMR spectroscopy.

10.2 Al^{3+}-nucleotide complexes

The Al^{3+} interaction with nucleotides was firstly evaluated by performing potentiometric titrations at different ionic strength values, different metal - ligand ratios, reported in the experimental section 3.2.2, and T = 298.15 K. More in detail, for Al^{3+}-*AMP* and -*ADP*, the investigations were carried out at I = 0.15 mol L^{-1}, whilst, in the case of *ATP*, measurements were performed at I = 0.1, 0.5, 1 mol L^{-1}. The results, shown in Table 10.2, are expressed as $\log\beta_{pqr}$, according to the equilibrium reaction (3.16).

The calculated speciation models related to Al^{3+}-*ADP* and -*ATP* systems are featured by the same species, namely MLH, ML, ML_2 and MLOH ones. The interaction between Al^{3+} and *AMP* provided the formation of ML, ML_2 and ML_3 species in a limited pH range, due to the formation of a sparingly soluble species, as already observed in the case of the -PO_4^{3-} ligand, discussed in the Chapter 8. For all the Al^{3+}-nucleotides systems, a common species, ML one, characterized by different stability, was found. For this species, $\log\beta$ = 6.66, 7.41, 8.113 for Al^{3+}-*AMP, -ADP, -ATP* systems, respectively, at I = 0.15 mol L^{-1} (I = 0.1 mol L^{-1} for Al^{3+}-*ATP)* and T = 298.15 K. These values indicate that the stability of ML species increases with the increasing of the number of the phosphate groups present in the molecule, thus following the trend: *AMP* < *ADP* < *ATP*. Nucleotides, therefore, show the same behaviour found for the oligophosphate ligands towards aluminium (already discussed in the Section 8.2), whose

speciation models are similar to the ones here reported. However, the stability of the complex species is highly different, resulting lower for nucleotides (logβ = 14.07, 13.53, 14.11 for ML species of Al^{3+}-*PO_4^{3-}, -PP, -TPP,* systems, respectively, at I = 0.15 mol L^{-1} and T = 298.15 K) (this thesis and [139]). This difference in stability is, probably, due to the steric hindrance of nucleotides.

Table 10.2 Experimental formation constants for Al^{3+}-*AMP, -ADP, -ATP* species (in NaCl), obtained by potentiometry at T = 298.15 K

		logβ [a]			
Ligand	**Species** [a]	I **= 0.1** [b]	I **= 0.15** [b]	I **= 0.5** [b]	I **= 1** [b]
AMP	**ML**	—	6.66 (6) [c]	—	—
	ML_2	—	12.76 (3)	—	—
	ML_3	—	18.63 (9)	—	—
ADP	**MLH**	—	10.73 (2)	—	—
	ML	—	7.41 (2)	—	—
	ML_2	—	11.96 (2)	—	—
	MLOH	—	1.98 (3)	—	—
ATP	**MLH**	10.852 (8) [c]	—	10.77 (2) [c]	10.35 (2) [c]
	ML	8.113 (6)	—	7.648 (8)	7.35 (1)
	ML_2	12.842 (8)	—	12.089 (7)	11.472 (9)
	MLOH	2.79 (1)	—	1.90 (1)	1.46 (2)

[a] According to the reaction (3.16), charges omitted for simplicity; [b] in mol L^{-1}; [c] least-squares errors on the last significant figure are given in parentheses.

The speciation profiles, drawn in Figs 10.1 - 10.3, denote the possibility of investigating Al^{3+}-*AMP* up to pH = 4.2 and Al^{3+}-*ADP*, -*ATP* up to physiological pH value, namely pH = 7.4. More in detail, in the Al^{3+}-*AMP* system, depicted in Fig. 10.1, the main species is the ML_3, which reaches an Al^{3+} maximum fraction of over 0.8 at pH = 4. At lower pH values, ML and ML_2 species predominate with a metal fraction of about 0.45 and 0.35, respectively, in the pH range between 3 and 3.5. In the case of Al^{3+}-*ADP* system, as reported in the Fig. 10.2, all the species achieve an Al^{3+} maximum fraction of about 0.7, except the hydrolytic mixed one, MLOH, which is formed in lower amount in the pH range 5 - 7.4. For Al^{3+}-*ATP* system, whose speciation profile is shown in Fig. 10.3, the main species are ML and ML_2, formed with maximum fractions of 0.85 and 0.65, respectively, in a wide pH range, from 2.5 to 7.4, at I = 0.1 mol L^{-1}. MLH and MLOH species reach lower, though significant, Al^{3+} fractions (about 0.5) at pH = 2.5 and 7, respectively. By increasing the ionic strength from 0.1 to 1 mol

L^{-1}, the fractions of MLH and MLOH species significantly change. More in detail, MLH increases from 0.5 to 0.6 at pH = 2.5 and MLOH decreases from 0.5 to 0.2 at pH = 7. ML and ML_2 species undergo a slight decrease and increase of their fractions, respectively.

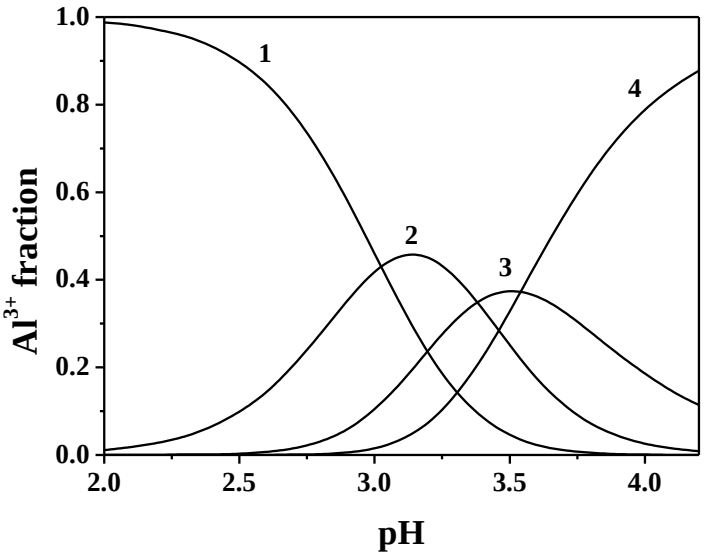

Fig. 10.1 Speciation diagram for Al^{3+}-*AMP* system in NaCl at I = 0.15 mol L^{-1}, T = 298.15 K. Experimental conditions: C_M = 0.5 mmol L^{-1}; C_L = 3 mmol L^{-1}. Species: **1. M; 2. ML; 3. ML_2; 4. ML_3.**

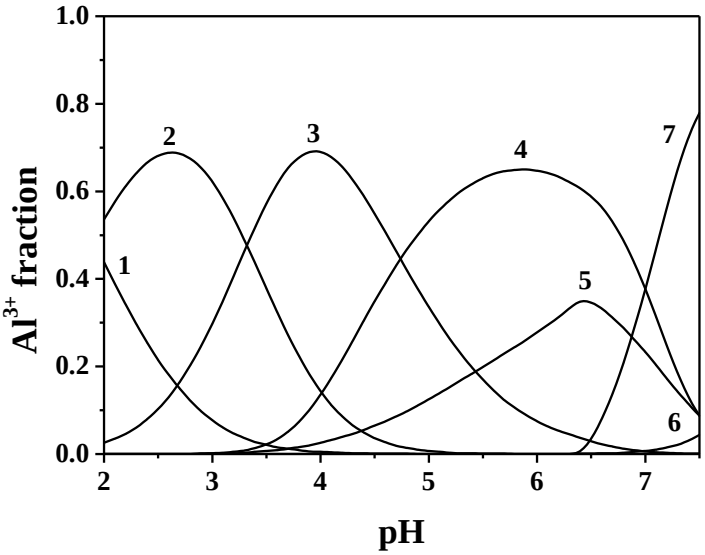

Fig. 10.2 Speciation diagram for Al^{3+}-*ADP* system in NaCl at I = 0.15 mol L^{-1}, T = 298.15 K. Experimental conditions: C_M = 2 mmol L^{-1}; C_L = 4 mmol L^{-1}. Species: **1. M; 2. MLH; 3. ML; 4. ML_2; 5. MLOH; 6. $M(OH)_4$; 7. $M_{13}(OH)_{32}$.**

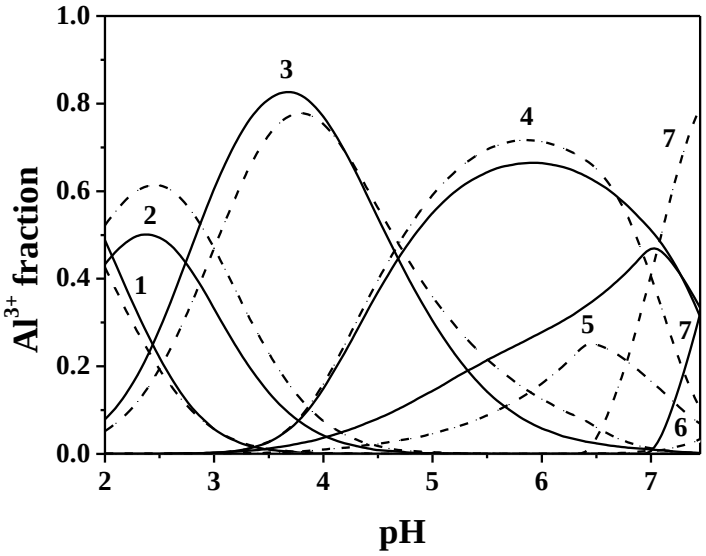

Fig. 10.3 Speciation diagram for Al^{3+}-*ATP* system in NaCl at I = 0.1 mol L^{-1} (solid line) and I = 1 mol L^{-1} (dotted line), T = 298.15 K. Experimental conditions: C_M = 2.5 mmol L^{-1}; C_L = 5 mmol L^{-1}. Species: **1. M; 2. MLH; 3. ML; 4. ML_2; 5. MLOH; 6. $M(OH)_4$; 7. $M_{13}(OH)_{32}$.**

10.3 Ionic strength dependence

The dependence of the formation constants on ionic strength was evaluated only for the Al^{3+}-*ATP* system, by using the Debye - Hückel type equation (3.23), expressed in the Section 3.7.3. The $\log^T\beta$ values for all the species, together with the empirical parameter C for the dependence on ionic strength are reported in Table 10.3.

The C parameter ranges from 0.0 to 2.1, differently from the oligophosphate and the other ligands under study. Moreover, concerning to the ML_2 species, it seems to be similar to the one obtained for Al^{3+}-*mal* with a values of 0.1 (this thesis and [66]).

Table 10.3 Formation constants for Al^{3+}-*ATP* species at infinite dilution, together with C parameter of eq. (3.23) in NaCl, at T = 298.15 K

Species [a]	Ligand	$\log^T\beta$	C
MLH	*ATP*	13.8 (3) [b]	2.1 (6) [b]
ML		10.8 (3)	1.6 (6)
ML_2		14.7 (3)	0.0 (6)
MLOH		5.0 (3)	0.5 (6)

[a] According to the reaction (3.16), charges omitted for simplicity; [b] least-squares errors on the last significant figure are given in parentheses.

10.4 Temperature dependence

For Al^{3+}-*ATP* system, enthalpy changes were obtained by means of calorimetric titrations, at T = 298.15 K and I = 0.1 mol L^{-1}. ΔH values of ligand protonations were previously determined under the same experimental conditions of ionic strength and temperature employed for the study of the complexes. Enthalpy changes, together with ΔG and $T\Delta S$ values of the protonated and complex species, are reported in Table 10.4. The driving force of the formation reactions of the species is the entropy, as expected by these type of interactions, typically hard-hard. For example, ΔH = 27.2 kJ mol^{-1} and $T\Delta S$ = 73.5 kJ mol^{-1} for the formation of ML species. Enthalpy change value for this species is almost the same of the one found for the ML species of the Al^{3+}-*TPP* system (ΔH = 27.8 kJ mol^{-1}, see Table 8.5). This highlights that the interaction between Al^{3+} and *ATP* may occur mainly through the phosphate groups. Moreover, it is comparable to the enthalpy change obtained for the simple metal - ligand species of the Al^{3+}-*tla* and -*mal* systems (ΔH = 28, 21 kJ mol^{-1}, respectively) (this thesis and [66, 120]).

Table 10.4 Thermodynamic parameters of *ATP* and Al^{3+}-*ATP* species obtained by titration calorimetry at I = 0.1 mol L^{-1} in NaCl and T = 298.15 K

Species [a]	Ligand	$-\Delta G$ [b]	ΔH [b]	$T\Delta S$ [b]
LH	*ATP*	36.9	6.1 (3) [c]	4.3
LH_2		59.7	-11.2 (8)	48.5
ML		46.3	27.2 (8)	73.5
ML_2		73	25 (2)	98

[a] According to the reaction (3.14), charges omitted for simplicity; [b] In kJ mol^{-1}; [c] least-squares errors on the last significant figure are given in parentheses.

10.5 ^{1}H NMR spectroscopy

Prior to carry out the titrations on Al^{3+}-*ATP* solutions, the study of the acid - base properties of the ligand was performed by means of ^{1}H NMR investigations as well, collecting spectra in H_2O/D_2O solutions with a ligand concentration of 8 mmol L^{-1}, at T = 298.15 K and I = 0.1 mol L^{-1} in NaCl and in a pH range between 1.85 and 8.05. Except for the signal indicated as CH(6) in Fig. 10.4, covered by the water band, all the other peaks can be observed as a single set of resonances which, as expected, undergo a shift with the pH variation, depending on the nucleus investigated. Moreover, the spectrum recorded at pH = 1.8, shown in Fig 10.5, can be considered with a good approximation as significant for the LH_2 species, since, on the basis of potentiometric data previously obtained by the research group [147], this species should be present in solution with a percentage of 99.4 at this pH value.

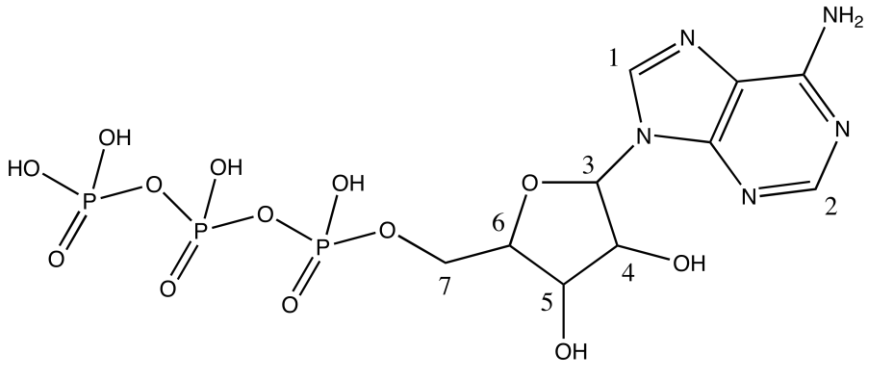

Fig 10.4 *ATP* molecule.

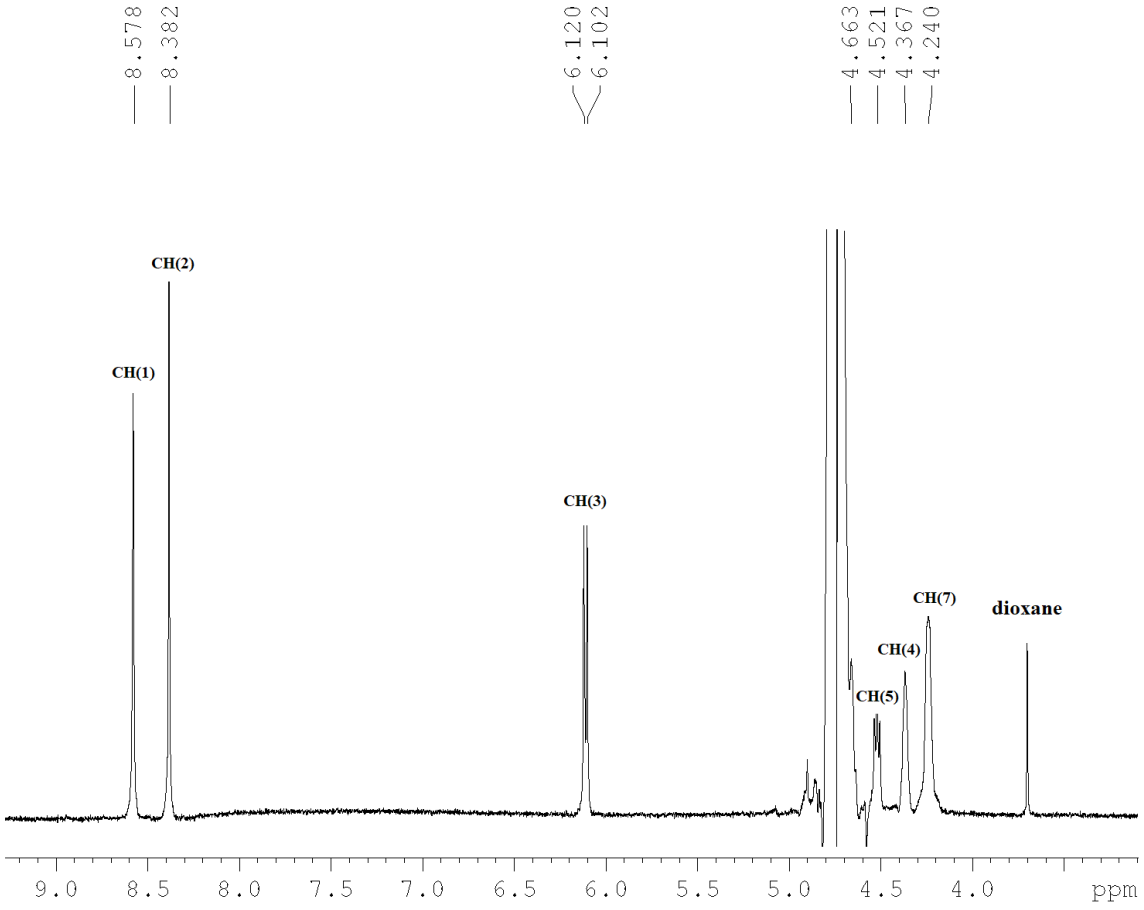

Fig. 10.5 ^{1}H NMR spectrum of *ATP* at C = 8 mmol L^{-1}, pH = 1.8, T = 298.15 K and I = 0.1 mol L^{-1} in NaCl.

Single resonances, attributed to aromatic protons, CH(1) and CH(2), start to undergo a considerable shielding from approx. pH = 3 up to pH = 5.5, thus indicating that the first

deprotonation occurs in proximity of these nuclei, probably due to the ammonium group, as already pointed out by Kiss *et al*. [148]. In addition, these two peaks remain unaltered at higher pH values. At the same time, the methylene group adjacent to the triphosphate group, indicated as CH(7), shows a similar trend to the previous ones, even though less pronounced. The formation of the totally deprotonated species occurs together with a deshilding of the CH(5) signal. The other peaks are characterized by continuous changes in chemical shift towards upfields, due to the pH increase. The chemical shifts obtained from each ^{1}H NMR spectrum, allowed to calculate, by HypNMR software program [76], the formation constants of the species and the chemical shift values for each complex. Moreover, the program can recalculate the average chemical shift at each experimental pH value. The results are reported in Table 10.5 and are in good accordance with the ones gained by potentiometry [147]. Furthermore, it was possible to obtain another protonation constant related to the LH_3 species with logβ = 12.9. As Al^{3+}-*ATP* system concerns, a wide number of spectra were collected by varying the metal - ligand ratio and the concentrations of metal and ligand as well (see Section 3.5.2). The presence of aluminum in solution causes significant changes in the recorded spectra, as a new set of broad resonances can be observed (indicated with the subscript “b”), in addition to the free ligand signals. The peaks related to the *ATP*, being always present in excess, appear and substantially overlap those recorded in the absence of metal. The only presence of this new observed pattern, beside the free ligand resonance, suggests that all complex species are also involved in a rapid mutual exchange on the NMR time scale, as already observed for the spectra recorded on *ATP* alone. Depending on the nucleus considered, the corresponding "bound" peaks are more shielded or more deshielded than those of the free ligand. For example, in the case of methylene group adjacent to triphosphate, CH(7), it is noted that the bound signal set is more deshielded with respect to the average of the free ligand resonances. This indicates a depletion of the electronic density on the *ATP*, due to the presence of aluminum, thus suggesting phosphate coordination, which cannot be observable from the simple comparison of the spectra. On the contrary, all the other bound signals present in the spectra are shifted to higher fields than those of the free ligand. This effect is very marked in the case of the proton designated as CH(3). ^{1}H NMR data, obtained for the Al^{3+}-*ATP* system, are reported in Table 10.6. The gained results, referred to the formation constants of the predominant species in the experimental conditions, namely ML, ML_2 and MLOH, are comparable to those collected by potentiometric titrations, as reported in Table 10.7. The formation constant value of the MLH species, calculated by potentiometry, was considered in the model and kept constant. The good agreement between experimental and calculated NMR parameters, as displayed in Fig. 10.6 for CH(2) and $CH(2)_b$ nuclei, allow to validate the speciation model provided by the potentiometric findings.

Table 10.5 Protonation constants and calculated chemical shifts of *ATP* species obtained by ^{1}H NMR at I = 0.1 mol L^{-1} (NaCl) and T = 298.15 K

Species [a)]	logβ	$\delta_{CH(1)}$	$\delta_{CH(2)}$	$\delta_{CH(3)}$	$\delta_{CH(4)}$	$\delta_{CH(5)}$	$\delta_{CH(7)}$
L	—	8.4891(8)[b)]	8.202(1) [b)]	6.078(1)[b)]	4.337(3)[b)]	4.576(8)[b)]	4.601(1)[b)]
LH	6.56(4)[b)]	8.459 (8)	8.200 (1)	6.086 (1)	4.347 (3)	4.5219 (8)	4.181 (1)
LH_2	10.64(4)	8.55 (8)	8.375 (1)	6.104 (1)	4.366 (3)	4.5228 (8)	4.238 (1)
LH_3	12.9(3)	8.5752 (8)	8.385 (1)	6.113 (1)	4.367 (3)	4.5202 (8)	4.241 (1)

[a)] According to the reaction (3.14), charges omitted for simplicity; [b)] least-squares errors on the last significant figure are given in parentheses.

Table 10.6 Formation constants and calculated chemical shifts of Al^{3+}-*ATP* species obtained by ^{1}H NMR at I = 0.1 mol L^{-1} (NaCl) and T = 298.15 K

Species [a)]	logβ	$\delta_{CH1(b)}$	$\delta_{CH2(b)}$	$\delta_{CH3(b)}$	$\delta_{CH7(b)}$
MLH	10.852	8.52 (1) [b)]	8.44 (1) [b)]	6.15 (7) [b)]	4.37 (2) [b)]
ML	8.0 (1) [b)]	8.53 (1)	8.28 (1)	6.08 (7)	4.15 (2)
ML_2	12.7 (2)	8.32 (1)	8.06 (1)	6.01 (7)	3.79 (2)
MLOH	3.1 (2)	8.29 (1)	8.04 (1)	5.97 (7)	5.21 (2)

[a)] According to the reactions (3.16), charges omitted for simplicity; [b)] least-squares errors on the last significant figure are given in parentheses.

Table 10.7 Comparison between experimental equilibrium constants of Al^{3+}-*ATP* species obtained by ^{1}H NMR and potentiometry at I = 0.15 mol L^{-1} (NaCl) and T = 298.15 K

Ligand	Species [a)]	$\log\beta_{H\ NMR}$	$\log\beta_{ISE\ H^+}$
ATP	**MLH**	10.852 [b)]	10.852(8) [c)]
	ML	8.0(1) [c)]	8.113(6)
	ML_2	12.7(2)	12.842(8)
	MLOH	3.1(2)	2.79(1)

[a)] According to the reaction (3.16), charges omitted for simplicity; [b)] potentiometric data kept constant in the calculations; [c)] least-squares errors on the last significant figure are given in parentheses

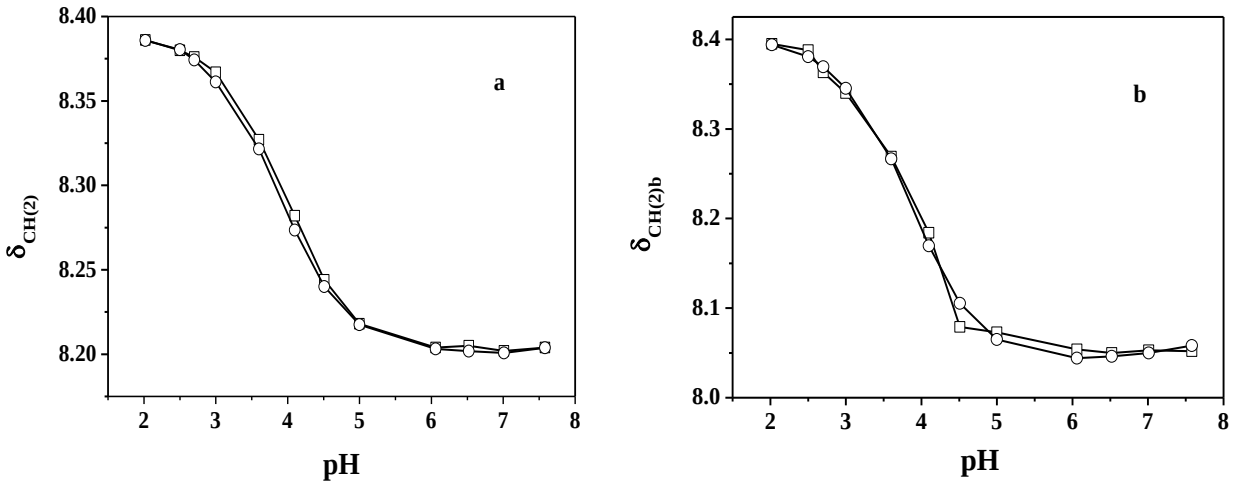

Fig. 10.6 Experimental (□) and calculated (○) values of the chemical shifts for CH(2) (a) and $CH(2)_b$ (b) of the ligand in Al^{3+}-*ATP* mixtures at C_M = 6 mmol L^{-1}, C_L = 8 mmol L^{-1} and *T* = 298.15 K.

10.6 Literature comparisons

To the best of our knowledge, few data are reported in the literature concerning the Al^{3+} interactions with the nucleosides under study, as shown in Table 10.8.

Kiss and other authors, in an article and afterward in a review [64, 148], reported the same speciation model for Al^{3+}-*ADP* and -*ATP*, similar to the ones here obtained and featured by MLH, ML, ML_2 and MLOH species. Kiss *et al*. outlined the presence also of the ML_2OH species at pH ≈ 7, probably due to the different experimental conditions in metal - ligand concentration ratios (from 1 : 1 to 1 : 10). More in detail, for Al^{3+}-*ADP* they found logβ = 10.98, 7.82, 2.94, 12.16 and for Al^{3+}-*ATP* logβ = 11.30, 7.92, 2.46, 12.47 related to MLH, ML, MLOH and ML_2 species, respectively, at *T* = 298.15 K and *I* = 0.2 mol L^{-1} in KCl. These values are in good agreement with the ones provided in this thesis (see Section 10.2, Table 10.2), by considering the different experimental conditions in metal - ligand concentrations and ionic strength.

For Al^{3+}-*AMP*, the speciation model reported by Kiss and other co-workers is different, with the only ML and ML_2 common species. In addition, they found the MLOH species, whilst in this thesis the ML_3 one is reported. The stability constants provided by Kiss (logβ = 6.17, 10.35 for ML and ML_2 species, respectively) result fairly different to the ones here reported (logβ = 6.66, 12.76 for ML and ML_2 species, respectively). It is due, also in this case, to the

different experimental conditions employed for the investigations (T = 298.15 K and I = 0.2 mol L^{-1} in KCl).

Moreover, in literature are also reported the protonation constants related to the three nucleotides. By taking into account the different experimental conditions, the protonation constant values, obtained by Kiss and others, are in good agreement with those here found, reported in Table 10.1 (logβ = 6.04, 9.78 for *AMP* and logβ = 6.19, 9.98 for *ADP*).

In addition, for *AMP* and *ADP* Smith *et al*., reported $\log\beta_1$ = 6.18, 6.31 and $\log\beta_2$ = 9.98, 10.25, respectively, at T = 298.15 K and I = 0.1 mol L^{-1} in NaCl [149], whilst Jackson and Voyi, provided $\log\beta_1$ = 6.08, 6.04 and $\log\beta_2$ = 9.89, 9.77 for *AMP* and *ADP* respectively, under the same experimental conditions employed for this study [150].

Table 10.8 Literature data on Al^{3+}-nucleotide systems

			logβ [a]				**Ref.**
***T*/K**	***I*/mol L^{-1}**	**Ligand**	**MLH**	**ML**	**ML_2**	**MLOH**	
298.15	0.2 [b]	*AMP*	—	6.17	10.35	—	[64, 148]
298.15	0.2 [b]	*ADP*	10.98	7.82	12.16	2.94	[148]
		ATP	11.30	7.92	12.47	2.46	[148]

[a] According to the reactions (3.16), charges omitted for simplicity; [b] in KCl.

Chapter 11

Sequestering ability and empirical relationships

11.1 Sequestering ability

The measure of the sequestration of a metal ion in solution is of great importance to assess the possibility of using a ligand as detoxifying agent in biomedical applications or to remove toxic metal ions from natural systems.

In general, for the evaluation of the metal ion complexation, all the complex species of a given system should be taken into account. As already pointed out, the stability of a complex is provided by the formation constant values of the species, which, in turns, are function of some parameters, such as temperature, pH, ionic strength, and composition of the medium. However, the simple analysis of the stability constants and percentage values of the different species is not sufficient to estimate the real binding ability of a ligand towards a metal cation. Other factors may influence the sequestering ability of a ligand, such as the ligand protonation, the hydrolysis equilibria of the metal and the possible interactions with other components, such as the supporting electrolyte.

By taking into account all these assertions, the sequestering ability of a ligand towards a metal cation can be evaluated by means of an empirical parameter, $pL_{0.5}$, already proposed in the past by the research group, which indicates the ligand concentration necessary to sequester the 50% of the metal cation present in traces. The $pL_{0.5}$ value can be calculated by the following sigmoidal type equation with asymptotes of 1 for $pL \rightarrow \infty$ and 0 for $pL \rightarrow 0$ [151, 152]:

$$\chi = \frac{1}{1+10^{(pL - pL_{0.5})}} \qquad (11.1)$$

where χ represents the sum of the molar fractions of the different species and pL is the cologarithm ($pL = -\log [L]_{tot}$) of the total ligand concentration ($[L]_{tot}$).

11.1.1 Carboxylic ligands

For the carboxylic ligands, the $pL_{0.5}$ parameter was determined at different pH values, I = 0.15 mol L^{-1} (I = 0.1 mol L^{-1} for *lac*) and T = 298.15 K. For Al^{3+}-*EDDS* system, this value was calculated also at physiological and natural water pH values (pH = 7.4 and 8.1, respectively), since this ligand totally suppresses the aluminium hydrolysis, as shown in Fig. 5.7. The obtained $pL_{0.5}$ values are reported in Table 11.1. More in detail, at pH = 5 and I = 0.15 mol L^{-1}, the $pL_{0.5}$ = 6.09, 5.84, 4.03, 4.15, 4.10, 10.69 for *mal*, *mala*, *tca*, *btc*, *mlt*, *EDDS*, respectively, and, as indicated in Fig. 11.1, follow the trend:

$$EDDS >> mal > mala > btc \approx mlt \approx tca$$

At pH = 5, it was not possible to assess the binding ability of *lac*, since the formation of a slightly soluble species occurred. Moreover, as expected, *EDDS* shows a higher sequestering ability toward Al^{3+} than the other ligands. The presence in its molecule of two amino groups, in addition to the four carboxylate ones, with the possibility of forming a six member chelate ring, can explain this behavior [7, 28].

Table 11.1 $pL_{0.5}$ values of polycarboxylates towards Al^{3+}, at different pH values, I = 0.15 mol L^{-1} and T = 298.15 K

Ligand	pH	$pL_{0.5}$
lac[a)]	4	2.84
mal	4	5.62
	5	6.09
mala	4	4.40
	5	5.84
tca	4	2.30
	5	4.03
btc	4	2.62
	5	4.15
mlt	4	3.03
	5	4.10
EDDS	4	8.56
	5	10.69
	7.4	10.63
	8.1	9.34

[a)] I = 0.1 mol L^{-1}.

The binding ability of *mal* and *mala* is comparable at pH = 5. Their fairly high $pL_{0.5}$ values are probably due to their capacity to act as bidentate ligands, forming cyclic structures. It is known that carboxylate with an additional donor group in α or β position, as in the case of *mala*, can providing structure of this type [153]. Moreover, for this ligand, Kiss and other coworkers, suggest a tridentate coordination by means of the alcoholic function [117]. In the case of *tca* and *btc*, the presence of one or two additional carboxylate groups, does not provide an increase of the binding capacity. Lastly, as *mlt* concerns, its lower sequestering ability with respect to the bicarboxylic ligands, *mal* and *mala*, is probably due to the rigidity of the structure provided by the benzene ring. Its $pL_{0.5}$ value is quite similar to the *tca* and *btc* ones.

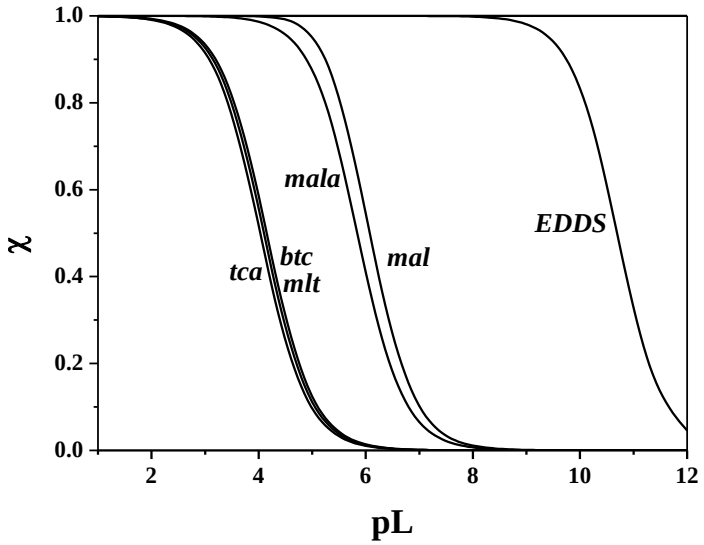

Figure 11.1 Sequestration diagram (sum of the molar fractions of the different species, χ, *vs.* cologarithm of the total ligand concentration, pL), for Al^{3+}-*mal*, -*mala*, -*tca*, -*btc*, -*mlt*, -*EDDS* species at pH = 5, I = 0.15 mol L^{-1} in NaCl, T = 298.15 K.

11.1.2 Thiocarboxylic ligands

For thiocarboxylic ligands, the sequestering ability was evaluated at pH = 4 and 5, I = 0.15 mol L^{-1} and T = 298.15 K. The obtained results are reported in Table 11.2.

As shown in the sequestration diagram, depicted in Fig. 11.2, a similar binding ability was found for *tla* and *mpa*, with a $pL_{0.5}$ = 3.18, 2.99, at pH = 5. In the case of *tma*, the presence of an additional carboxylate group in its molecule with respect to the *tla* and *mpa* ones, produces a significant increment of the $pL_{0.5}$ parameter ($pL_{0.5}$ = 5.47). This value is fairly similar to those reported for *mal* and *mala* towards Al^{3+} ($pL_{0.5}$ = 6.09, 5.84, respectively) in the same experimental conditions (this thesis and [66]). Furthermore, taking into account the $pL_{0.5}$ values of lactate and thiolactate at pH = 4, the sequestering ability is fairly comparable for

both ligands, even though it results slightly higher for *lac*. Also in the case of *tma* and *mala*, the sequestering ability is higher for the ligand having the -OH group, as shown in Fig. 11.3. These results were expected, since Al^{3+}, being a hard metal cation, tends to bind more strongly to O-donor group, thus forming more stable complexes with the hydroxyl group.

Table 11.2 $pL_{0.5}$ values of thiocarboxylates towards Al^{3+}, at different pH values, I = 0.15 mol L^{-1} and T = 298.15 K

Ligand	pH	$pL_{0.5}$
tla	4	2.58
	5	3.18
mpa	4	2.49
	5	2.99
tma	4	3.44
	5	5.47

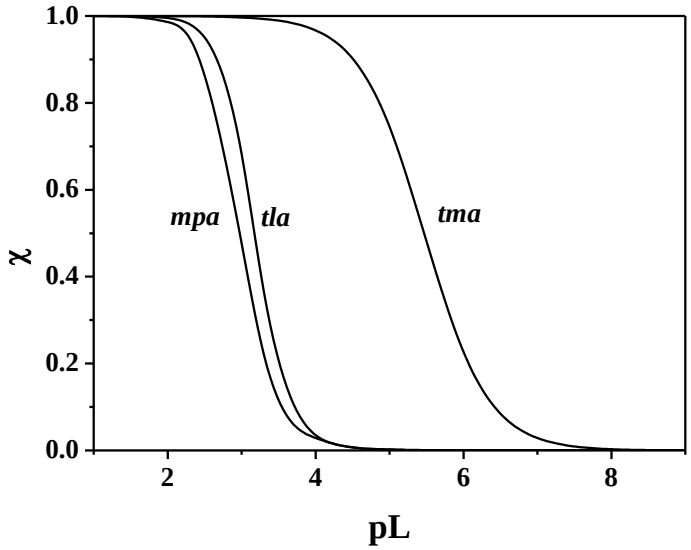

Fig. 11.2 Sequestration diagram (sum of the molar fractions of the different species, χ, *vs.* cologarithm of the total ligand concentration, pL), for Al^{3+}-*tla* -*mpa*, -*tma* species at pH = 5, I = 0.15 mol L^{-1} in NaCl, T = 298.15 K.

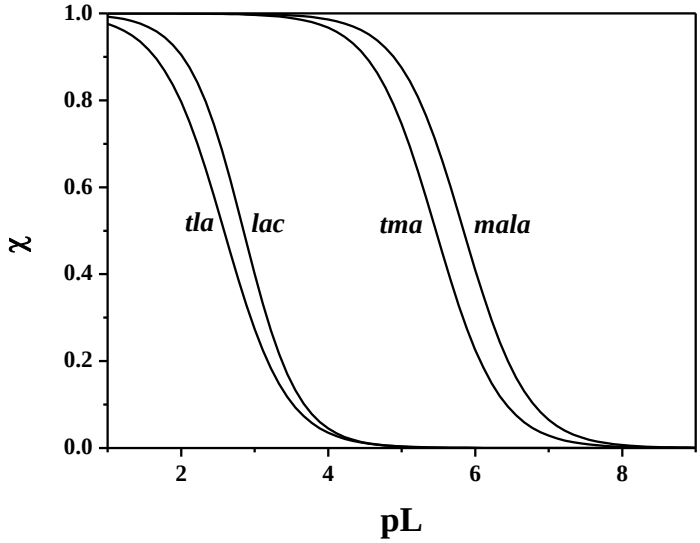

Fig. 11.3 Sequestration diagram (sum of the molar fractions of the different species, χ, *vs.* cologarithm of the total ligand concentration, pL), for Al^{3+}-*tla* and -*lac* species at pH = 4 and Al^{3+}-*tma* and -*mala* species at pH = 5, T = 298.15 K and I = 0.15 mol L^{-1} in NaCl (for *lac* I = 0.1 mol L^{-1}).

11.1.3 Amino acids

For the amino acids under study, $pL_{0.5}$ parameter at pH = 4 and 5, I = 0.15 mol L^{-1} and T = 298.15 K was calculated. The obtained values are collected in Table 11.3. As shown in Fig. 11.4, at pH = 5, I = 0.15 mol L^{-1} and T = 298.15 K, the sequestering ability of *Gly*, *Cys* and *tranex* ($pL_{0.5}$ = 2.51, 3.74, 3.91) follows the trend:

$$tranex \approx Cys > Gly$$

For *Cys* and *tranex*, the $pL_{0.5}$ parameter is fairly similar, but higher than the one of *Gly* of over one logarithmic unit in the same experimental conditions.

Table 11.3 $pL_{0.5}$ values of *Gly*, *Cys*, *tranex* towards Al^{3+}, at different pH values, I = 0.15 mol L^{-1} and T = 298.15 K

Ligand	pH	$pL_{0.5}$
Gly	4	2.19
	5	2.51
Cys	4	1.62
	5	3.74
tranex	4	2.44
	5	3.91

At pH = 5, *Cys* and *tranex* binding capacity is higher to the ones obtained for Al^{3+}-*tla* and -*mpa* systems, ($pL_{0.5}$ = 3.18, 2.99 respectively) under the same pH and ionic strength conditions (this thesis and [120]). Moreover, the comparison between *Gly*, *mpa* and *Cys*, values at pH = 5 ($pL_{0.5}$ = 2.51, 2.99, 3.74 respectively), suggests that the sequestering ability of the ligands having an O- donor group and a N- or S- additional one (*Gly* and *mpa*) is lower than a ligand with an O- donor group and two N- and S- additional ones, such as *Cys*.

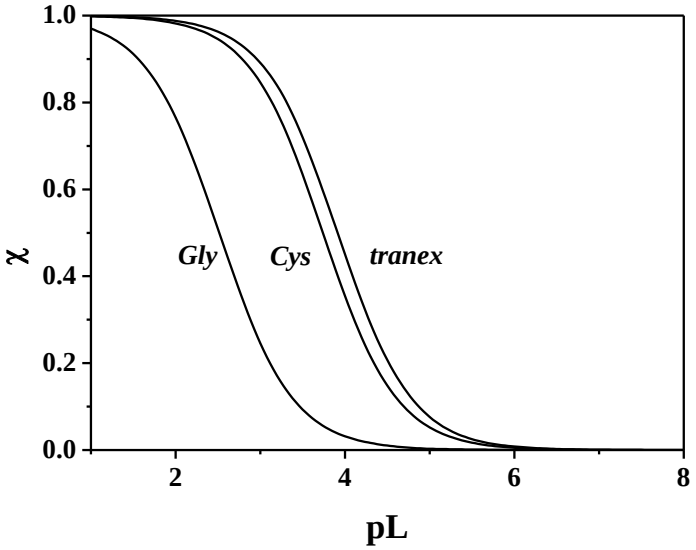

Fig. 11.4 Sequestration diagram (sum of the molar fractions of the different species, χ, *vs.* cologarithm of the total ligand concentration, pL), for Al^{3+}-*Gly*, -*Cys*, -*tranex* species (in NaCl) at pH = 5, I = 0.15 mol L^{-1}, T = 298.15 K.

11.1.4 Oligophosphate ligands

For Al^{3+}-oligophosphate systems, the sequestering ability was evaluated at pH = 4 and 5, I = 0.15 mol L^{-1} and T = 298.15 K. As concerns *PP* and *TPP* ligands, the $pL_{0.5}$ value was calculated also at physiological pH. The gained results are reported in Table 11.4.
At pH = 4, I = 0.15 mol L^{-1} and T = 298.15 K, $pL_{0.5}$ = 3.94, 7.74, 9.55, 6.63, for PO_4^{3-}, *PP, TPP, HMP,* respectively and, as shown in Fig 11.5, the binding ability follows the trend:

$$TPP > PP > HMP > PO_4^{3-}$$

Therefore, it increases with the increasing of the phosphate groups, except for *HMP,* which is a complex mixture of polyphosphates (see Section 2.5). At physiological pH, *TPP* also shows the highest sequestering ability toward Al^{3+}. Probably, it is due to the possibility to form a stable six membered ring *via* two adjacent phosphate oxygens, as suggested by NMR and LD MS investigations (see Section 8.5 and 8.6).

Moreover, the binding ability of oligophophates towards aluminium is much higher than carboxylate, thiocarboxylate and amino acid ones (this thesis and [66, 116, 120, 129, 139]). Among carboxylates, only *EDDS* sequestering ability ($pL_{0.5}$ = 10.69 at pH = 5, I = 0.15 mol L^{-1} and T = 298.15 K) results an intermediate between *PP* and *TPP* one ($pL_{0.5}$ = 9.44, 11.27, respectively, in the same conditions) (this thesis and [66]).

Table 11.4 $pL_{0.5}$ values of oligophosphates towards Al^{3+}, at different pH values, I = 0.15 mol L^{-1} in NaCl (in $NaNO_3$, only for *HMP*) and T = 298.15 K

Ligand	pH	$pL_{0.5}$
PO_4^{3-}	4	3.94
	5	5.73
PP	4	7.74
	5	9.44
	7.4	7.08
TPP	4	9.55
	5	11.27
	7.4	7.74
HMP	4	6.63
	5	7.64

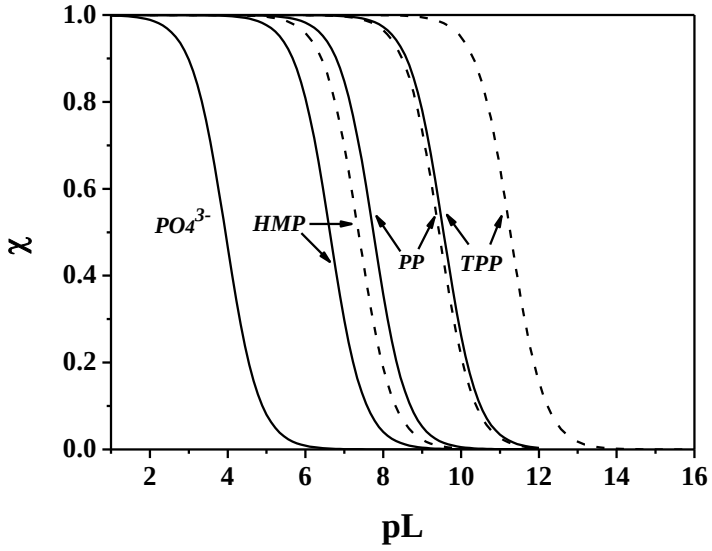

Fig. 11.5 Sequestration diagram (sum of the molar fractions of the different species, χ, *vs.* cologarithm of the total ligand concentration, pL), for Al^{3+}-PO_4^{3-}, -*PP*, -*TPP*, -*HMP* species at pH = 4 (solid line) and pH = 5 (dotted line), I = 0.15 mol L^{-1}, T = 298.15 K.

11.1.5 Other inorganic ligands

For the other inorganic ligands, the sequestering ability was evaluated at I = 0.15 mol L^{-1}, T = 298.15 K and pH = 2.5 and 4 for Al^{3+}-F^- , -CO_3^{2-} systems, respectively.
It was not possible for both systems to assess the binding capacity at higher pH values, owing to the formation of poorly soluble species. The obtained results are reported in Table 11.5.
For CO_3^{2-}, $pL_{0.5}$ = 4.36 at pH = 4, which is comparable to the one of *mala* in the same experimental condition ($pL_{0.5}$ = 4.40) (this thesis and [66]).
Moreover, as shown in Fig 11.6, the sequestering ability results fairly higher for CO_3^{2-} with the respect to the PO_4^{3-} one ($pL_{0.5}$ = 3.94) at I = 0.15 mol L^{-1}, T = 298.15 K and pH = 4 (this thesis and [139]).

Table 11.5 $pL_{0.5}$ values of -CO_3^{2-} and F^- towards Al^{3+}, at different pH values, I = 0.15 mol L^{-1} in NaCl and T = 298.15 K

Ligand	pH	$pL_{0.5}$
CO_3^{2-}	4	4.36
F^-	2.5	5.78

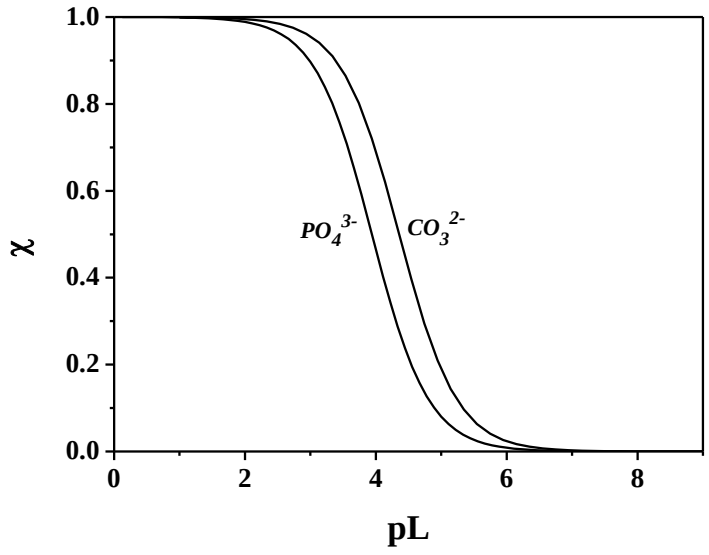

Fig. 11.6 Sequestration diagram (sum of the molar fractions of the different species, χ, *vs.* cologarithm of the total ligand concentration, pL), for Al^{3+}-CO_3^{2-} and -PO_4^{3-} species at pH = 4, I = 0.15 mol L^{-1}, T = 298.15 K.

11.1.6 Nucleotides

For Al^{3+}-nucleotides systems, the sequestering ability was evaluated at pH = 4 and 5, I = 0.15 mol L^{-1} (I = 0.1 mol L^{-1} for *ATP*) and T = 298.15 K. In addition, for *ADP* and A*TP*, the $pL_{0.5}$ value was calculated also at physiological pH. The obtained results are reported in Table 11.6. As shown in Fig 11.7, at pH = 4, the binding ability follows the trend:

$$ATP > ADP > AMP$$

with $pL_{0.5}$ = 4.31, 4.99, 5.36 for *AMP*, *ADP* and *ATP,* respectively. The same trend is observed at pH = 5 and 7.4 for *ADP* and *ATP*.

Table 11.6 $pL_{0.5}$ values of *AMP*, *ADP* and *ATP* towards Al^{3+}, at different pH values, I = 0.15 mol L^{-1} in NaCl and T = 298.15 K

Ligand	pH	$pL_{0.5}$
AMP [a)]	4	4.31
ADP	4	4.99
	5	6.04
	7.4	3.17
ATP	4	5.36
	5	6.55
	7.4	3.83

[a)] I = 0.1 mol L^{-1}.

Therefore, the sequestering ability increases with the increasing of the number of phosphate groups, as in the case of the oligophosphate ligands. Despite this, their binding capacity results lower than the corresponding phosphate ligand ones, probably because of the larger structure of nucleotides, which does not allow the same mobility. Moreover, for *ADP* and *ATP* the $pL_{0.5}$ values result comparable to the ones of *mal* and *mala* in the same experimental conditions. (This thesis and [66]).

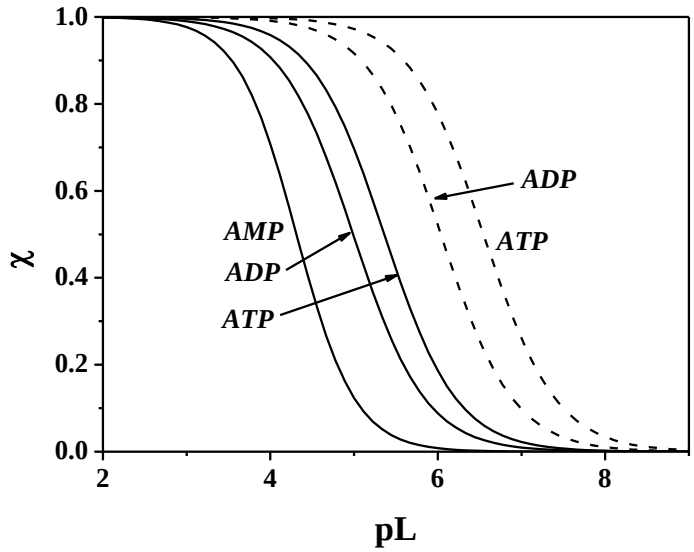

Fig. 11.7 Sequestration diagram (sum of the molar fractions of the different species, χ, *vs.* cologarithm of the total ligand concentration, pL), for Al^{3+}-*AMP, -ADP, -ATP* species at pH = 4 (solid line) and pH = 5 (dotted line), I = 0.15 mol L^{-1} (I = 0.1 mol L^{-1} for ATP), T = 298.15 K.

11.2 Empirical relationships

Speciation and sequestration studies on metal cations are of great importance for their possible application to real systems, such as natural waters and biological fluids, featured by very variable composition, temperature, ionic strength, pH and pressure.

The determination of the possible interactions of all the components in a particular system, in its specific conditions of *I, T*, pH and concentrations, may be result a crucial task. For this reason, although the experimental determination is the best approach, modelling studies can be very useful as well. With this kind of study, it is possible to predict the reactivity of a specific metal cation towards different ligand classes typically present in real systems.

The stability of metal - ligand complexes, for the same metal cation and homogeneous ligand classes, can be considered as a function of the number and kind of functional groups of the ligand. The formation constant of a complex may be roughly estimated by adding the contribution of single functional groups involved in the complexation (Additivity Factors Approach) [154-157]. Accordingly, the stability constant can be expressed by the following equation:

$$\log K = \sum n_{\text{x-donor}} \qquad (11.1)$$

where $n_{\text{x-donor}}$ could be a S-, N- or O-donor group.

By considering log$K$ values at I = 0 mol L^{-1} and T = 298.15 K for MLH_2, MLH and ML complex species of Al^{3+} with amino acids, namely *Gly*, *Cys*, *tranex,* thiocarboxylates, namely

tla, *mpa*, *tma*, and carboxylates, namely *mal*, *tca*, *btc*, it was possible to calculate the single contribution values, by the following equation:

$$\log K = 2.93n_{COO^-} + 6.5n_{SH^-} + 4.5n_{NH2} \quad (11.2)$$

The contributions for carboxylate, thiolate and amino group result equal to 2.93 and 6.5, 4.5, respectively, with a log*K* ± 0.8 (95% confidence interval) estimated precision [66, 120, 129]. For this type of calculation, it is not considered the chelation or other specific effects.

This trend may seem surprising since generally S-donor groups do not show a good affinity towards hard metal cations, such as Al^{3+}. However, as already pointed out, for ligands containing more than one group potentially coordinating the metal cation, if thiolate groups are in α or β position with respect to an O-donor group, their binding ability may significantly increase [28].

In Fig 11.8 the formation constant values calculated by the equation 11.2 are plotted *vs.* the corresponding experimental data with a fairly good agreement (correlation coefficient, r^2 = 0.92; slope = 0.9 9 ± 0.03) By taking into account the obtained contribution values calculated by the equation 11.2, the stability constant value of ML species for *Cys*, given by the sum of carboxylate, thiolate and amino groups contributions (log*K* =13.9, at *I* = 0 mol L^{-1}), results quite comparable to the one reported in Table 7.3, obtained by the experimental data (log*K* =13.31 at *I* = 0 mol L^{-1}).

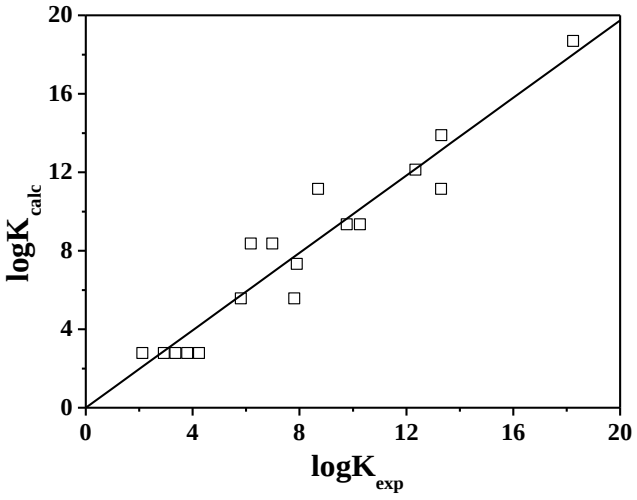

Fig. 11.8 Calculated formation constants, by eq. (11.2), of MLH_2, MLH and ML species (as stepwise equilibria, eq. (3.17)) formed by Al^{3+} with *Gly*, *Cys*, *tranex*, *tla*, *mpa*, *tma*, *mal*, *tca*, and *btc* at *I* = 0 mol L^{-1} and *T* = 298.15 K, *vs.* experimental ones.

Chapter 12

Conclusions

In this thesis, the results of a thermodynamic and spectroscopic study in aqueous solution on the Al^{3+} interactions with several ligands of biological and/or environmental interest were reported. The attention was focused on the study of the complexing ability of different ligand classes present in natural systems and biological fluids. These were classified in:

1. Carboxylic acids, or O-donor ligands;
2. Thiocarboxylic acids or O-, S-donor ligands;
3. Amino acids, or O-, N-donor ligands;
4. Oligophosphates (O-donor ligands) and other inorganic ligands;
5. Nucleotides.

Molecules with these functions may be involved in Al^{3+} transport and uptake processes into living organisms, playing a very important role in its sequestration.

Before to evaluate the metal cation interaction with the ligands, a thorough analysis of literature data and a subsequent experimental study on aluminum hydrolysis was conducted at T = 298.15 K and ionic strength between 0.1 and 1 mol L^{-1}, in NaCl, $NaNO_3$ and NaCl/$NaNO_3$ mixed solutions.

For the different metal - ligand systems, the speciation models were proposed on the basis of experimental results obtained by potentiometry, which is considered the most suitable analytical technique for the speciation studies in aqueous solution. In addition, in some cases, UV and ^1H NMR spectroscopic measurements, MALDI-MS and MS/MS investigations were performed to confirm the speciation models provided by potentiometric data and to have more information about the complex species, such as the spectroscopic properties, the geometry, the fragmentation pathways and the elemental composition. Moreover, UV - spectrophotometric technique allowed to use lower concentrations, extending the investigated pH range, which is limited in the case of metal cations characterized by strong hydrolysis, such as aluminium.

From the obtained results, the following conclusions can be done:

- The stability of the simple ML species related to Al^{3+}-polycarboxylate systems follows the trend: *lac* < *mala* ≤ *tca* < *btc* ≈ *mlt* < *mal* < *EDDS*. The higher value of *mal*, with respect to the other ligands, except *EDDS*, is probably due to its ability to act as bidentate ligand, forming cyclic structures;

- The affinity of Al^{3+} towards thiocarboxylic ligands increases with the number and the basicity of the donor groups. Formation constant values related to the ML species indicate a higher stability for Al^{3+}-*tma* complexes than Al^{3+}-*tla* and -*mpa* species. It is probably due to the presence on *tma* molecule of another carboxylic group with respect to *tla* and *mpa*, which have only a carboxylate and a thiolate as potential binding site;

- The analysis of Al^{3+}-amino acid results allowed to obtain the stability trend, *Gly* < *Cys* < *tranex*. It clearly indicates that the additional presence of an additional -SH group in the cysteine molecule with respect to the glycine strongly affects the binding ability of this compounds and the complex stability;

- For Al^{3+}- oligophosphate systems, the stability of ML species is quite similar in the case of PO_4^{3}, *PP* and *TPP* ligands and follows the trend: *HMP* << *PP* < *P* ≈ *TPP*. For *TPP*, ^{1}H NMR and LD - MS investigations suggested that this ligand interacts with aluminium through two adjacent phosphate oxygens, leading to a six membered ring structure. The same results were provided for *HMP* by means of LD - MS and MS/MS analysis;

- For Al^{3+}-CO_3^{2-} system, the speciation model is featured by the only MLH species and its formation constant value is lower than the one of Al^{3+}-PO_4^{3-}. Moreover, by considering the simple binary Al^{3+}-*lac* and Al^{3+}-F^{-} species previously studied, it was found a ternary species, M(l*ac*)F^{-}, with a significant formation percentage;

- The stability of ML species, for Al^{3+}-nucleotide systems, increases with the increase of the number of the phosphate groups present in the molecule structure, thus following the trend: *AMP* < *ADP* < *ATP*. These biomolecules show approximatively the same behaviour found for the oligophosphate ligands towards aluminium, suggesting that the interaction occurs primarily with phosphate groups.

12.1 Peculiarity of this thesis

In addition to potentiometric investigations, for all the metal - ligand systems (except for Al^{3+}-*lac*, -CO_3^{2-}, -F^-, -*AMP*, -*ADP*), enthalpy change values were determined by means of calorimetric titrations. As expected, it was found that the contribution to the free energy is mainly entropic in nature, typically of hard-hard interactions. ΔH values, here obtained at T = 298.15 K, allow to calculate stability constant values of the complex species at other temperatures through the Van't Hoff equation (3.24). The assessment of these thermodynamic parameters it is necessary to evaluate the temperature effect on the speciation.

For all the Al^{3+}-ligand systems (except for Al^{3+}-*mlt*, -PO_4^{3-}, -*AMP*, -*ADP*), the dependence on ionic strength was studied by means of the Debye - Hückel type equation (3.23) or (3.28). Formation constant values obtained at infinite dilution, together with the empirical parameters C for the dependence on ionic strength are necessary to calculate the stability constants of the complex species at any ionic strength over the range investigated. The dependence on both ionic strength and temperature is of great importance for the application to real systems, such as natural waters and biological fluids, featured by a very variable composition.

For Al^{3+}-*mpa* and -*Cys* systems, UV spectrophotometric investigations were performed in order to study the spectroscopic properties and to confirm the potentiometric findings.

Moreover, for at least one ligand of each different class, (precisely *mal*, *mala*, *Cys*, *tranex*, *TPP* and *ATP*) the speciation models and the stability constants of the main complex species were confirmed by ^{1}H NMR or ^{31}P -{^{1}H} NMR spectroscopy. The results obtained were in good agreement between them and, in the case of Al^{3+}-*TPP*, these investigations allowed to obtain information about the geometry of the complex species.

For the latter system, MALDI LD-MS and MS/MS measurements confirmed the way of ligand chelation, through two adjacent phosphate oxygens, leading to a six membered cyclic structure, also suggested for the Al^{3+}-*HMP* one.

In addition, for polycarboxylates, thiocarboxylate and amino acids, an empirical relationship was proposed. Although the experimental determination is the best approach, modeling studies can be very useful to predict the stability of metal - ligand complexes for the same homogeneous ligand classes. For these systems, by this empirical relationship it is possible to calculate roughly the stability of Al^{3+}-ligand species, for compounds containing O-, N-, S-donor groups.

Lastly, the sequestering ability was investigated for all the systems under study by the calculation of the $pL_{0.5}$ values. In general, it is influenced by several factors such as ionic strength, pH, metal - ligand concentration ratio and temperature. As expected, the results show an increase of the sequestering capacity with the increase of the number and the hard character of the donor groups. For example, at pH = 5, I = 0.15 mol L^{-1} and T = 298.15 K, the

sequestering ability of *mal*, having two -COOH groups, results higher ($pL_{0.5}$ = 6.09) than *tranex* one ($pL_{0.5}$ = 3.91), having a -COOH and a $-NH_2$ group, and higher than *mpa* and *tla* ones ($pL_{0.5}$ = 2.59, 3.18, respectively), having a -COOH and a -SH group.

References

1. G. Berthon, *Chemical speciation studies in relation to aluminium metabolism and toxicity.* Coord. Chem. Rev., 1996, **149**, 241-280.
2. D.M. Templeton, F. Ariese, R. Cornelis, L.G. Danielsson, H. Muntau, H.P. Van Leeuwen, R. Łobinsky, *Guidelines for terms related to chemical speciation and fractionation of elements. Definitions, structural aspects, and methodological approaches.* Pure Appl. Chem., 2000, **72**(8), 1453-1470.
3. A.M. Ure, C.M. Davidson, *Chemical Speciation in the Environment*, ed. n. edition. 2002: Blackwell Science.
4. M. Filella, P.M. May, *Reflections on the calculation and publication of potentiometrically-determined formation constants.* Talanta 2005, **65**, 1221-1225.
5. T. Kiss, *From coordination chemistry to biological chemistry of aluminium.* J. Inorg. Biochem., 2013, **128**, 156-163.
6. D.R. Parker, *Encyclopedia of soils in the environment.* Elsevier, 2005, 50-56.
7. R.A. Yokel, *Aluminum chelation principles and recent advances.* Coord. Chem. Rev., 2002, **228**, 97.
8. G. Crisponi, V.M. Nurchi, V. Bertolasi, M. Remelli, G. Faad, *Chelating agents for human diseases related to aluminium overload.* Coord. Chem. Rev., 2012, **256**, 89-104.
9. I. McNeil, *The light metals, aluminium and magnesium*, in *An Encyclopedia of the History of Technology*, Routledge, Editor. 2002.
10. R. Quentin, J. Skrabec, *Aluminum in America: A History*. 2016, Jefferson, North Carolina: McFarland.
11. A. Agnihotri, S. Rai, N. Wahradpande, *Carbon dioxide Management-Aluminium industry perspective*. Carbon Utilization: Applications for the Energy Industry, ed. Malti;, Goel;, M. Sudhakar. 2017: Springer.
12. *Aluminium* in *Meyler's Side Effects of Drugs:The International Encyclopedia of Adverse Drug Reactions and Interactions*, J.K. Aronson, Editor. 2016, Elsivier. 187-197.
13. R.A. Yokel, *Aluminum*, in *Elements and their compounds in the environment - Occurrence, analysis and biological relevance*, E. Merian, M. Anke, M. Ihnat, M. Stoeppler, Editors. 2004, Wiley-VCH. 635-658.
14. R.B. Martin, *Ternary complexes of Al^{3+} and F^- with a third ligand* Coord. Chem. Rev., 1996, **141**, 23-32.
15. P. Rubini, A. Lakatos, D. Champmartin, T. Kiss, *Speciation and structural aspects of interactions of Al(III) with small biomolecules.* Coord. Chem. Rev., 2002, **228**, 137-152.
16. R.B. Martin, *The Importance of Aluminium Chemistry in Biological Systems*, in *Aluminium Toxicity in infants' Health and Disease*, P.F. Zatta, A.C. Alfrey, Editors. 1998, World Scientific. 3 -15.
17. V. Bertolasi, G. Crisponi, G. Faa, V.M. Nurchi, M. Remelli, *Aluminium-dependent human diseases and chelating properties of aluminium chelators for biomedical applications*, in *Metal Ions in Neurological Systems*, W. Linert, H. Kozlowski, Editors. 2012, Springer-Verlag: Wien. 103-123.
18. K. Satake, E.J.M. Temminghoff, W. Van Riemsdijk, L. Weng, *Aluminum speciation in natural waters: measurement using Donnan membrane technique and modeling using NICA-Donnan.* Water Res., 2002, **36**(17), 4215-4226.
19. C. Exler, *Darwin, natural selection and the biological essentiality of aluminium and silicon.* Trends Biochem. Sci., 2009, **34**, 589-593.

20. D. Krewski, R.A. Yokel, E. Nieboer, D. Borchelt, J. Cohen, J. Harry, S. Kacew, J. Lindsay, A.M. Mahfouz, V. Rondeau, *Human health risk assessment for aluminium, aluminium oxide and aluminium hydroxide.* J. Toxicol. Environ. Health B. Crit. Rev., 2007, **10**(1-269).
21. Z. Rengel, *Aluminium cycling in the soil-plant-animal-human continuum.* BioMetals, 2004, **17**, 669–689.
22. A. Sanz-Medel, A.B. Soldado Cabezuelo, R. Milacic, T.B. Polak, *The chemical speciation of aluminium in human serum.* Coord. Chem. Rev., 2002, **228**, 373-383.
23. I.S. Parkinson, M.K. Ward, D.N. Kerr, *Dialysis encephalopathy, bone disease and anaemia:the aluminium intoxication syndrome during regular haemodialysis.* J. Clin. Pathol., 1981, **34**(11), 1285-1294.
24. S. Maya, T. Prakash, K. Das Madhu, D. Goli, *Multifaceted effects of aluminium in neurodegenerative diseases: A review.* Biomed. Pharmacother., 2016, **83**, 746-754.
25. R.B. Martin, *The Chemistry of Aluminium as related to biology and medicine.* Clin. Chem., 1986, **32**(10), 1797-1806.
26. G. Crisponi, V.M. Nurchi, *Thermodynamic remarks on chelating ligands for aluminium related diseases.* J. Inorg. Biochem., 2011, **105**, 1518-1522.
27. T. Kiss, I. Sovago, I. Toth, A. Lakatos, R. Bertani, A. Tapparo, G. Bombi, R.B. Martin, *Complexation of aluminium (III) with several bi- and tri-dentate amino acids.* J. Chem. Soc., Dalton Trans., 1997, 1967-1972.
28. A.E. Martell, R.D. Hancock, R.M. Smith, R.J. Motekaitis, *Coordination of Al(III) in the environment and in biological systems.* Coord. Chem. Rev., 1996, **311-328**, 149
29. E.M. Thurman, *Organic Geochemistry of Natural Waters*. 1985: Martin Nijhoff/Dr. W. Junk Publishers.
30. M.L. Goodwin, J.E. Harris, A. Hernández, L.B. Gladden, *Blood lactate measurements and analysis during exercise: a guide for clinicians.* J. Diabetes Sci. Technol., 2007, **1**(4), 558–569.
31. F.A. Castillo Martinez, E.M. Balciunas, J.M. Salgado, J.M. Domínguez González, A. Converti, R. Pinheiro de Souza Oliveira, *Lactic acid properties, applications and production: A review.* Trends Food Sci Technol., 2013, **30**(1), 70-83.
32. A.B. Pardee, V.R. Potter, *Malonate Inhibition of Oxidations in the Krebs Tricarboxylic Acid Cycle.* J. Biol. Chem., 1948, **178**, 241–250.
33. C.S. Ough, M.A. Amerine, *Methods For Analysis of Musts and Wines*. 1988: John Wiley and Sons. 67.
34. J.M. Llobet, J.L. Domingo, M. Gómez, J.M. Tomás, J. Corbella, *Acute toxicity studies of aluminium compounds: antidotal efficacy of several chelating agents.* Pharmacol. Toxicol., 1987, **60**(4), 280-283.
35. J.B. Russell, N. Forsberg, *Production of tricarballylic acid by rumen microorganisms and its potential toxicity in ruminant tissue metabolism.* British Journal of Nutrition, 1986, **53**, 153-162.
36. J.D. George, C.J. Price, M.C. Marr, C.B. Myers, G.D. Jahnke, *Developmental toxicity evaluation of 1,2,3,4-butanetetracarboxylic acid in Sprague Dawley (CD) rats.* Reproductive Toxicology, 2001, **15**(413-420).
37. F. Crea, D. Milea, S. Sammartano, *Enhancement of hydrolysis through the formation of mixed hetero-metal species.* Talanta, 2005, **65**, 229-238.
38. C. De Stefano, A. Gianguzza, T. Leggio, S. Sammartano, *Dependence on ionic strength of hydrolysis constants for dioxouranium(VI) in $NaCl_{(aq)}$ and $NaNO_{3(aq)}$, at pH < 6 and t = 25°C.* J. Chem. Eng. Data, 2002, **47**(3), 533-538.

39. N.J. Velupula, G.J. Tedros, M.C. Andrew, *Determination of Copper and Iron Using [S,S]-Ethylenediaminedisuccinic Acid as a Chelating Agent in Wood Pulp by Capillary Electrophoresis.* Anal. Sci., 2007, **23**, 493−496.
40. J.A. Neal, N.J. Rose, *Stereospecific Ligands and Their Complexes. I. A Cobalt(III) Complex of Ethylenediaminedisuccinic Acid.* Inorganic Chemistry, 1968, **7**(11), 2405-2412.
41. C. Bretti, R.M. Cigala, C. De Stefano, G. Lando, S. Sammartano, *Understanding the bioavailability and sequestration of different metal cations in the presence of a biodegradable chelant S,S-EDDS in biological fluids and natural waters.* Chemosphere, 2016 **150**, 341-356.
42. J. Buffle, *Complexation reactions in aquatic systems: An Analytical approach.* 1988, Chichester, England: Ellis Horwood Limited.
43. J. Zhang, F. Wang, J.D. House, B. Page, *Thiols in wetland interstitial waters and their role in mercury and methylmercury speciation.* Limnol. Oceanogr., 2004, **49**, 2276-2286.
44. V. Krishnan, P. Patil, *Thiomalates of divalent Zinc, Cadmium, Mercury and Lead.* J. Inorg. Nucl. Chem., 1978, **40**, 1255-1257.
45. G.R. Lenz, A.E. Martell, *Metal chelates of mercaptosuccinic and alfa, alfa'-dimercaptosuccinic acids.* Inorg. Chem., 1965, **4**(3), 378-384.
46. P. Gillet, *Pharmacokinetics of tiopronin after repeated oral administration in rheumatoid arthritis.* Fundam. Clin. Pharmacol., 1995, **9**, 205-206.
47. M. Priori, *Medicina e chirurgia estetica del viso e del collo*, ed. Elsevier. 2007.
48. E. Sabbagh, D. Cuebas, H. Schulz, *3-Mercaptopropionic Acid, a Potent Inhibitor of Fatty Acid Oxidation in Rat Heart Mitochondria.* J. Biol. Chem., 1985, **260**(12), 7337-7342.
49. D. Cuebas, J.D. BeckrnannSg, F.E. FrermanS, H. Schulz, *Mitochondrial Metabolism of 3-Mercaptopropionic Acid.* J. Biol. Chem., 1985, **260**(12), 7330-7336.
50. U. Heresco-Levy, D.C. Javitt, M. Ermilov, C. Mordel, G. Silipo, M. Lichtenstein, *Efficacy of High-Dose Glycine in the Treatment of Enduring Negative Symptoms of Schizophrenia.* Arch. Gen. Psychiatry, 1999, **56**(1), 29-36.
51. E. Bottari, M.R. Festa, *On the behaviour of cysteine as ligand of cadmium(II).* Talanta, 1997, **44**, 1705-1718.
52. S.S. Khaloo, M.K. Amini, S. Tangestaninejad, S. Shahrokhian, R. Kia, *Voltammetric and Potentiometric study of cysteine at Cobalt(II) Phtalocyanine modified carbon-paste electrode.* J. Ir. Chem. Soc., 2004, **1**, 128-135.
53. M.F. Khan, M.F. Khan, M. Ashfaq, G.M. Khan, *Synthesis and characterization of some novel tranexamic acid derivatives and their copper(II) complexes.* The Sciences, 2001, **1**(5), 327-333.
54. F.J. Millero, *Chemical Oceanography*. 2nd ed, ed. F.J. Millero. 1996 Boca Raton, FL: CRC Press.
55. P. Djurdjevic, R. Jelic, D. Dzajevic, M. Cvijovic, *Solution equilibria between aluminum(III) ion and L-Histidine or L-tyrosine.* Met. Based Drugs, 2002, **8**(5), 235-248.
56. A.M. Ho, M.D. Johnson, D.M. Kingsley, *Role of the mouse ank gene in control of tissue calcification and arthritis.* Science, 2000, **289**(5477), 265–270.
57. K. Schrödter, G. Bettermann, T. Staffel, F. Wahl, T. Klein, T. Hofmann, *Phosphoric Acid and Phosphates*, in *Ullmann's Encyclopedia of Industrial Chemistry*, Wiley-VCH, Editor. 2008: Weinheim.
58. P. Wiilknitz, *Cleaning power and abrasivity of European toothpastes.* Adv. Dent. Res., 1997, **11**(4), 576-579.

59. H. AraiIwao, I. Maruta, T. Kariyone, *Study of detergency. II. Effect of sodium tripolyphosphate.* J. Am. Oil Chem. Soc., 1966, **43**(5), 315-316.
60. F. Rashchi, J.A. Finch, *Polyphosphates: a review their chemistry and application with particular reference to mineral processing.* Miner. Eng., 2000, **13**(10-11), 1019-1035.
61. F.J. Millero, A. Gianguzza, E. Pelizzetti, S. Sammartano, *Chemical Processes in Marine Environments*. 2000, Berlin: Springer. 9-42.
62. C. De Stefano, C. Foti, A. Pettignano, S. Sammartano, *Binding of fluoride and carbonate by open chain polyammonium cations.* Talanta, 2004, **64**, 510-517.
63. Z.M.Y. Abouleish, *Evaluation of fluoride levels in bottled water and their contribution to health and teeth problems in the United Arab Emirates.* Saudi. Med. J., 2016, **28**, 194-202.
64. T. Kiss, P. Zatta, B. Corain, *Interaction of aluminium(III) with phosphate-binding sites: biological aspects and implications.* Coord. Chem. Rev., 1996, **149**, 329-346.
65. D.L. Nelson, M.M. Cox., *I principi di biochimica di Lehninger*, ed. 6. 2014: Zanichelli. 1312.
66. P. Cardiano, F. Giacobello, O. Giuffrè, S. Sammartano, *Thermodynamic and spectroscopic study on Al^{3+}-polycarboxylate interaction in aqueous solution.* J. Mol. Liq., 2017, **232**, 45-54.
67. D.A. Skoog, D.M. West, F.J. Holler, S.R. Crouch, *Foundamentals of Analytical Chemistry*. 9th ed. 2014: Brooks/Cole, Cengage Learning.
68. A. Rouessac, F. Rouessac, *Potentiometric methods, Chemical Analysis. Modern Instrumentation Methods and Techniques*, ed. J.W. Sons. 1994.
69. A. De Robertis, C. De Stefano, O. Giuffré, S. Sammartano, *Binding of Carboxylic Ligands by Protonated Amines.* J. Chem. Soc. Faraday Trans., 1996, **92**, 4219-4226.
70. R.M. Silverstein, F.X. Webster, D.J. Kiemle, D.L. Bryce, *Identificazione spettrometrica di composti organici*. 3 ed. 2016: Casa Editrice Ambrosiana.
71. C. De Stefano, C. Foti, O. Giuffrè, P. Mineo, C. Rigano, S. Sammartano, *Binding of tripolyphosphate by aliphatic amines: formation, stability and calculation problems.* Ann. Chim. (Rome), 1996, **86**
72. C. De Stefano, S. Sammartano, P. Mineo, C. Rigano, *Computer Tools for the Speciation of Natural Fluids*, in *Marine Chemistry - An Environmental Analytical Chemistry Approach*, A. Gianguzza, E. Pelizzetti, S. Sammartano, Editors. 1997, Kluwer Academic Publishers: Amsterdam. 71-83.
73. A. De Robertis, C. De Stefano, C. Rigano, *Computer analysis of equilibriumdata in solution. ES5CM Fortran and basic programs for computing formation enthalpies from calorimetric measurements.* Thermochim. Acta, 1986, **138**.
74. C. De Stefano, P. Mineo, C. Rigano, S. Sammartano, *Ionic strenght dependence of formation constants. XVII. The calculation of equilibrium concentrations and formation constants.* Ann. Chim. (Rome), 1993, **83**, 243-277.
75. P. Gans, A. Sabatini, A. Vacca, *Determination of equilibrium constants from spectrophometric data obtained from solutions of known pH: THE PROGRAM pHab.* Ann. Chim. (Rome), 1999, **89**, 45-49.
76. C. Frassineti, S. Ghelli, P. Gans, A. Sabatini, M.S. Moruzzi, A. Vacca, *Nuclear Magnetic Resonance as a Tool for Determining Protonation Constants of Natural Polyprotic Bases in Solution.* Anal. Biochem., 1995, **231** 374-382
77. C.W. Davies, *Ion Association*. 1962, London.
78. C. Bretti, F. Crea, O. Giuffrè, S. Sammartano, *The effect of different aqueous ionic media on the acid-base properties of some open chain polyamines.* J. Solution Chem., 2008, **37**, 183-201.

79. F. Crea, C. De Stefano, A. Irto, D. Milea, A. Pettignano, S. Sammartano, *Modeling the acid-base properties of molybdate(VI) in different ionic media, ionic strengths and temperatures, by EDH, SIT and Pitzer equations.* J. Mol. Liq., 2017, **229**, 15-26.
80. C.F. Baes, R.E. Mesmer, *The hydrolysis of cations*. 1976, New York: John Wiley & sons.
81. A. Sarpola, H. Hellman, V. Hietapelto, J. Jalonen, J. Jokela, J. Ramo, J. Saukkoriipi, *Hydrolysis products of water treatment chemical aluminium sulfate octadecahydrate by electrospray ionization mass spectrometry.* Polyhedron, 2007, **26**, 2851-2858.
82. L.D. Pettit, K.J. Powell, *IUPAC Stability Constants Database.* 2001, Academic Software, IUPAC.
83. R.M. Cigala, C. De Stefano, A. Giacalone, A. Gianguzza, *Speciation of Al^{3+} in fairly concentrated solutions (20 –200mmol L^{-1}) at I = 1 mol L^{-1} ($NaNO_3$), in the acidic pH range, at different temperatures.* Chem. Spec. Bioavail., 2011, **23**(11), 33-37.
84. A.E. Martell, R.M. Smith, R.J. Motekaitis, *Critically Selected Stability Constants of Metal Complexes*, NIST Critically selected stability constants of metal complexes database, Editor. 2004: National Institute of Standard Technology, Garthersburg, MD.
85. P.M. May, K. Murray, *Database of chemical reactions designed to achieve thermodynamic consistency automatically* J. Chem. Eng. Data, 2001, **46** 1035-1040.
86. E. Gumienna-Kontecka, G. Berthon, I.O. Fritsky, R. Wieczorek, Z. Latajka, H. Kozlowski, *2-(Hydroxyimino)propanohydroxamic acid, a new effective ligand for aluminium.* J. Chem. Soc., Dalton Trans., 2000, 4201-4208.
87. E. Marklund, L.O. Öhman, *Equilibrium and Structural Studies of Silicon (IV) and Aluminium (III) in Aqueous solution. 24. A Potentiometric and ^{27}Al NMR Study of Polynuclear Aluminium (III) Hydroxo Complexes with Lactic Acid.* Acta Chem. Scand., 1990, **44**, 228-234.
88. T. Hedlund, L.O. Öhman, S. Sjöberg, *Equilibrium and Structural Studies of Silicon (IV) and Aluminium (III) in Aqueous Solution. 15. A Potentiometric Study of Speciation and Equilibria in the $Al(^{3+})$-$CO_{2(g)}$-OH^- system.* Acta Chem. Scand., 1987, **41**, 197-207.
89. P. Sipos, S.G. Capewell, P.M. May, G. Hefter, G. Laurenczy, F. Lukács, R. Roule, *Spectroscopic studies of the chemical speciation in concentrated alkaline aluminate solutions.* J. Chem. Soc., Dalton Trans., 1998, 3007-3012.
90. P.L. Brown, R.N. Sylva, G.E. Batley, J. Ellis, *The hydrolysis of metal ions. Part 8. Aluminium(III).* J. Chem. Soc., Dalton Trans., 1985, 1967-1970
91. A. De Robertis, C. De Stefano, C. Foti, *Medium effects on the protonation of carboxylic acids at different temperatures.* J. Chem. Eng. Data, 1999, **44**, 262-270.
92. A. De Robertis, C. De Stefano, C. Foti, *Studies on Polyfunctional O-Ligands. Protonation in Different Ionic Media and Alkali and Alkaline Earth Metal Complex Formation of Benzenehexacarboxylate.* Ann. Chim. (Rome), 1996, **86**, 155-166.
93. C. Bretti, R.M. Cigala, C. De Stefano, G. Lando, S. Sammartano, *Understanding the bioavailability and sequestration of different metal cations in the presence of a biodegradable chelant S,S-EDDS in biological fluids and natural waters.* Chemosphere, 2016, **150**, 341-356.
94. C. Bretti, O. Giuffrè, G. Lando, S. Sammartano, *Solubility, protonation and activity coefficients of some aminobenzoic acids in NaClaq and (CH3)4NClaq, at different salt concentrations, at T=298.15K.* J. Mol. Liq., 2015, **212**, 825-832.
95. C. De Stefano, O. Giuffrè, S. Sammartano, *Protonation constants of ethylenediamine, diethylenetriamine and spermine in $NaCl_{aq}$, NaI_{aq}, $(CH_3)_4NCl_{aq}$ and $(C_2H_5)_4NI_{aq}$, at different ionic strengths and t = 25 °C.* J. Chem. Eng. Data, 2005, **50**, 1917-1923.

96. F. Crea, P. Crea, C. De Stefano, O. Giuffrè, A. Pettignano, S. Sammartano, *Thermodynamic Parameters for the Protonation of Poly(allylamine) in concentrated LiCl(aq) and NaCl(aq).* J. Chem. Eng. Data, 2004, **49**, 658-663.
97. A. De Robertis, C. Foti, O. Giuffrè, S. Sammartano, *The dependence on ionic strength of enthalpies of protonation for polyamines in $NaCl_{(aq)}$.* J. Chem. Eng. Data, 2002, **47**, 1205-1212.
98. F. Crea, G. Falcone, C. Foti, O. Giuffrè, S. Materazzi, *Thermodynamic data for Pb^{2+} and Zn^{2+} sequestration by biologically important S-donor ligands, at different temperatures and ionic strengths.* New J. Chem., 2014, **38**, 3973-3983.
99. D. Chillè, C. Foti, O. Giuffrè, *Thermodynamic parameters for the protonation and the interaction of arsenate with Mg^{2+}, Ca^{2+} and Sr^{2+}: Application to natural waters.* Chemosphere, 2017, **190**, 72-79.
100. C. De Stefano, C. Foti, O. Giuffrè, D. Milea, *Complexation of Hg^{2+}, CH_3Hg^{+}, Sn^{2+}, and $(CH_3)_2Sn^{2+}$ with phosphonic NTA derivatives.* New J. Chem., 2016, **40**, 1443-1453.
101. C. Foti, O. Giuffrè, S. Sammartano, *Thermodynamics of HEDPA protonation in different media and complex formation with Mg^{2+} and Ca^{2+}.* J. Chem. Thermodynamics, 2013, **66**, 151-160.
102. G. Bruno, A. De Robertis, O. Giuffrè, A. Rotondo, S. Sammartano, *Binding of benzene-1,2,3,4,5,6-hexacarboxylate by polyammonium cations.* Polyhedron, 2009, **28**, 2703–2709.
103. C. De Stefano, O. Giuffrè, A. Pettignano, S. Sammartano, *Thermodynamics of proton association of polyacrilates and polymethacrylates in $NaCl_{(aq)}$.* J. Solution Chem., 2003, **32**(11), 967-976.
104. C. De Stefano, C. Foti, O. Giuffrè, S. Sammartano, *Dependence on ionic strength of protonation enthalpies of polycarboxylic anions in NaCl aqueous solution.* J. Chem. Eng. Data, 2001, **46**, 1417-1424.
105. C. De Stefano, A. Gianguzza, O. Giuffrè, A. Pettignano, S. Sammartano, *Interaction of methyltin(IV) compounds with carboxylate ligands. Part 2: Formation thermodynamic parameters, predictive relationships and sequestering ability.* Appl. Organomet. Chem., 2008, **22**, 30-38.
106. C. Bretti, C. De Stefano, C. Foti, S. Sammartano, *Acid-base properties, solubility, activity coefficients and Na^{+} ion pair formation of complexons in $NaCl_{(aq)}$ at different ionic strengths ($0 \leq I \leq 4.8$ mol L^{-1})* J. Solution Chem., 2013, **42**, 1452-1471.
107. G. Falcone, C. Foti, A. Gianguzza, O. Giuffrè, A. Napoli, A. Pettignano, D. Piazzese, *Sequestering ability of some chelating agents towards methylmercury(II).* Anal. Bioanal. Chem., 2013, **405**(2), 881-893.
108. P. Cardiano, G. Falcone, C. Foti, O. Giuffrè, S. Sammartano, *Methylmercury(II)-sulphur containing ligand interactions: a potentiometric, calorimetric and ^{1}H-NMR study in aqueous solution.* New J. Chem., 2011, **35**(4), 800 - 806.
109. P. Cardiano, D. Cucinotta, C. Foti, O. Giuffrè, S. Sammartano, *Potentiometric, calorimetric and ^{1}H-NMR investigation on Hg^{2+}-mercaptocarboxylate interaction in aqueous solution.* J. Chem. Eng. Data, 2011, **56**, 1995-2004.
110. P. Cardiano, O. Giuffrè, L. Pellerito, A. Pettignano, S. Sammartano, M. Scopelliti, *Thermodynamic and spectroscopic study of the binding of dimethyltin(IV) by citrate at 25°C.* Appl. Organomet. Chem., 2006, **20**, 425-435.
111. K. Gajda-Schrantz, L. Nagy, T. Fiore, L. Pellerito, T. Gajda, *Equilibrium and spectroscopic studies of diethyltin(IV) complexes formed with hydroxymono- and di-carboxylic acids and their thioanalogues.* J. Chem. Soc., Dalton Trans., 2002, 152-158.

112. J. Findlow, J. Duffield, D. Williams, *The chemical spéciation of aluminum in milk.* Chem. Spec. Bioavail., 1990(2), 3-32.
113. G.E. Jackson, *Studies on the chelation of aluminum for biological application. Part 1. Citric acid.* S. Afr. J. Chem., 1982, **35**(3), 89-92.
114. H.K.J. Powell, R.M. Town, *Aluminum(III)-Malonate Equilibria: a Potentiometric Study.* Australian J. Chem., 1993, **46**(5), 721-726.
115. M. Venturini-Soriano, G. Berthon, *Aluminum speciation studies in biological fluids Part 7. A quantitative investigation of aluminum(III)–malate complex equilibria and their potential implications for aluminum metabolism and toxicity.* J. Inorg. Biochem., 2001, **85**, 143-154.
116. P. Cardiano, R.M. Cigala, F. Crea, F. Giacobello, O. Giuffré, A. Irto, G. Lando, S. Sammartano, *Sequestration of Aluminium(III) by different natural and synthetic organic and inorganic ligands in aqueous solution.* Chemosphere, 2017, **186**, 535-545.
117. T. Kiss, I. Sovago, R.B. Martin, J. Pursiainen, *Ternary complex formation between Al(III)-adenosine-5'-phosphates and carboxylic acid derivatives.* J. Inorg. Biochem., 1994, **55**(1), 53-65.
118. K.M. Elkins, D.J. Nelson, *Spectroscopic approaches to the study of the interaction of aluminum with humic substances.* Coord. Chem. Rev., 2002, **228**, 205-225.
119. C. Bretti, C. De Stefano, C. Foti, O. Giuffrè, S. Sammartano, *Thermodynamic protonation parameters of some sulphur-containing anions in NaClaq and $(CH_3)_4NCl_{aq}$ at t = 25 °C* J. Solution Chem., 2009, **38**(10), 1225-1245.
120. P. Cardiano, F. Giacobello, O. Giuffrè, S. Sammartano, *Thermodynamics of Al^{3+}-thiocarboxylate interaction in aqueous solution.* J. Mol. Liq., 2016, **222**, 614-621.
121. P. Cardiano, R.M. Cigala, F. Crea, C. De Stefano, O. Giuffrè, S. Sammartano, G. Vianelli, *Potentiometric, UV and ^1H NMR study on the interaction of penicillin derivatives with Zn(II) in aqueous solution.* Biophys. Chem., 2017, **223**, 1-10.
122. P. Cardiano, F. Crea, C. Foti, O. Giuffrè, S. Sammartano, *Potentiometric, UV and ^1H NMR study on the interaction of Cu^{2+} with ampicillin and amoxicillin in aqueous solution* Biophys. Chem., 2017, **224**, 59-66.
123. P. Cardiano, C. Foti, O. Giuffrè, *On the interaction of N-acetylcysteine with Pb^{2+}, Zn^{2+}, Cd^{2+} and Hg^{2+}.* J. Mol. Liq., 2016, **223**, 360-367.
124. C. De Stefano, C. Foti, O. Giuffrè, S. Sammartano, *Acid-base and UV behaviour of 3-(3,4-dihydroxyphenyl)-propenoic acid (caffeic acid) and complexing ability towards different divalent metal cations in aqueous solution.* J. Mol. Liquids, 2014, **195**, 9–16.
125. G. Falcone, O. Giuffrè, S. Sammartano, *Acid-base and UV properties of some aminophenol ligands and their complexing ability towards Zn^{2+} in aqueous solution.* J. Mol. Liquids, 2011 **159**, 146-151.
126. S. Desroches, S. Dayde, G. Berthon, *Aluminum speciation studies in biological fluids Part 6. Quantitative investigation of aluminum(III)–tartrate complex equilibria and their potential implications for aluminum metabolism and toxicity.* J. Inorg. Biochem., 2000, **81**, 301-312.
127. M. Venturini-Soriano, G. Berthon, *Aluminum speciation studies in biological fluids. Part 4. A new investigation of aluminum-succinate complex formation under physiological conditions, and possible implications for aluminum metabolism and toxicity.* J. Inorg. Biochem., 1998, **71**, 135-145.
128. G. Berthon, *Aluminium speciation in relation to aluminium bioavailability, metabolism and toxicity.* Coord. Chem. Rev., 2002, **228**, 319-341.

129. P. Cardiano, F. Giacobello, O. Giuffré, S. sammartano, *Thermodynamic and spectroscopic study of Al^{3+} interaction with glycine, L-Cysteine and tranexamic acid in aqueous solution.* Biophys. Chem., 2017, **230**, 10-19.
130. C. Bretti, O. Giuffrè, G. Lando, S. Sammartano, *Modeling solubility and acid-base properties of some amino acids in aqueous NaCl and (CH3)4NCl aqueous solutions at different ionic strengths and temperatures.* SpringerPlus, 2016.
131. V.K. Sharma, F. Casteran, F.J. Millero, C. De Stefano, *Dissociation Constants of Protonated Cysteine Species in NaCl Media.* J. Solution Chem., 2002, **31**(10), 783-792.
132. P. Cardiano, C. De Stefano, O. Giuffrè, S. Sammartano, *Thermodynamic and spectroscopic study for the interaction of dimethyltin(IV) with L-cysteine in aqueous solution.* Biophys. Chem., 2008, **133**, 19-27.
133. P. Cardiano, G. Falcone, C. Foti, S. Sammartano, *Sequestration of Hg^{2+} by some biologically important thiols* J. Chem. Eng. Data, 2011, **56**, 4741-4750.
134. D. Bohrer, V. Gabbi Polli, P. Cicero do Nascimento, J.K.A. Mendonca, L. Machado de Carvalho, S. Garcia Pomblum, *Ion-exchange and potentiometric characterization of Al-cystine and Al-cysteine complexes.* J. Biol. Inorg. Chem., 2006, **11**, 991-998.
135. S. Daydé, V. Brumas, D. Champmartin, P. Rubini, G. Berthon, *Aluminum speciation studies in biological fluids Part 9. A quantitative investigation of aluminum(III)–glutamate complex equilibria and their potential implications for aluminum metabolism and toxicity.* J. Inorg. Biochem., 2003, **97**, 104-117.
136. S. Daydé, D. Champmartin, P. Rubini, G. Berthon, *Aluminium speciation studies in biological fluids. Part 8. A quantitative investigation of Al(III) /amino acid complex equilibria and assessment of their potential implications for aluminium metabolism and toxicity.* Inorg. Chim. Acta, 2002, **339**, 513-524.
137. P.G. Daniele, A. De Robertis, C. De Stefano, A. Gianguzza, S. Sammartano, *Salts Effects on the Protonation of Ortho-Phosphate Between 10 and 50 °C, in Aqueous Solution. A Complex formation Model.* J. Solution Chem., 1991, **20**, 495-515.
138. C. De Stefano, C. Foti, A. Gianguzza, *Ionic Strength Dependence of Formation Constants. Part XIX. The Effect of Tetramethylammonium, Sodium and Potassium Chlorides on the Protonation Constants of Pyrophosphate and Triphosphate at Different Temperatures.* J. Chem. Res., 1994, (S) 464 (M) 2639-2661.
139. D. Aiello, P. Cardiano, R.M. Cigala, P. Gans, F. Giacobello, O. Giuffré, S. Sammartano, *Sequestering ability of oligophosphate ligands towards Al^{3+} in aqueous solution.* Accepted by J. Chem. Eng. Data, 2017.
140. H. Maki, M. Tsujito, T. Yamada, J. Sol. Chem., 2013, **42**, 1063-1074.
141. K. Atkari, T. Kiss, R. Bertani, R.B. Martin, *Interactions of Aluminum(III) with phosphates.* Inorg. Chem., 1996, **35**, 7089-7094.
142. P. Cardiano, G. Falcone, C. Foti, O. Giuffrè, A. Napoli, *Binding ability of glutathione towards alkyltin(IV) compounds in aqueous solution.* J. Inorg. Biochem., 2013, **129**, 84-93.
143. P. Cardiano, O. Giuffrè, A. Napoli, S. Sammartano, *Potentiometric, ^{1}H-NMR, ESI-MS investigation on dimethyltin(IV) cation-mercaptocarboxylate interaction in aqueous solution.* New J. Chem., 2009, **33**, 2286-2295.
144. W.R. Harris, *Equilibrium model for speciation of aluminum in serum.* Clin. Chem., 1992, **38**, 1809-1818.
145. F. Crea, C. De Stefano, A. Gianguzza, D. Piazzese, S. Sammartano, *Protonation of Carbonate in Aqueous Tetraalkylammonium Salts at 25°C.* Talanta, 2006, **68**(4), 1102-1112.

146. M.S. Cordillon, M.A. Olazabal, J.M. Madariaga, *Potentiometric study of aluminium-fluoride complexation equilibria and definition of the thermodynamic model.* J. Sol. Chem., 2008, **37**(567-579).
147. C. De Stefano, D. Milea, A. Pettignano, S. Sammartano, *Modeling ATP protonation and activity coefficients in $NaCl_{aq}$ and KCl_{aq} by SIT and Pitzer equations.* Biophys. Chem., 2006, **121**, 121-130.
148. T. Kiss, I. Sovago, R.B. Martin, *Al^{3+} binding by adenosine 5'-phosphates: AMP, ADP, and ATP*. Inorg. Chem., 1991, **30**, 2130 - 2132.
149. R.M. Smith, A.E. Martell, Y. Chen, *Critical evaluation of stability constants for nucleotide complexes with protons and metal ions and the accompanying enthalpy changes.* Pure Appl. Chem., 1991, **63**(7), 1015-1080.
150. G.E. Jackson, K.V. Voyi, *Studies on the chelation of aluminium for biological application—IV. AMP, ADP and ATP*. Polyhedron, 1987, **6**(12), 2095-2098.
151. A. Gianguzza, O. Giuffrè, D. Piazzese, S. Sammartano, *Aqueous solution chemistry of alkyltin(IV) compounds for speciation studies in biological fluids and natural waters.* Coord. Chem. Rev., 2012, **256**, 222-239.
152. F. Crea, C. De Stefano, C. Foti, D. Milea, S. Sammartano, *Chelating agents for the sequestration of mercury(II) and monomethyl mercury(II).* Curr. Med. Chem., 2014, **21**(33), 3819-3836.
153. P.G. Harrison, K. Lambert, T.J. King, B. Majee, *The Mössbauer recoil-free fraction and structure. Part 3. Triorganotin arylazobenzoates.* J. Chem. Soc., Dalton Trans., 1983(2), 363-369.
154. D. Cucinotta, C. De Stefano, O. Giuffrè, G. Lando, D. Milea, S. Sammartano, *Formation, stability and empirical relationships for the binding of Sn2+ by O-, N- and S- donor ligands.* J. Mol. Liq., 2014, **200**, 329-339.
155. C. Foti, O. Giuffrè, G. Lando, S. Sammartano, *Interaction of Inorganic Mercury(II) with Polyamines, Polycarboxylates, and Amino Acids.* J. Chem. Eng. Data, 2009, **54**, 893–903.
156. C. De Stefano, A. Gianguzza, O. Giuffrè, D. Piazzese, S. Orecchio, S. Sammartano, *Speciation of organotin compounds in NaCl aqueous solution: Interaction of mono-, di- and triorganotin(IV) cations with nucleotides 5' monophosphates.* Appl. Organomet. Chem., 2004, **18**(12), 653-661.
157. C. De Stefano, O. Giuffrè, D. Milea, C. Rigano, S. Sammartano, *Speciation of phytate ion in aqueous solution. Non covalent interactions with biogenic polyamines.* Chem. Spec. Bioavail., 2003, **15**(2), 29-36.

Acknowledgments

I would like to thank my supervisor, Prof. Ottavia Giuffrè, for helping me in the realization of this thesis, for her continuous support and for being close to me over the years.
Thanks also to Prof. Silvio Sammartano, for helping me with his great scientific knowledge, Prof. Paola Cardiano, for contributing to this study with NMR measurements and Prof. Anna Napoli, for the collaboration with MALDI LD-MS investigations.